The Role of Sarcolipin in Calcium Handling and Obesity

by

Eric Bombardier

A thesis
presented to the University of Waterloo
in fulfillment of the
thesis requirement for the degree of
Doctor of Philosophy
in
Kinesiology

Waterloo, Ontario, Canada, 2010

AUTHOR'S DECLARATION

I hereby declare that I am the sole author of this thesis. This is a true copy of the thesis, Including any required final reversions, as accepted by my examiners.

I understand that my thesis may be made electronically available to the public.

Eric Bombardier

ABSTRACT

Sarcolipin (SLN), a small molecular weight, hydrophobic protein found in skeletal muscle, is a known regulator of sarco(endo)plasmic reticulum Ca^{2+} ATPase (SERCA) pumps. Earlier *in vitro* reconstitution experiments have shown that SLN uncouples ATP hydrolysis from Ca^{2+} transport by the SERCA pumps and increases the amount of heat released per mol of ATP hydrolyzed by inducing an increased rate of "slippage" during the reaction cycle of SERCA pumps. In order to determine whether SLN causes slippage of SERCA activity by uncoupling ATP hydrolysis from Ca^{2+} transport under more physiological conditions, comparisons were made between skeletal muscle Ca^{2+} ATPase activity and Ca^{2+} uptake in homogenates from soleus muscle of wild-type (WT) and *Sln*-null (KO) mice under conditions in which a Ca^{2+} gradient was preserved across the sarcoplasmic reticulum (SR) vesicles. Ca^{2+} ATPase activity, measured in the absence of the Ca^{2+} ionophore, A23187, was 15-25% lower in KO muscles, compared with WT, consistent with the proposal that SLN increases "slippage" and reduces the extent of back-inhibition of the Ca^{2+} ATPase. Ca^{2+} uptake, measured in homogenates without oxalate, was not different ($p>0.05$) in SR vesicles from WT and KO mice, indicating that the calculated Ca^{2+} transport efficiency (coupling ratio) in KO mice was increased by about 20% ($P<0.04$). The basal oxygen consumption (VO_2) of soleus muscles isolated from WT and KO mice and the contribution of energy utilized by SERCA was also compared. Surprisingly, basal VO_2 was not lower in the soleus of KO mice, but the contribution of energy utilized by SERCA pumps was about 7% lower ($P<0.0001$). It was also found that uncoupling protein 3 (UCP-3) was expressed at a higher ($P<0.03$) concentration in soleus muscle of KO compared to WT. Thus UCP-3 could, potentially, provide compensation, resulting in higher basal VO_2 in KO mice than expected. These data show that at physiological

SLN:SERCA ratios, SLN uncouples ATP hydrolysis from SR Ca^{2+} uptake in skeletal muscle, resulting in a lower contribution of Ca^{2+} handling to basal VO_2. Thus, SLN is a key regulator of both ATP utilization in Ca^{2+} handling and of overall energy metabolism in skeletal muscle.

To further examine the role of SLN in adaptive thermogenesis, obesity and glucose intolerance, KO and WT mice were placed on a high fat diet (HFD; 42% of kcal derived from fat) for an eight week period. Whole body metabolism, weight gain, glucose tolerance and insulin tolerance were measured before and after the HFD. Fat pads, liver, pancreas, hindlimb muscles and plasma samples were collected from standard chow fed control and HFD WT and KO mice. KO mice gained more weight ($P<0.05$) and became more obese ($P<0.05$) than WT mice after consuming the HFD. The comprehensive laboratory animal monitoring system (CLAMS) revealed no differences in whole body metabolic rate (ml O_2/kg/hr) between KO and WT mice pre diet; however, daily metabolic rate was lower ($P<0.05$) in KO mice compared with WT mice after the HFD which may explain the increased obesity in KO mice. Western blotting analyses revealed SLN protein content to be 3.8 fold higher ($P<0.05$) in WT soleus post HFD compared to control. Phospholamban (PLN), a homologue of SLN, was found to be 2.1 fold higher ($P<0.05$) in brown adipose tissue (BAT) in both WT and KO mice post HFD. Protein contents of other Ca^{2+} handling proteins (SERCA1a, SERCA2a, PLN and calsequestrin) within fast (white gastrocnemius) and slow (soleus) twitch muscle were not different between KO and WT mice following the HFD. Collectively, these results suggest that PLN and SLN could play a role in adaptive diet-induced thermogenesis. On the other hand, compared with chow fed control mice, the metabolic cost of Ca^{2+} handling in soleus muscle was significantly reduced post HFD in both WT and KO mice, although to a greater extent ($P<0.05$) in KO mice than WT mice. Moreover, there were no differences in resting

energy expenditure of soleus muscles between WT and KO mice following the HFD. These observations can be accounted for by diet-induced increases in sympathetic nervous system activity in KO mice and other adaptive responses leading to increased energy expenditure of soleus in both WT and KO mice. Therefore, differences in whole body metabolic rate and obesity between high fat fed WT and KO mice do not appear to be due to adaptive thermogenesis mechanisms in skeletal muscle involving SLN. Interestingly, soleus and EDL muscle weights increased proportionately to body weight in high fat fed WT mice but not KO mice. Therefore, lower lean body tissue mass may explain the lower whole body metabolic rate and increased susceptibility to obesity in KO mice compared with WT mice. With increased obesity, KO mice became extremely glucose intolerant ($P<0.05$) post HFD compared to WT mice who also demonstrated glucose intolerance ($P<0.05$) compared to the pre-HFD values. Surprisingly, the insulin tolerance test responses were not different between KO and WT mice post HFD suggesting that KO mice did not develop greater whole body insulin resistance despite being more obese than WT mice. Blood serum analysis showed that non-esterified fatty acids (NEFA) and LDL cholesterol levels were also increased more ($P<0.05$) in KO mice compared to the WT mice post HFD. Overall, it is concluded that SLNs impact on Ca^{2+} handling influences not only ATP consumption by SERCA pumps in resting soleus muscle via uncoupling of ATP hydrolysis from SR Ca^{2+} uptake but also blunts the negative effect of high fat feeding by increasing resistance to diet-induced obesity and glucose intolerance in mice through mechanisms which are currently unidentified.

.

ACKNOWLEDGEMENTS

First and foremost I must thank my wife, Robina, for the acceptance and support she has given me as a forty year old student with a young family.

I would also like to acknowledge my supervisor, Dr. A Russell Tupling for giving/pushing this project on me, over much discussion and beers many ideas came to light concerning the role of this small protein in skeletal muscle. These discussions laid the foundation for the laboratory work/experiments and the final product, this thesis. As a mentor, Dr. Tupling gave me the needed insight into amalgamating large quantities of data into an efficient and concise document.

The work of Ryan Sayer, Sarah Norris and Chris Vigna from Dr. Tupling's laboratory cannot be ignored as this thesis often felt more like a team effort than an individual endeavor. Marg Burnett must also be mentioned as she helped perform the catecholamine analysis in Chapter 3, as well as many other administrative duties allowing for a smooth functioning laboratory.

The donation of *Sln*-null mice by Dr. Muthu Periasamy at Ohio State University was also greatly appreciated as it allowed for the creation of a breeding colony at the University of Waterloo. Dr. Periasamy and Subash Gupta from Ohio State University should also be recognized for the work they performed on some of the Western blotting analysis. Finally I must thank my parents, Michel and Francine Bombardier, for providing not only financial support, but also for encouraging me to start, continue and ultimately finish this journey called a PhD degree.

DEDICATION

This thesis is dedicated to my hot and beautiful wife, Robina, and our two darling daughters, Kyra and Kayla. Through the past five years, the trials and tribulation of raising a young family has often kept me ground during stagnant and unproductive periods in the laboratory.

TABLE OF CONTENTS

LIST OF TABLES

LIST OF FIGURES

LIST OF ABBREVIATIONS

ADP – adenosine diphosphate

Akt – protein kinase B

AMP – adenosine monophosphate

ATP – adenosine triphosphate

BAT – brown adipose tissue

$[Ca^{2+}]_f$ – intracellular free calcium concentration

CAMKII – Ca^{2+}/calmodulin-dependent protein kinase

cAMP – cyclic AMP

CLAMS –comprehensive laboratory animal monitoring system

CPA – cyclopiazonic acid

CSQ – calsequestrin

DHPR – dihydropyrodine receptor

DXA – dual energy X-ray absorptiometry

EDL – extensor digitorum longus muscle

E – epinephrine

HDL – high density lipoprotein

HFD – high fat diet

GLUT 4 – glucose transporter type 4

GT – glucose tolerance

GTT – glucose tolerance test

IRS-1 – insulin receptor substrate 1

IT – insulin tolerance

ITT – insulin tolerance test

L_o – optimum muscle length for maximum twitch force

LDL – low density lipoprotein

NE – Norepinephrine

NEFA – non-esterified fatty acid

PAGE – polyacrylamide gel electrophoresis

pCa^{2+} – negative logarithm of $[Ca^{2+}]_f$

pCa_{50} – $[Ca^{2+}]_f$ required to achieve 50% of V_{max}

PI – phosphatidylinositol

PLN – phospholamban

PKC – protein kinase C

PVDF – polyvinylidene difluoride

RER – respiratory exchange ratio

RG – red gastrocnemius

RYR – ryanodine receptors

SDS - Sodium dodecyl sulfate

SERCA – sarco(endo)plasmic reticulum Ca^{2+} ATPase

SLN – sarcolipin

SOC-3 – suppressor of cytokine signalling-3

SR – sarcoplasmic reticulum

TA – tibialis anterior

TAG – triacylglycerol

UCP-3 – uncoupling protein 3

Vmax – maximal enzyme activity

VO_{2max} – maximal aerobic capacity

VO_2 – oxygen consumption

WG – white gastrocnemius

WT– wild type

CHAPTER I

INTRODUCTION, REVIEW OF THE LITERATURE AND STATEMENT OF THE PROBLEM

INTRODUCTION

Sarcolipin (SLN), a small molecular weight proteolipid found embedded in the sarcoplasmic reticulum (SR) of skeletal muscle, is a known modulator of sarco(endo)plasmic reticulum Ca^{2+}ATPase (SERCA) function (MacLennan et al.,2003; MacLennan and Kranias, 2003; Odermatt et al., 1998; Asahi et al., 2002; Asahi et al., 2003). Through its effects on SERCA activity, SLN is a key modulator of Ca^{2+} transient amplitude and kinetics and muscle relaxation *in vivo* (Tupling et al., 2002; Babu et al., 2005; 2006; 2007a; Ottenheijm et al., 2008). SLN may also play an important role in thermogenesis through the uncoupling of Ca^{2+} uptake from ATP hydrolysis by the SERCA pumps, thereby generating heat. This has been demonstrated previously *in vitro*, where the presence of SLN in reconstituted membrane vesicles containing SERCA resulted in uncoupled ATP hydrolysis (Smith et al., 2002) and increases in the amount of heat released per mol of ATP hydrolyzed (Mall et al., 2006). This suggests that alterations of SLN levels within skeletal muscle will influence SERCA efficiency and ultimately metabolism. The studies in the current thesis will examine the physiological role of SLN in skeletal muscle and whole body metabolism through the use of a *Sln*-null transgenic mouse model. Secondly, susceptibility to diet-induced obesity and glucose intolerance will be investigated in the *Sln*-null mouse model.

Ca^{2+} signaling and excitation-contraction coupling

Calcium is essential for living organisms, playing a pivotal role in cell physiology where its movement between cellular compartments (i.e. endoplasmic reticulum to cytoplasm) serves as a signal for various cellular processes. Intracellular Ca^{2+} is involved in signal transduction pathways in a variety of tissues including neurotransmitter release from neurons,

insulin release from β-cells in the pancreas and in reproduction (Vander et al., 1990; Henquin, 2009). Extracellular Ca^{2+} is important in maintaining potential difference across excitable cell membranes as well as bone formation (Vander et al., 1990). Ca^{2+} is a dominant signaling and regulatory molecule in skeletal muscle which is important not only for excitation-contraction coupling but it also plays a significant role in energy expenditure, second messenger signaling, activation of transcription factors and apoptosis (Berchtold et al., 2000). In all muscle cells, the SR is the major organelle responsible for regulating the concentration of intracellular free Ca^{2+} ($[Ca^{2+}]_f$).

Excitation-contraction coupling and relaxation in skeletal muscle consists of a series of inter-related processes involving the 3 major energy consuming processes. Stimulation of the motor end plate by the chemical transmitter, acetylcholine, results in depolarization (influx of Na^+ through voltage gated ion channels) that spreads along the sarcolemma and down into the transverse-tubules (t-tubules). Membrane repolarization is rapid due to opening of the K^+ channels and the efflux of K^+ out of the cell. Propagation of the resulting action potential into the t-tubules activates the voltage sensitive dihydropyrodine receptors (DHPRs) found in the t-tubules causing them to undergo conformational changes which ultimately triggers the opening of the ryanodine receptors (RyRs) in the SR. The ensuing Ca^{2+} efflux out of the SR binds to troponin C, removing the inhibitory actions of tropomyosin on actin and allows for the activation of actomyosin ATPase and formation of strong binding cross bridges, ultimately leading to muscle contraction and force production. Termination of the action potential and accompanying closure of RYR, together with the activation of SERCA pumps due to elevated $[Ca^{2+}]_f$ results in the removal of cytosolic Ca^{2+} back into the SR and relaxation of the muscle. Restoration of Na^+ and K^+ gradients must follow each action potential to protect membrane

excitability. This is accomplished by the Na^+/K^+ ATPase pumps which uses the energy from the hydrolysis of 1 ATP to transport 3 Na^+ out of the cell and 2 K^+ into the cell.

In resting muscle, $[Ca^{2+}]_f$ is regulated predominately by the activity of the SERCA pumps. SERCA pumps are 95-110-kDa integral membrane proteins consisting of 10 trans-membrane helices (M1-M10) and three cytoplasmic domains (actuator, nucleotide binding and phosphorylation; Toyoshima et al., 2000; Figure 1.1). These highly conserved P-type ATPase pumps are found in all tissues and are responsible for Ca^{2+} regulation. In rodents and humans, SERCA pumps are encoded by three different genes (ATP2A1-3) giving rise to three major isoforms, SERCA1, SERCA2 and SERCA3 (Lytton et al., 1992; Wu and Lyttton, 1993). The two predominant SERCA isoforms found in adult skeletal muscle are SERCA1a and SERCA2a which are highly conserved with 84% of the amino acid sequence being identical. The SERCA1a isoform consists of 1001 amino acids and is expressed predominately in adult fast twitch skeletal muscle whereas SERCA2a is made up of 997 amino acids and is highly expressed in heart and slow twitch skeletal muscle (Wu and Lytton, 1993). Fast and slow twitch skeletal muscles are also known to have different SR Ca^{2+} leak rates and SERCA coupling ratios (Ca^{2+} transported per ATP hydrolyzed), which translates into differences in SERCA pump efficiency and heat production/energy utilization (Reis et al., 2002 Reis et al., 2001; Murphy et al., 2009). Specifically, fast twitch muscles have a higher density of SERCA pumps and lower $[Ca^{2+}]_f$ within the SR due to a higher volume of SR and concentration of calsequestrin (CSQ) when compared to slow twitch muscle (Murphy et al., 2009). The high density of SERCA pumps likely accounts for the higher Ca^{2+} leak rates found in fast twitch muscle as the SERCA pumps themselves appear to be the major pathway for leakage of Ca^{2+} out of the SR (Inesi and deMeis, 1989; Murphy et al., 2009). The higher rate

of Ca^{2+} leak from the SR in fast twitch muscle could account for the lower coupling ratio and hence greater heat production in fast muscle compared to slow muscle (Reis et al., 2002), due to increased ATP hydrolysis by SERCA pumps.

Coupling ratio and reaction cycle

Expanding upon the previous definition, the SERCA coupling ratio refers to the amount of Ca^{2+} transported into the lumen of the SR from the cytoplasm per ATP hydrolyzed. A coupling ratio of 2 Ca^{2+}:1 ATP is considered to be optimal as it corresponds to the stoichiometry of two Ca^{2+} binding sites and one ATP binding site on each Ca^{2+} pump subunit (Smith et al., 2002; Inesi et al., 1978; de Meis, 2001a; MacLennan et al., 1997; Toyoshima and Inesi, 2004). With the recent improvement in resolution of the SERCA crystal structure in different conformations as determined by X-ray crystallography, detailed mechanisms for Ca^{2+} transport into the SR can be inferred (Toyoshima and Inesi, 2004; Toyoshima et al., 2000; Toyoshima et al., 2003; Toyoshima and Nomura, 2004). Assuming optimal stoichiometry, the reaction cycle of SERCA would proceed as shown in Figure 1.2 (reactions 1 – 6). The cycle begins with 2 Ca^{2+} ions from the cytoplasm binding with high affinity to the Ca^{2+} binding pocket formed by four (M4, M5, M6 and M8) of the 10 transmembrane helices found in the transmembrane domain in the E_1 conformation of the Ca^{2+}-ATPase pump (Lee, 2002). ATP then binds to the nucleotide binding domain and is hydrolyzed, forming a high energy phospho-protein intermediate (reactions 1 – 2). Upon the phosphorylation of SERCA, conformational change in the cytoplasmic/transmembrane domain occurs via alterations in the stalk domain so the 2 Ca^{2+} binding sites change to a state of low Ca^{2+} binding affinity and face the lumen, causing the Ca^{2+} ions to be released into the lumen of the SR (reactions 3 – 4).

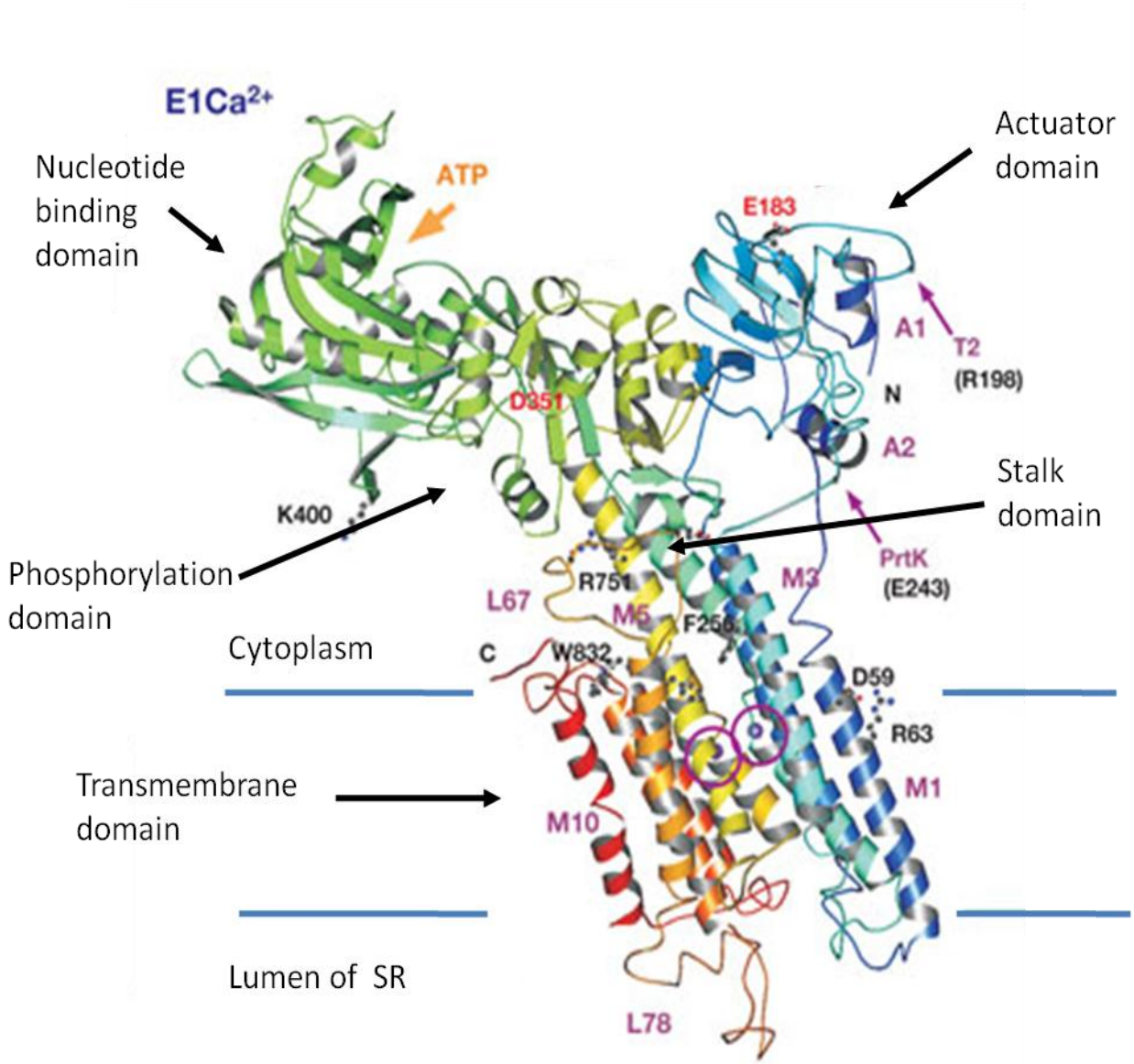

Figure 1.1: Ribbon schematic showing the crystal structure of rabbit skeletal muscle SERCA1a. Colours change gradually from the amino terminus (blue) to the carboxy terminus (red). Two purple spheres (circled) in $E1Ca^{2+}$ represent bound Ca^{2+}. The cytoplasmic portion is composed of three interacting domains: the nucleotide binding domain, phosphorylation domain and the actuator domain. SERCA pumps also possess a transmembrane domain consisting of 10 helical transmembrane segments, including the 2 Ca^{2+} binding sites, which are link to the cytoplasmic domains via the stalk domain. Adapted from Toyoshima and Nomura 2004, originally published by Toyoshima et al., 2000.

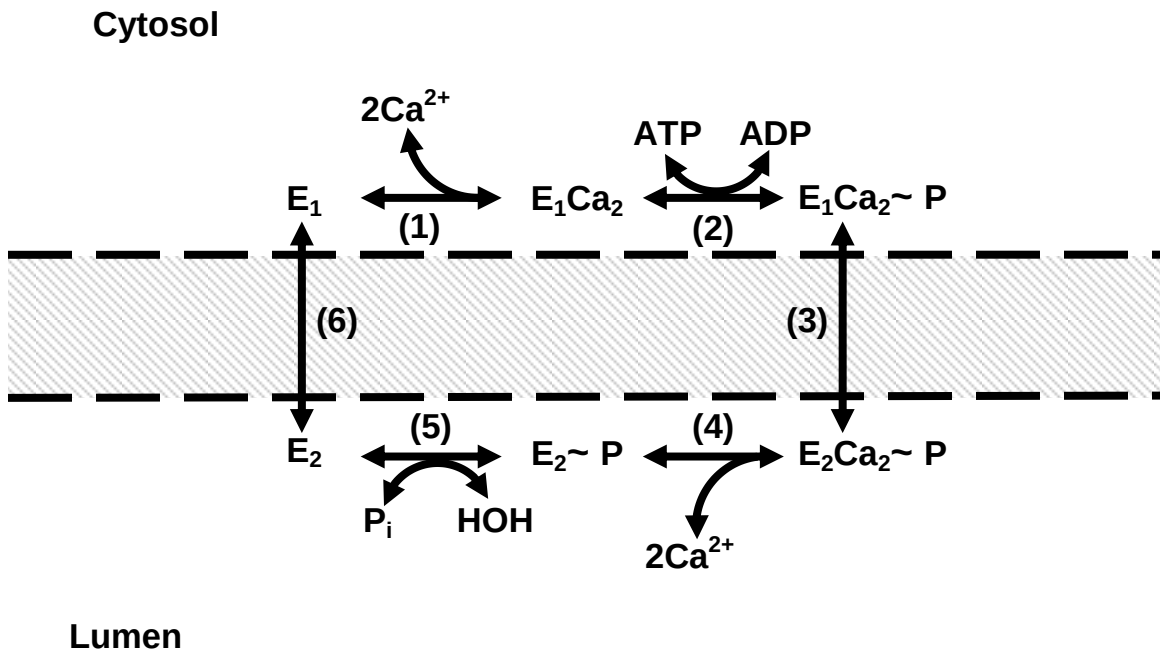

Figure 1.2: Schematic of the partial reactions of the catalytic and transport cycle of the SR Ca^{2+} pump showing coupled Ca^{2+} transport reactions (1-6 forward) in the absence of a Ca^{2+} gradient. Under these leaky conditions, reaction 4 is irreversible forcing the sequence to flow forward to reaction 6. The sequence includes two distinct enzyme conformations, E_1 and E_2. (Figure redrawn from Inesi, 1985; de Meis and Vianna, 1979)

Dephosphorylation then allows for the recycling of SERCA from the E_2 conformation back to the E_1 conformation (reactions 5 – 6).

Under physiological conditions where a Ca^{2+} gradient across the SR membrane is present, due to high lumenal [Ca^{2+}] within the SR (millimolar; Rasmussen, 1986), the coupling ratio of 2 Ca^{2+} transported for every ATP hydrolyzed is greatly diminished. Previous *in vitro* studies with rabbit fast and slow twitch hindlimb muscle SR vesicles showed that the coupling ratio of Ca^{2+} transported/ATP hydrolyzed varies between 0.3 and 0.6 for fast twitch, and up to 1.0 for slow twitch muscle, in the presence of a Ca^{2+} gradient (de Meis, 2001b; Reis et al., 2001; McWhirter et al., 1987; Reis et al., 2002). A number of experimental procedures and conditions including altered ADP/ATP ratio, $[Ca^{2+}]_f$, hyperthyroidism and sarcolipin also cause

a reduction in the SERCA coupling ratio through changes in the reaction cycle of the Ca^{2+} pump (Smith et al., 2002; Mall et al., 2006; Reis et al., 2002; Inesi and de Meis , 1989; de Meis, 1998; de Meis 2000; Arruda et al., 2003).

A reduction in the coupling ratio of SERCA pumps (i.e. <2 Ca^{2+}:1 ATP) can arise from three potential sources. The first is through passive Ca^{2+} efflux by the Ca^{2+} pump which occurs when a high Ca^{2+} concentration in the lumen of the SR promotes the binding of Ca^{2+} to the E_2 conformation of the enzyme prior to conversion back to E_1 which is called uncoupled Ca^{2+} efflux or passive leak (Mall et al., 2006; Inesi and de Meis, 1989; Berman, 2001; de Meis, 2001a; reactions 7 – 9 in Figure 1.3). Secondly, a high Ca^{2+} concentration in the lumen of the SR will slow down the forward conformational reaction between E_1Ca_2~P and E_2Ca_2~P (reaction 3 in Figure 1.3), increasing the number of Ca^{2+}ATPase pumps found in the E_1Ca_2~P conformation and promoting cleavage of Pi prior to Ca^{2+} translocation (i.e. uncoupled ATPase activity) (Yu and Inesi, 1995; Bermen, 2001; de Meis, 2001a; reaction 10 in Figure 1.3). Lastly, the premature release of the Ca^{2+} ions to the cytoplasmic side of the SR rather than to the lumenal side during the conformational change between E_1Ca_2~P and E_2Ca_2~P (reaction 3 in Figure 1.3) is called slippage (Smith et al., 2002; Mall et al., 2006; Berman, 2001; reaction 11 in Figure 1.3). Slippage is believed to result from a decrease in Ca^{2+} affinity of the E_1Ca_2~P state as a consequence of high lumenal Ca^{2+} and/or the presence of SERCA regulatory proteins such as SLN and phospholamban (PLN), which physically interact with helices M2, M4, M6 and M9 of the transmembrane domain of the Ca^{2+} ATPase pumps (Morita et al., 2008; Bhupathy et al., 2007; Odermatt et al., 1998). Two of these helices (M4 and M6) make up part of the Ca^{2+} binding pocket, so the physical presence of SLN or PLN in this area could alter Ca^{2+} binding affinity, thereby resulting in the early release of Ca^{2+} back into the cytosol.

Although these three reactions of uncoupled ATP hydrolysis are different, the net result is that a higher fraction of the total chemical energy derived from ATP hydrolysis is converted into heat as opposed to osmotic energy (ie. Ca^{2+} transported into the SR) (Mall et al., 2006; Reis et al., 2002; de Meis, 1998; de Meis 2000; de Meis , 2002).

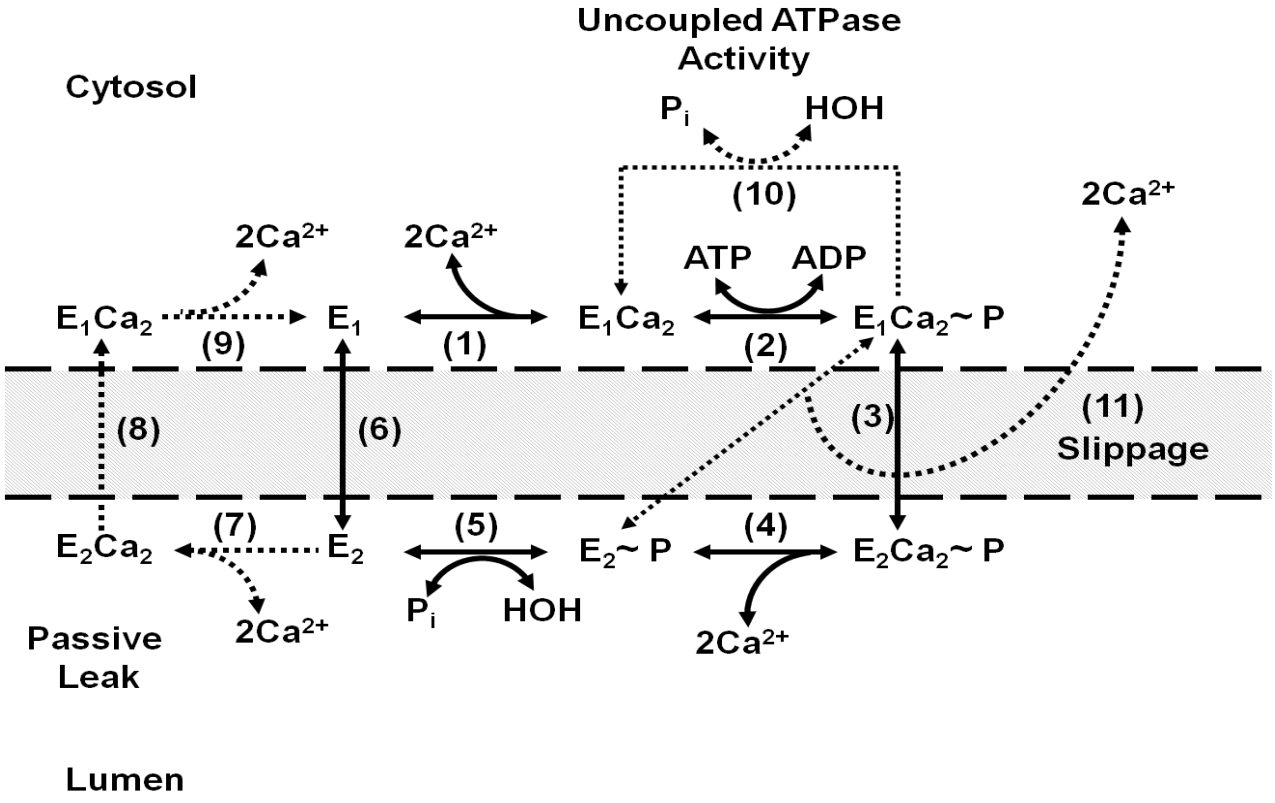

Figure 1.3. Schematic of the partial reactions of the catalytic and transport cycle of the SR Ca^{2+} pump showing coupled Ca^{2+} transport reactions (1-6 forward), passive leak reactions (7-9), uncoupled ATPase activity (reaction 10) and slippage (reaction 11). (Figure redrawn from de Meis, 2001 and Mall et al., 2006)

SERCA Regulatory proteins: SLN and PLN

SERCA pump activity is highly regulated through gene transcription and by protein-protein interactions with small hydrophobic regulatory proteins, namely SLN and PLN (Vangheluwe et al., 2005a). In the heart, SERCA2a associates with PLN, a 52 amino acid transmembrane protein, resulting in a lower apparent Ca^{2+} affinity for the PLN-SERCA2a complex (Simmerman and Jones,1998). The inhibited complex can be disrupted by phosphorylation of PLN or elevation of cytosolic Ca^{2+}, leading to the reversal of SERCA2a inhibition (Simmerman and Jones,1998). SLN, a 31 amino acid protein, shows significant sequence identity and gene structure to PLN (Wawrzynow et al., 1992; Odermatt et al., 1997) and, like PLN, is an effective inhibitor of SERCA molecules (Odermatt et al., 1998; Asahi et al., 2002; Asahi et al., 2003). Sequencing of SLN revealed a 7-residue hydrophilic N-terminal domain, a 19-residue hydrophobic trans-membrane α-helical domain and a 5-residue hydrophilic C-terminal domain (Wawrzynow et al., 1992; MacLennan et al., 2002). It was originally identified as a proteolipid that co-purified with SERCA1a in rabbit fast twitch skeletal muscle (MacLennan et al., 1972; 1974). Subsequently, SLN was found to be highly expressed in both human and rabbit fast twitch skeletal muscle and to a lesser extent in slow twitch and cardiac muscle based on mRNA levels (Odermatt et al., 1997). Recently, SLN-specific antibodies have been developed and used to determine the tissue-specific distribution pattern of SLN protein expression in different species (Vangheluwe et al., 2005a; Babu et al., 2007b). In small mammals (i.e. mouse and rat) it was found that SLN was highly expressed in tongue, diaphragm, soleus and atria but not ventricle whereas in large mammals (i.e. rabbit and dog) SLN was abundant in all skeletal muscles examined and atria but not ventricle. PLN is a well characterized regulator of the SR Ca^{2+} pumps in cardiac muscle (Simmerman and

Jones,1998) and is a major modulator of cardiac contractility, which became clear through functional analysis of *Pln*-null (Luo, 1994) and over-expression of superinhibitory monomeric and pentameric PLN mutant hearts (Zhai et al., 2000; Zvaritch et al., 2000). Overexpression of PLN decreases the apparent Ca^{2+} affinity of SERCA2a, negatively influences the kinetics of the Ca^{2+} transient and hence contractility resulting in impaired ventricular systolic function *in vivo* (Kadambi et al., 1996). Accordingly, PLN ablation increases left ventricular contractility and systolic function (Luo et al., 1994).

The physiological role of SLN is less understood. SLN was originally co-purified with SERCA over thirty years ago, however only recently has the function of this proteolipid been investigated in cardiac muscle and to a much lesser degree in skeletal muscle. Work by both the MacLennan (Gramolini et al., 2006) and Periasamy (Babu et al., 2005) groups has shown that overexpression of SLN in cardiac muscle causes a decreased Ca^{2+} affinity of SERCA pumps and reduces Ca^{2+} trasnsient amplitude and kinetics resulting in decreased myocyte contractility. The role of SLN in cardiac physiology was recently investigated in knockout mice (Babu et al., 2007a), which established SLN as a key regulator of SERCA2a in the atria. Importantly ablation of *SLN* enhances SR Ca^{2+} transport and atrial contractility (Babu et al., 2007a).

In skeletal muscle, Tupling et al. (2002) assessed the physiological function of SLN, using intramuscular injection and electro-transfer of plasmid cDNA to over-express NF-SLN (SLN tagged N-terminally with a FLAG epitope) in rat soleus. It was found that NF-SLN reduced maximal Ca^{2+} transport activity in post-nuclear homogenates by 31% and reduced maximal tetanic force and rates of contraction and relaxation (Tupling et al., 2002). It has since been shown that slowing of SR Ca^{2+} uptake and speed of relaxation in both slow and fast

twitch skeletal muscle from nebulin knockout mice is associated with profound up-regulation of SLN protein (>20-fold) (Ottenheijm et al., 2008). Most recently, Tupling et al. (2008) examined the effects of SLN ablation on SERCA function in skeletal muscle and skeletal muscle contractility. They found increased oxalate-dependent Ca^{2+} uptake activity in the soleus and mixed gastrocnemius but not in EDL of *Sln*-null mice compared with wild type which was accompanied by faster rates of relaxation of soleus muscle in the *Sln*-null mice (Figure 1.4A; Tupling et al., 2008). Repeated tetanic stimulation of the soleus muscle revealed an increase in relaxation rate at the last tetanus (10^{th}) in wild type (WT) mice but not in the *Sln*-null mice suggesting that the inhibitory effect of SLN is relieved upon repeated tetanic stimulation (Figure 1.4B). This is supported by recent evidence showing phosphorylation of threonine-5 on the cytosolic tail of SLN by Ca^{2+}/calmodulin dependent protein kinase II (CAMKII) is a key mechanism in the regulation of SLN in cardiac myocytes (Bhupathy et al., 2009). Thus, SLN has been established as a key modulator of SERCA pump function and skeletal muscle relaxation *in vivo*; however, conceptually it is unclear how expression of a SERCA pump inhibitor might be beneficial for skeletal muscle contractile performance which led us to question the physiological role of SLN in skeletal muscle.

Reconstitution experiments in artificial membranes have shown that SLN uncouples ATP hydrolysis from Ca^{2+} transport by the SR Ca^{2+} pump (Smith et al., 2002) and increases the amount of heat released per mol of ATP hydrolyzed (Mall et al., 2006). A potential explanation for these results could be that SLN causes an increased rate of slippage on the Ca^{2+} pumps (Figure 1.3, reaction 11; Smith et al., 2002; Mall et al., 2006) thereby decreasing the fraction of energy released during ATP hydrolysis that is converted into osmotic energy (Ca^{2+} transport) and increasing the amount of heat released (de Meis, 2001b; de Meis, 2002). It has

been suggested that SLN could have an important role in thermogenesis (Smith et al., 2002; Mall et al., 2006), ultimately affecting cellular energy balance and metabolic rate. In these reconstitution experiments, SLN was shown to have no effect on Ca^{2+} ATPase activity even with un-physiologically high SLN concentrations (Smith et al., 2002; Mall et al., 2006); however, SLN did decrease Ca^{2+} uptake into reconstituted vesicles at a molar ratio of SLN:SERCA as low as 2:1 (Smith et al., 2002). This data suggests that alterations in transport efficiency/coupling ratio through genetic manipulation (SLN-knockout) of mice could significantly influence the energy cost of Ca^{2+} handling in skeletal muscle and therefore whole body metabolism. Specifically, *Sln*-null mice should have increased Ca^{2+} pumping efficiency (i.e. less ATP required to achieve a given Ca^{2+} transport rate), a lower whole body metabolic rate and increased susceptibility to obesity and type II diabetes.

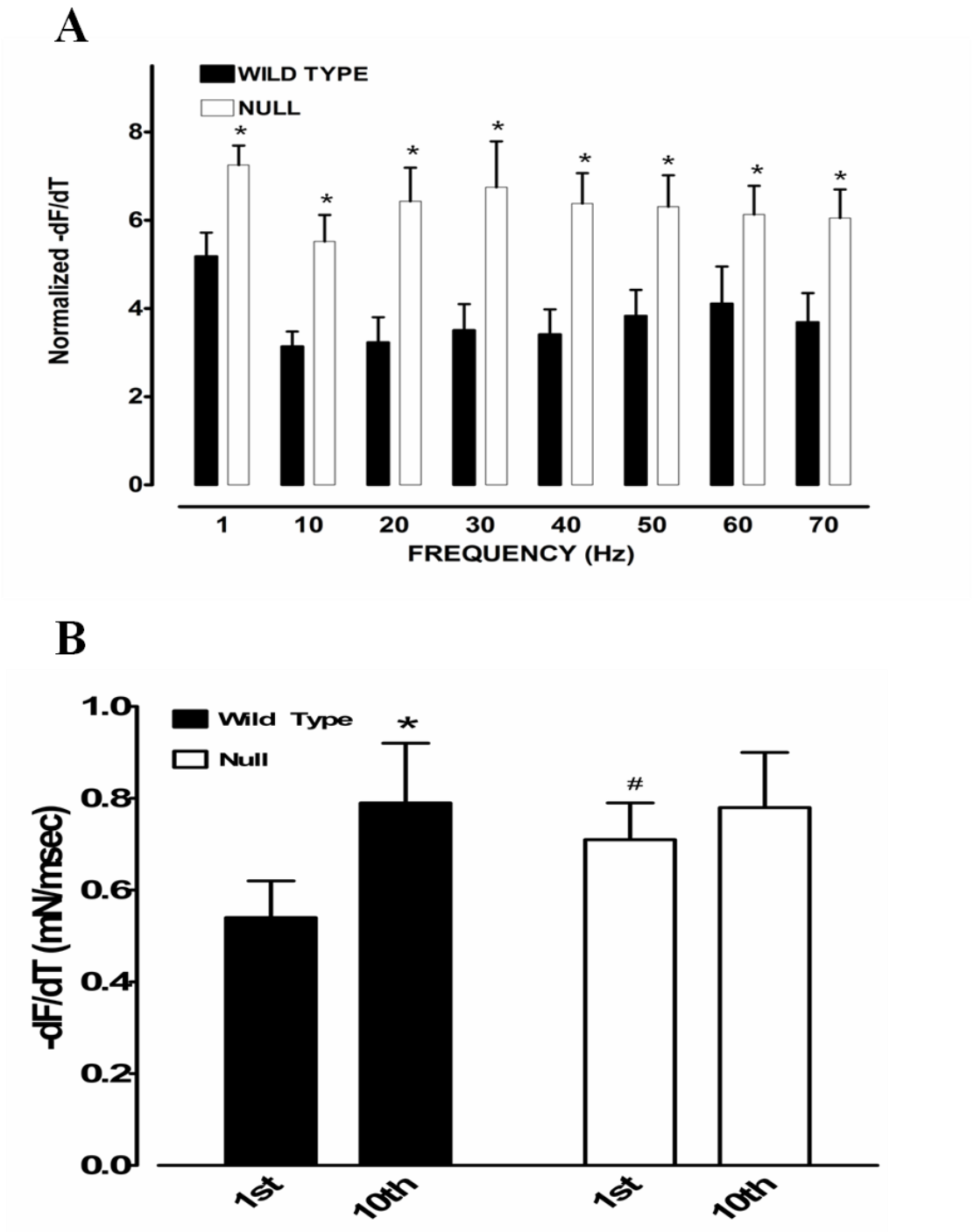

Figure 1.4 (A) Relaxation rates (-dF/dT) from force frequency experiments on isolated soleus muscles from wild type and *Sln*-null mice. * significant, $p<0.05$ versus wild type (B) Soleus muscles from wild type and *Sln*-null mice were electrically stimulated repeatedly using a protocol consisting of 350-ms trains at 70 Hz once every 1 s for a total of 10 contractions and comparisons were made between the 1st and 10th contractions for –dF/dt. * Significant, $p<0.05$ versus 1st contraction. # Significant, $p<0.05$ versus wild type. Taken from Tupling et al., 2008.

Obesity and adaptive thermogenesis

The incidence of obesity in the western industrial world has risen dramatically over the past 30 years and it is believed that it will continue to rise in future decades (Laaksonen et al., 2004). Prevalence data, show that since 1985 the number of Canadians with extreme obesity (body mass index (BMI) > 35 kg/m^2) has increased by more than 500% (Katzmarzyk and Mason, 2006). Obesity is considered a primary risk factor associated with many other life threatening diseases such as cardiovascular disease, hypertension and type II diabetes (Kopelman, 2000; Calle et al., 1999; Must et al., 1999). Obesity results from a chronic imbalance between energy intake (i.e. feeding) and energy expenditure (i.e. metabolic rate).

Adaptive thermogenesis is a mechanism involved in regulating energy expenditure and hence energy balance by increasing heat production during prolonged periods of excess energy intake (i.e. high fat diet; Levine et al., 1999) or cold exposure (Lowell and Spiegelman, 2000). This is believed to occur predominately in the mitochondria of brown adipose tissue (BAT) and skeletal muscle through the uncoupling of protons from the electron transport chain by membrane bound uncoupling proteins (UCPs), resulting in the conversion of osmotic energy into heat (Lowell and Spiegelman, 2000). BAT is highly innervated by the sympathetic nervous system and can be rapidly activated through β-adrenergic-receptor stimulation due to cold exposure and diet (i.e. elevated leptin levels; Haynes et al., 1997). Chronic high fat feeding increases white adipose tissue mass which in turn releases a greater quantity of leptin into the plasma thereby activating the sympathetic nervous system ultimately resulting in BAT activation as well as elevating uncoupling protein 1 (UCP-1) mRNA and protein levels in small rodents (Cusin et al., 1998; Cannon and Nedergard, 2003).

In humans and other large mammals, which possess only a small quantity of BAT, other mechanisms for adaptive thermogenesis are needed for regulating energy metabolism. Uncoupling protein 3 (UCP-3), a homologue of UCP-1, is found predominately in skeletal muscle and has uncoupling activity similar to UCP-1, making it a potential key player in adaptive thermogenesis in skeletal muscle. However studies have demonstrated a lack of response of UCP-3 mRNA to cold exposure in humans (Schrauwen et al., 2002) as well as rodents (Lin et al., 1998). Other potential functions for UCP-3 that have recently emerged include mitochondrial lipid export (Schrauwen et al., 2006), maintenance of glucose homeostasis (Clapham et al., 2000) and decreasing generation of mitochondrial reactive oxygen species (Echtay et al., 2003). Independent of UCP-3 function the resultant transport of protons into the mitochondrial matrix consequently results in the production of heat, thereby increasing skeletal muscle metabolism and potentially affecting metabolic rate (Schrauwen and Hesselink, 2004). Another potential site for adaptive thermogenesis in skeletal muscle would be futile ion (i.e. Ca^{2+}, Na^{+}, K^{+}) cycling giving rise to elevated energy expenditure and heat production (Lowell and Spiegelman, 2000).

Ca^{2+} handling in skeletal muscle has previously been calculated to make up approximately 5% of the basal metabolic rate in skeletal muscle (Clausen et al., 1991) rising up to 20-50% during periods of muscular exertion (i.e. exercise) (Clausen et al., 1991; Homsher,1987; Szentesi et al., 2001). Based on these values, Ca^{2+} handling in skeletal muscle, and more specifically, SERCA pump activity, would account for 7-15% of total daily energy expenditure. However, with the use of calorimetric measurements, Chinet et al. (1992) found that up to 24% of heat produced by resting mouse soleus muscle could be attributed to SERCA activity. These results were confirmed in similar experiments on mouse soleus and EDL

muscles which showed that 18 – 22% of resting energy expenditure in both muscles is related to SR Ca^{2+} uptake (Dulloo *et al.*, 1994). More recently, resting muscle oxygen consumption of isolated soleus and EDL was measured polaragraphically at 30 ºC using the TIOX tissue bath system, where it was discovered through the use of cyclopiazonic acid (CPA), a highly specific SERCA inhibitor (Goeger & Riley, 1989; Seidler *et al.*, 1989), that Ca^{2+} cycling in muscle contributes approximately 50% of basal metabolism in both fast and slow twitch skeletal muscle (Norris et al., 2010). This data would suggest that previous estimates on the cost of Ca^{2+} handling have been largely underestimated. In agreement, Zhang et al. (2006) estimated the energetic cost of Ca^{2+} handling in fast twitch (EDL) skeletal muscle during sub-maximal contraction to be approximately 80% of total energy expenditure. Even with the more conservative estimate of 30-40% of the energy cost associated with muscle contraction coming from ATPase activity of SERCA pumps (for review see Barclay et al., 2007), the SR Ca^{2+} pumps would account for approximately 25% of the total daily energy expenditure.

If chronic excess caloric intake (i.e. through high fat feeding) results in altered Ca^{2+} handling in skeletal muscle such that the energy requirements for Ca^{2+} handling are increased under basal conditions and/or during exercise, then it could be concluded that diet-induced (adaptive) thermogenesis at least partly involves adaptations in skeletal muscle Ca^{2+} handling. Given that SLN appears to be an important regulator of SERCA pump energetics through its effects on the coupling ratio of SERCA pumps (Smith et al., 2002; Mall et al., 2006), diet-induced increases in SLN expression could provide a potential mechanism for adaptive thermogenesis, but this has yet to be investigated.

The ability to influence the metabolic cost of Ca^{2+} handling in skeletal muscle and BAT through genetic manipulation could represent a potential treatment for obesity and its

complications. The use of genetic manipulation to alter metabolism has been previously demonstrated in other transgenic mouse models, specifically by overexpressing the mitochondrial uncoupling proteins (UCPs) in skeletal muscle and BAT resulting in an increase in metabolic rate and resistance to genetic and diet-induced obesity in mice (Li et al., 2000; Kopecky et al., 1995; Clapham et al., 2000; Son et al., 2004). Currently, it is understood that the UCPs and the SERCA pumps in skeletal muscle are two major systems involved in non-shivering thermogenesis (Block, 1994; de Meis, 2001b) and could potentially have important implications in adaptive thermogenesis (Lowell and Spiegelman, 2000). Therefore targeting SERCA and Ca^{2+} handling as a potential site in skeletal muscle and BAT to promote energy "wasting" or inefficient metabolism, while maintaining functional capacity would provide a novel approach in the prevention and/or treatment of obesity. Therefore, mice with varying levels of SLN expression in skeletal muscle and potentially in BAT are ideal for studying the effects of altered Ca^{2+} pump efficiency on metabolic rate and susceptibility to obesity.

STATEMENT OF THE PROBLEM:

The primary objectives for this thesis are: 1) to investigate the role of SLN in skeletal muscle and its influence on SR Ca^{2+} transport efficiency, resting skeletal muscle metabolic rate and resting whole body metabolic rate in mice; 2) to examine the effects of SLN ablation on diet-induced thermogenesis and susceptibility to diet-induced obesity and glucose intolerance.

Study 1:

Transgenic *Sln*-null (KO) mice were used in order to examine the effects of SLN on Ca^{2+} transport efficiency and skeletal muscle and whole body metabolism.

The primary objectives for study 1 were:

1. To determine the expression pattern of SLN in cardiac and different skeletal muscles as well as in BAT.
2. To determine whether SLN ablation results in compensatory changes in the expression of major Ca^{2+} regulatory proteins and/or UCP-3 in skeletal muscle.
3. The determine if SLN reduces the coupling ratio (Ca^{2+} uptake/Ca^{2+}-ATPase activity) of SERCA pumps in both fast (EDL) and slow (soleus) twitch skeletal muscle.
4. To examine the effects of SLN ablation on basal metabolism and the contribution of SERCA pumps to basal metabolism in isolated soleus muscles.
5. To examine the effects of SLN ablation on basal, sub-maximal and maximal whole body energy expenditure.

Study 1 Hypotheses

The specific hypotheses are:

1. SLN will be expressed abundantly in atrium, diaphragm, soleus and BAT whereas little to no SLN will be found in ventricle, EDL or other fast twitch skeletal muscles.
2. SLN ablation will not result in compensatory changes in the expression of any of the major Ca^{2+} regulatory proteins or UCP-3 in skeletal muscle or BAT.
3. The coupling ratio of SERCA pumps (Ca^{2+} transported in to the lumen of the SR per ATP hydrolyzed) in skeletal muscle homogenates will be higher in KO than wild type (WT) mice.
4. Resting metabolic rate (VO_2) of isolated soleus muscles from KO mice will be lower compared with WT mice due to lower energy consumption by SERCA pumps in KO mice.
5. Whole body metabolic rate at rest and during sub-maximal treadmill exercise, but not VO_2max, will be lower in KO mice compared with WT mice.

STUDY 2

To investigate the role of SLN in adaptive thermogenesis and on susceptibility to diet-induced obesity, KO and WT mice were placed on a high fat diet for 8 weeks (HFD; 42% of kcal derived from fat).

The primary objectives for study 2 were:

1. To determine whether KO mice are more susceptible to diet-induced obesity and glucose intolerance than WT mice.

2. To determine if SLN plays a role in adaptive thermogenesis by examining the effects of the HFD on: a) SLN expression in skeletal muscle, b) energy consumption by SERCA pumps and total energy expenditure in resting skeletal muscle and c) resting whole body energy expenditure in both WT and KO mice.
3. To determine whether the HFD results in compensatory changes in other major Ca^{2+} regulatory proteins and/or UCP-3 in either skeletal muscles or BAT in KO and WT mice.

Study 2 Hypotheses

The specific hypotheses are:

1. KO mice fed a HFD will gain more weight, become more obese as indicated by a higher adiposity index, become more glucose and insulin intolerant and display greater hyperglycemia, hyperinsulinemia and dyslipidemia compared to WT mice.
2. Relative whole body metabolic rate will be lower in both KO and WT mice following the HFD; however, WT mice will have a higher metabolic rate compared to KO mice.
3. Basal VO_2 of isolated soleus muscles from both KO and WT mice will be higher following the HFD; however, soleus muscles from WT mice will display a higher metabolic rate compared to soleus muscles from KO mice.
4. The % contribution of SERCA pump activity to basal metabolism in isolated soleus muscles will increase in response to the HFD in WT mice but not in KO mice.
5. There will be no compensatory changes in the expression of any of the major Ca^{2+} regulatory proteins or in UCP-3 in either skeletal muscle or BAT in response to the HFD in either KO or WT mice.

CHAPTER II

EFFECTS OF SARCOLIPIN ABLATION ON CALCUIM HANDLING AND SKELETAL MUSCLE AND WHOLE BODY METABOLISM

OVERVIEW

Earlier *in vitro* reconstitution experiments have shown that sarcolipin (SLN) uncouples ATP hydrolysis from Ca^{2+} transport by the sarco(endo)plasmic reticulum Ca^{2+} ATPase (SERCA) and increases the amount of heat released per mol of ATP hydrolyzed by inducing an increased rate of "slippage" during the reaction cycle of SERCA pumps. In this study, we compared skeletal muscle Ca^{2+} ATPase activity and Ca^{2+} uptake in homogenates from fast (extensor digitorum longus; EDL) and slow (soleus) twitch muscle of wild-type (WT) and *Sln*-null (KO) mice under conditions in which a Ca^{2+} gradient was preserved across the sarcoplasmic reticulum (SR) vesicles in order to determine whether SLN causes slippage of SERCA activity by uncoupling ATP hydrolysis from Ca^{2+} transport under more physiological conditions. Western blotting analysis revealed SLN to be present in soleus muscle and to a much lesser extent in the EDL of WT mice. SLN protein expression in WT mice was also abundant in atrium, diaphragm, red gastrocnemius and tibialis anterior and was absent from ventricle, white gastrocnemius, quadriceps and brown adipose tissue (BAT). SERCA activity measured without ionophore A23187 (presence of a Ca^{2+} gradient) was ~15-25% lower ($P<0.05$) in soleus muscle of KO mice compared with WT which is consistent with the idea that SLN increases "slippage" and thus reduces the extent of back-inhibition on the SERCA pumps. Ca^{2+} uptake, measured in homogenates of soleus and EDL in the presence of a Ca^{2+} gradient was not different ($p>0.05$) in SR vesicles from WT and KO mice, indicating that the calculated Ca^{2+} transport efficiency (Ca^{2+}uptake/Ca^{2+}-ATPase activity) in the presence of a Ca^{2+} gradient in the soleus was higher by 19% ($P<0.04$) in KO mice, while there were no differences between KO and WT mice for EDL. Resting, sub-maximal and maximal whole body metabolic rates, as well as basal oxygen consumption (VO_2) of isolated soleus muscle

and the contribution of energy utilized by SERCA under basal conditions were also assessed in both WT and KO mice. Resting, sub-maximal and maximal whole body metabolic rate, food consumption and cage activity levels were not different between KO and WT mice. Similarly, basal VO_2 was not lower in the isolated soleus of KO mice, but the contribution of energy utilized by SERCA pumps was 6.8% lower ($P<0.0003$) in the KO mice soleus. It was also found that uncoupling protein 3 (UCP-3) was expressed at a higher ($P<0.03$) concentration in soleus muscle of KO compared to WT mice. Thus UCP-3 could, potentially, provide compensation, resulting in higher basal VO_2 in KO mice than expected. These data show that at a physiological SLN:SERCA ratio, SLN uncouples ATP hydrolysis from SR Ca^{2+} uptake in skeletal muscle resulting in a lower contribution of Ca^{2+} handling to basal VO_2. Therefore it is construed that SLN is a key regulator of ATP utilization in Ca^{2+} handling and hence energy metabolism in skeletal muscle.

INTRODUCTION

Muscle contraction and relaxation are energy-dependent processes that are regulated by Ca^{2+}. In all muscle cells, the sarcoplasmic reticulum (SR) is the major organelle responsible for the regulation of intracellular free calcium ($[Ca^{2+}]_f$). Under basal conditions in skeletal muscle, the sarco(endo)plasmic reticulum Ca^{2+}-ATPase (SERCA) pumps are responsible for maintaining a $>10^4$-fold Ca^{2+} concentration gradient across the SR membrane and for keeping $[Ca^{2+}]_f$ below 100 nM (Toyoshima, 2008)). In working muscle, SERCA pumps must rapidly pump large Ca^{2+} loads from the cytoplasm into the lumen of the SR, thereby inducing muscle relaxation and restoring SR Ca^{2+} stores that are utilized in the next contraction cycle. SERCA pumps require energy in the form of ATP to pump Ca^{2+} from the cytosol into the SR. It is well established that the ATPase activity of SERCA pumps contributes 30-40% of the energy cost associated with muscle contraction (for review see Barclay et al., 2007). It was recently established that ATP consumption by SERCA pumps is responsible for ~50% of the resting metabolic rate in both mouse fast (extensor digitorum longus; EDL) and slow twitch (soleus) skeletal muscles (Norris et al., 2010).

Under optimized states, SERCA pumps transport 2 mol of Ca^{2+} across the SR membrane by hydrolysis of 1 mol of ATP (see forward reactions 1 – 6, Fig. 1.2) (Inesi et al., 1978; de Meis, 2001a; Smith et al., 2002). However, a number of experimental procedures and conditions have been shown to lead to partial uncoupling of Ca^{2+} transport from ATP hydrolysis through changes in the reaction cycle of the SERCA pump (Smith et al., 2002; Mall et al., 2006; Reis et al., 2002; Inesi and de Meis, 1989; de Meis, 1998; de Meis 2000; Arruda et al., 2003). For example, passive Ca^{2+} efflux by the pump occurs when a high Ca^{2+} concentration in the lumen of the SR promotes binding of Ca^{2+} to the E_2 form of the enzyme,

leading to its conversion back to E_1 (reactions 7 – 9, Fig. 1.3) (Mall et al., 2006; Inesi and de Meis, 1989; Berman, 2001; de Meis, 2001a). A high Ca^{2+} concentration in the lumen of the SR can also increase the steady state level of E_1Ca_2~P, which promotes cleavage of Pi prior to Ca^{2+} translocation (*i.e.* uncoupled ATPase activity) (reaction 10, Fig. 1.3) (Yu and Inesi, 1995; Bermen, 2001; de Meis, 2001a). Finally, slippage is a process that is defined by the reaction whereby E_1Ca_2~P releases 1-2 Ca^{2+} ions to the cytoplasmic side of the membrane rather than to the lumenal side (reaction 11, Fig. 1.3) (Smith et al., 2002; Mall et al., 2006; Berman, 2001). Although the reactions of uncoupled ATP hydrolysis vary, the net result is the same: ultimately most of the energy derived from ATP hydrolysis is converted into heat (Mall et al., 2006; Reis et al., 2002; de Meis, 1998; de Meis 2000; de Meis , 2002).

Sarcolipin (SLN) is a 31 amino acid protein that regulates the activity of SERCA pumps in skeletal muscle (MacLennan et al., 2003). *In vitro* reconstitution experiments in SR vesicles by the Lee and East group have demonstrated that SLN not only uncouples ATP hydrolysis from Ca^{2+} transport by the SR Ca^{2+} pump (Smith et al., 2002) but also increases the amount of heat released per mol of ATP hydrolyzed (Mall et al., 2006). It was proposed that SLN induces an increased rate of slippage by the Ca^{2+} pump (Figure 1.3, reaction 11), thereby decreasing the fraction of energy released during ATP hydrolysis that is converted into osmotic energy (Ca^{2+} transported into the SR) and hence increasing the amount of heat released (de Meis, 2001; de Meis, 2002). These authors have suggested that SLN could have an important role in thermogenesis (Smith et al., 2002; Mall et al., 2006), which would ultimately affect cellular energy expenditure and metabolic rate but this has not been examined in systems more closely approximating the *in vivo* state.

In this study, a *Sln*-null (KO) mouse model was employed to characterize the metabolic function of SLN**.** Because SLN has been shown to uncouple Ca^{2+} transport from ATP hydrolysis by the SR Ca^{2+} pumps, it was postulated that the soleus muscle from KO mice would have a higher coupling ratio (Ca^{2+} transported into lumen per ATP hydrolyzed) compared with littermate wild type (WT) mice. It was further hypothesized that isolated soleus from KO mice would have a lower basal oxygen consumption (VO_2) resulting in lower basal whole body metabolism when compared to WT mice. Spectrophotometric and spectrofluorometeric assays were utilized to determine Ca^{2+} dependent Ca^{2+}-ATPase activity and Ca^{2+}uptake in the presence of a Ca^{2+} gradient, respectively, allowing for the assessment of the SERCA coupling ratio under more physiological conditions. Polaragraphic measurements of VO_2 from isolated soleus muscle at 30 ºC using the TIOX tissue bath system and measurements of basal metabolism by the Comprehensive Lab Animal Monitoring System (CLAMS) were also used to investigate these hypotheses.

METHODS

Sln-null (KO) mice

Transgenic mice, *Sln*-null, donated by Dr. Muthu Periasamy, Ohio State University, were utilized to establish a continuous breeding colony at the University of Waterloo. Breeding of the heterozygous *Sln*-null mice produced wild type (+/+; WT), heterozygous (+/-) and homozygous (-/-; KO) mice. At 3-4 weeks of age all mice were ear notched and tagged. Genotyping was then performed on the DNA extracted from ear notches using a pureLink Genomic DNA mini kit (Invitrogen, Carlsbad, CA). RT-PCR was then performed to amplify the DNA of interest. Briefly, approximately 50 ng of DNA was added to a Taq DNA

polymerase mix (Fermentas, Canada) containing 3mM $MgCl_2$, 200 µM dNTP, 0.625 units of Taq DNA polymerase and 0.4 µM each of the appropriate 5' and 3' primers for both WT and SLN-null (SLN-WT, forward, 5'-TGT CCT CAT CAC CGT TCT CCT-3'and reverse 5'-GCT GGA GCA TCT TGG CTA ATC-3'; SLN-null, Forward, 5'- GTG GCC AGA GCT TTC CAA TA-3'and reverse 5'-CAA AAC CAA ATT AAG GGC CA-3'). Samples were placed in a thermal cycler (MJ MINI, Bio-Rad, Canada) and denatured for 3 min at 94°C followed by 30 cycles of denaturation for 30 sec at 94°C, annealing for 30 sec at 54°C, and extension for 60 sec at 72°C, followed by a final extension at 72°C for 7 min. The amplified products were then separated on a 1% agrose gel containing 0.01% ethidium bromide (BioShop, Canada) and identified using a bio-imaging system and densitometric analysis performed using the GeneSnap software (Syngene, Frederick, MD).

Once the animals had been genotyped, the WT and KO mice were separated into individual cages. Animals were housed in an environmentally controlled room with a standard 12:12 light/dark cycle and allowed access to food (Tekland 22/5 Rodent Diet, Harland-Tekland, Madison, WI) and water *ad libitum.* The study was approved by the Animal Care Committee at the University of Waterloo and all procedures were performed in accordance with the Canadian Council on Animal Care.

Muscle homogenate

Cardiac muscle (ventricle and atrium) and skeletal muscle (soleus, EDL, quadriceps, tibialis anterior, diaphragm, red and white gastrocnemius) and brown adipose tissue (BAT) from three WT mice were diluted 10:1 (vol/wt) in ice cold PMSF buffer (250mM sucrose, 5 mM HEPES, 10mM NaN_3 and 0.2 mM phenylmethanesulfonyl fluoride, pH 7.5) and

homogenized using a hand held polytron homogenizer and frozen immediately in liquid nitrogen and stored at –80 °C (Tupling et al., 2001; Tupling and Green, 2002; Tupling et al., 2004). These homogenates were used to examine the tissue distribution of endogenous SLN using Western blotting analysis. This experiment was repeated on 2 separate occasions with equivalent results.

A total of 15 WT and 15 KO mice were sacrificed and the soleus and EDL from 3 animals were pooled (n=5) and homogenized in PMSF buffer as previously described. These homogenates were then used for assessment of SR Ca^{2+}-ATPase activity and Ca^{2+} uptake and for Western blotting analysis. BAT and white gastrocnemius were also excised and homogenized in PMSF buffer from these WT and KO mice to determine SR protein (SLN, SERCA1a, SERCA2a, PLN and calsequestrin (CSQ)) content using Western blotting analysis. Total protein concentration of the homogenates was measured by the method of Lowry, as modified by Schacterle and Pollock (Schacterle & Pollock, 1973).

SDS-PAGE and Western blotting

Endogenous SLN content was detected in cardiac tissue (ventricle and atrium), skeletal muscles (soleus, EDL, quadriceps, tibalis anterior, diaphragm, red and white gastrocnemius) and BAT to determine SLN distribution in WT mice. Skeletal muscle (soleus and white gastrocnemius) and BAT homogenates were also used to determine the relative expression and protein content of endogenous SLN, SERCA1a, SERCA2a, PLN, UCP-3 and CSQ. Sodium dodecyl sulfate (SDS) polyacrylamide gel electrophoresis (PAGE) was initially performed on samples to separate proteins of interest by size (Laemmli, 1970). Equal quantities of protein were loaded in each well. Due to the large discrepancy in size between the proteins to be

measured, different densities and types of gels were utilized (8% polyacrylamide gels [Mini-PROTEAN II, Bio-Rad, Canada] for SERCA1a, SERCA2a, CSQ and UCP-3; 14% and16% Tricine gel [Sigma-Aldrich] for PLN and SLN, respectively). After separation, proteins were transferred to a polyvinylidene difluoride membrane (PVDF membrane, Bio-Rad, Canada) using a semi dry transfer unit at 23mV for 45 min (Trans-Blot Cell, Bio-Rad, Canada). After blocking with 5% skim milk in Tris-buffered saline (pH 7.5) for 1 hour at room temperature, the membranes were incubated with the primary anti-rabbit CSQ antibody (1:5,000), anti-rabbit PLN antibody (1:3,000), anti-rabbit UCP-3 antibody (1:1,000), anti-mouse SERCA2a antibody (1:4,000; Affinity Bioreagents), anti-rabbit SLN antibody (1:3,000; Babu et al., 2007), and anti-mouse SERCA1a antibody (1:20,000; A52 gift from Dr. MacLennan) and anti-mouse α-actin antibody (1:5000; Sigma-Aldrich) which was used as a loading control in BAT. After washing in Tris-buffered saline 0.1% Tween, the membranes were then treated for 1 hour with the appropriate horseradish peroxidase-conjugated anti-mouse or anti-rabbit secondary antibody (Santa Cruz Biotechnology, Santa Cruz, CA). Lastly, the membranes were washed again and the signals were detected with an enhanced chemiluminescence kit (Amersham Pharmacia Biotech, Piscataway, NJ) using a bio-imaging system and densitometric analysis performed using the GeneSnap software (Syngene, Frederick, MD).

Ca^{2+} dependent Ca^{2+}-ATPase Activity

Homogenates (n=5) from the pooled soleus and EDL of WT and KO mice were used to determine Ca^{2+} dependent Ca^{2+}-ATPase activity using a spectrophotometric assay developed by Simonides & Van Hardeveld (1990) and modified by our laboratory to accommodate a 96-well plate reader (SPECTRAmax Plus; Molecular Devices, Toronto, ON; Duhamel et al.,

2007). Briefly, reaction buffer (200 mM KCl, 20 mM HEPES (pH 7.0), 15 mM $MgCl_2$, 1 mM EGTA, 10 mM NaN_3, 5 mM ATP and 10 mM PEP) containing 18 U/mL of both LDH and PK, as well as homogenate were added to test tubes containing 15 different concentrations of Ca^{2+}, ranging between 7.6 and 4.7 pCa units in the presence and absence of ionophore A23187 (4.2 µM). In the absence of the ionophore, Ca^{2+} accumulates inside the SR vesicle and causes back-inhibition of SERCA pumps, which is more relevant to the physiological system found in skeletal muscle. Aliquots (100 µl) were then transferred in duplicate to a clear bottom 96-well plate (Costar, Corning Incorporated, NY), where 0.3 mM NADH was added to start the reaction. The plate was read at a wavelength of 340 nm for 30 min at 37°C. The different concentrations of Ca^{2+} in the wells were used to determine the maximal enzyme activity (Vmax) and pCa_{50}, which is defined as the $[Ca^{2+}]_f$ required to achieve 50% of Vmax. Lastly, cyclopiazonic acid (CPA; 40 µM), a highly specific SERCA inhibitor (Seidler et al., 1989), was used to determine background activity which was subtracted from the total Ca^{2+}-ATPase activity measured in muscle homogenate.

All data were then plotted against the negative logarithm of $[Ca^{2+}]_f$ (pCa) using basic statistatical software (GraphPad Prism™ version 4) to determine Vmax and pCa_{50}. pCa_{50} was determined by non-linear regression curve fitting using the sigmoidal dose response equation (Equation 2.1),

$$Y = Y_{bot} + (Y_{top} - Y_{bot}) / (1 + {}^{10(LogCa_{50}-x)} * n_H) \qquad \text{Equation 2.1}$$

where Y_{bot} is the bottom of the plateau, Y_{top} is the top of the plateau, Log Ca_{50} is the logarithm of pCa_{50} and n_H is the hill coefficient. pCa_{50} was determined using only activity values between 20 and 80 % of maximal activity.

The accurate measurement of $[Ca^{2+}]_f$ used for the ATPase activity assay was measured using the Ca^{2+} fluorophore, indo-1 on a spectrofluorometric plate reader (SPECTRAmax Gemini XS; Molecular Devices, Toronto, ON) as previously described (Duhamel et al., 2007). The 15 $[Ca^{2+}]_f$ concentrations ranging from 7.6 to 4.7 pCa units and all other components found in the above assay cocktail were added with the addition of indo-1 (1.5 µM); note however that NADH was not added, as it has extremely fluorescent properties which can interfere with the Indo-1 signal. In addition, two other Ca^{2+} concentrations were required for Ca^{2+} measurement, a zero Ca^{2+} and a max Ca^{2+} concentration (1mM). These were then added into a black 96 well plate (Costar, Corning Incorporated, NY) in duplicate and read on a spectrofluorometric plate reader (SPECTRAmax Gemini XS; Molecular Devices, Toronto, ON) after a 15min incubation period at 37 °C. This assay is based on the difference in the maximal emission wavelength between Ca^{2+} bound indo-1 (F) and Ca^{2+} free indo-1 (G) complexes which have emission wavelengths of 405 and 485 nm upon excitation with a 355 nm wavelength, respectively. The ratio (R) of bound (F) to free (G) indo-1 complexes is used to calculate $[Ca^{2+}]_f$ with the following equation (Grynkiewicz et al., 1985):

$$[Ca^{2+}]_f == K_d * (G_{max}G_{min}) * (R-R_{min})/(R_{max}-R) \qquad \text{Equation 2.2}$$

where K_d is the equilibrium constant for the interaction between Ca^{2+} and indo-1, R_{min} is the minimum value of R with zero Ca^{2+}, G_{max} is the maximum value of G with zero Ca^{2+}, R_{max} is the maximum value of R at max Ca^{2+} (1mM) and G_{min} is the minimum value of G at max Ca^{2+} (1mM). The K_d value of the indo-1 Ca^{2+} dye complex is 250 for muscle homogenates (Grynkiewicz et al., 1985).

Ca^{2+} uptake measurement

Homogenates (n=5) from the pooled soleus and EDL of WT and KO mice were used to determine Ca^{2+} uptake using the Ca^{2+} fluorophore, indo-1 as has been described in detail previously (O'Brien et al., 1991; Tupling and Green, 2002). Fluorescence signals produced by Indo-1 were collected on a dual emission wavelength spectrofluorometer (Ratiomaster™ system, Photon Technology International, Birmingham, NJ). As described above, $[Ca^{2+}]_f$ measurements are based on the difference in Ca^{2+} bound Indo-1 (F) and Ca^{2+} free Indo-1 (G) complexes which have emission wavelengths of 405 and 485 nm upon excitation with a 355 nm wavelength, respectively.

Two ml of reaction buffer (200 mM KCl, 20 mM HEPES, 10mM NaN_3, 5 µM TPEN and 15mM $MgCl_2$, pH 7.0 at 37 °C) were added to a four sided cuvette and mixed 1.5 µM Indo-1. $CaCl_2$ (3µl) was then added to achieve an initial $[Ca^{2+}]_f$ between 3 and 3.5 µM. Prior to the addition homogenate (approx. 500µg protein), data collection was initiated using Felix software (Photon Technology International, Birmingham, NJ), after which ATP (5mM) was added to initiate Ca^{2+} uptake. Each sample was run in duplicate. Measurements of Ca^{2+} uptake rates in soleus and EDL homogenates were made without the Ca^{2+} precipitating anion, oxalate. In the absence of the oxalate, Ca^{2+} accumulates inside the SR vesicle and causes back-inhibition of SERCA pumps, which is more relevant to the physiological system found in skeletal muscle.

The decrease in $[Ca^{2+}]_f$ with Ca^{2+} uptake increases G and decreases F causing the F to G ratio (R) to decrease. As previously mentioned using equation 2.2, ionized Ca^{2+} concentration was calculated using the Felix software (Photon Technology International, Birmingham, NJ). The generated curve ($[Ca^{2+}]_f$ versus time) was smooth over 21 points using

the Savitsky-Golay algorithm. Linear regression was then performed on values ranging ±100nM at $[Ca^{2+}]_f$ of 500 nM and 1500 nM and the rate of Ca^{2+} uptake determined by differentiating the linear fit curve and expressed as μmoles•g protein^{-1}• min^{-1}. To determine the role of SLN on the Ca^{2+} transport efficiency of the SERCA pumps, the Ca^{2+} uptake and SERCA activity rates were assessed in the presence of a Ca^{2+} gradient (i.e. without oxalate and without ionophore) at *p*Ca 7.0 and the coupling ratio (Ca^{2+} uptake/SERCA activity) was calculated.

Serum collection and catecholamine measurements

All mice were fasted for 4 hrs prior to being anaesthetized using 0.65mg of somnitol per kg body weight. Blood (approx. 700μl) was collected from the left ventricle and spun down at 5000g for 8 min; resulting serum was then collected and stored at -80°C until analysis. Catecholamines, epinephrine (E) and norepinephrine (NE) were determined using high-performance liquid chromatography and electrochemical detection as described by Weicher et al. (1984) and modified by Green et al. (1991).

Indirect calorimetry of whole-body basal metabolic rate

A total of 30 sexually mature (4-6 months old) WT and KO mice were acclimated to single housed clear mesh bottom cages for a period of one week prior to being placed in a 12-chamber CLAMS (Oxymax series; Columbus Instruments, Columbus, OH). During this period the mice were also fed powdered rat chow (Tekland 22/5 Rodent Diet, Harland-Tekland, Madison, WI) in a feeding apparatus similar to that found within the CLAMS. The CLAMS is an open circuit indirect calorimeter with a positive air flow of 0.5 l/min, allowing for the

sampling of air within the individual chambers. The air samples are pumped through a drier assembly before being analyzed by the oxygen and carbon dioxide sensors which were calibrated by highly purified gas prior to the experiment. The percent O_2 and CO_2 gas levels of the animal chambers (20 cm x 10 cm x 12.5 cm) are measured periodically between reference readings of room air and are used to compute the O_2 consumption (VO_2) of the animal. The daily metabolic rate of each mouse, within the 12 cages was measured individually every 26 minutes. In addition to metabolic rate, this system is equipped with a feed scale for monitoring mass of food consumed and X and Z activity sensors for monitoring ambulatory activity counts (when 2 adjacent X axis beams are broken in succession), rearing activity and total activity.

A total of 5 different groups of 6 WT and KO mice were monitored simultaneously on four separate occasions. The first trail was routinely discarded as individual data were variable and VO_2 values were considerably higher than subsequent trials. Mice were allowed a 24 hour acclimation period in the metabolic chamber prior to data collection after which data were collected at 26-min intervals over a 24 hour period under a controlled environmental temperature (23°C). During these studies, mice had ad libitum access to standard powdered mouse chow (Tekland 22/5 Rodent Diet, Harland-Tekland, Madison, WI) and water. O_2 consumption was averaged over a 24h period as well as divided into sleeping metabolic rate (readings with a total activity count ≤ 4) and resting (awake) metabolic rate, allowing for a better estimate of the O_2 cost associated with the activity counts. The respiratory exchange ratio (RER) was also calculated (VCO_2/VO_2) and reported as a 24h average (total), sleeping and awake. The simultaneous measure of food consumption, total activity and the metabolic rate were utilized to make accurate assessments of basal metabolism between WT and KO

mice. Of the 30 mice used in each group, 2WT and 2KO mice could not be used as their data were very erratic resulting in either loss of weight or hyper-activity during all of the final three trials.

Measurements of whole body O_2 consumption during treadmill exercise

A total of 12 sexually mature (4-6 months old) WT and KO mice were assessed for sub-maximal and maximal aerobic capacity (VO_{2max}) during forced exercise, by running them on an enclosed motorized treadmill using an open-flow respirometry system (Oxymax series; Columbus Instruments, Columbus, OH). This was performed at room temperature (23°C) using a positive pressure, flow-through respirometry system as described above to calculate the rate of oxygen consumption (VO_2). Mice were acclimated prior to the actual assessment by placing them in the enclosed treadmill on three separate occasions and having them walk/run at a low speed (8m/min). For both sub-maximal and maximal aerobic capacity measurements, mice were placed in the enclosed treadmill for 30 min prior to testing. Sub-maximal tests were performed at 3 different speeds for ten minutes using the open flow system, with a flow rate of 0.8 L/min and sampling every 30 sec. The mice exercised at a running speed of 8m/min for 10 min followed by 10 min at 16m/min and a further 10 min at 24 m/min. On a separate occasion VO_{2max} was determined using a slightly modified version of a standardized protocol (Rezende et al., 2006). Briefly, after the 30 min acclimation period, mice were run at 7 m/min for 90 sec, allowing for 3 air samples, the speed was then increased by 3m/min for 90 sec. This was repeated until a plateau in VO_2 was reached or the mouse is incapable of continuing.

Oxygen consumption in isolated intact mouse skeletal muscles

Measurements of oxygen consumption in resting intact soleus muscles were performed as previously described by Norris et al., (2010). A total of 22 KO and 21 WT mice were anesthetized using 65 mg/kg sodium pentobarbital and the soleus muscles were carefully removed from both hind limbs with tendons intact. Care was taken not to damage the muscles and to excise as much tendon as possible as they were needed to tie the muscle to the apparatus. Isolated soleus muscles were mounted in the TIOX tissue bath system (Figure 2.1; Hugo Sachs Electronik-Harvard Apparatus, Germany) for the measurement of resting muscle oxygen consumption (VO_2). The TIOX tissue bath system consists of a moveable platform which supports the muscle and a force transducer (F30 type 372) for measuring contractile force. A movable jacketed tissue chamber that is fitted with a temperature probe and a Clarke type PO_2 electrode (model 1302) is also mounted onto the platform. The jacketed reservoir is connected to a thermocirculator to maintain constant chamber temperatures. Two platinum parallel plate electrodes are located on both sides of the muscle for stimulation protocols enabling simultaneous measurement of force production and oxygen consumption. All components of the TIOX system are connected and controlled by individual PLUGSYS-modules and the data acquired from the individual modules is compiled, filtered, displayed and stored by the HSE-HA ACAD data acquisition software (Hugo Sachs Electronik-Harvard Apparatus, Germany).

Using 4/0 surgical silk, the isolated muscle was mounted onto a fixed lower hook attached to the platform and a top hook which passes through a hole in the lid of the platform and connects to the external force transducer. After mounting the muscle, the tissue chamber was closed to the atmosphere by gently raising it to the platform and tightly sealing it with

bolts and wing nuts to fasten the chamber in place. The system was made air tight by closing off the hole in the lid of the platform using grease (baysilone paste, GE Bayer Silicones). The chamber was then filled with Ringer solution (121mM NaCl, 5mM KCl, 0.5mM $MgCl_2$, 0.4mM NaH_2PO_4, 24mM $NaHCO_3$, 5.5mM glucose and 0.1mM EDTA, pH 7.3), which was pre-heated to 30ºC and aerated with 95% oxygen and 5% carbon dioxide, through a port on the bottom of the bath until it overflowed out of the ventilation cap in the lid of the platform which was then sealed. For each experiment, care was taken to ensure that there were no bubbles within the chamber once it was filled with Ringer solution and closed off to the atmosphere as bubbles will increase the rate of oxygen leak out of the solution. The contents of the chamber were constantly stirred with a magnetic bar and stirrer located directly under the oxygen electrode to ensure consistent oxygen concentration throughout the solution. The muscle length was adjusted to achieve optimal length (l_o) for force production and then the muscle was given 10 minutes to equilibrate inside the chamber prior to initiating data collection.

PO_2 measurements were recorded every 4 seconds for a duration of 30min for each of 3 separate experimental trials at 30ºC designed to quantify resting muscle VO_2 and SERCA pump energetics. The PO_2 in the bath (~620 mmHg) should enable adequate diffusive oxygen supply to support resting muscle metabolism of mouse soleus (Barclay et al., 2005); however, to prevent the formation of hypoxic cores in the muscle, all experiments were terminated before the PO_2 of the Ringer solution fell below 580 mmHg. First, the decrease in PO_2 of the Ringer solution was recorded in the presence of a resting muscle at l_o for 30 minutes. Secondly, the muscle was lengthened until sarcomere overlap (approx. 1.4 l_o) was eliminated and no force could be detected during a single twitch. The bath was then emptied and refilled with fresh Ringer solution and the PO_2 was recorded for 30 minutes. Lastly, to calculate the

contribution of SERCA to basal metabolism, with the muscle still pre-stretched, the bath was emptied and refilled with fresh Ringer solution and 10µM CPA was added with a Hamilton syringe through the vent in the lid of the platform and PO_2 was recorded for 30 minutes. 10µM of CPA was found to be the concentration which was optimal for inhibiting SERCA without having a toxic effect on the muscle (Norris et al., 2010). As in the Norris et al., (2010) study, after the initial rest trial, the isolated muscles were stretched until the actin/myosin overlap was completely eliminated, where VO_2 was not different than the rest trial alone. This would remove the contribution of myosin ATPase to VO_2 as well as eliminate creeping in force upon addition of CPA in the following trial (Barclay, 1996; Barclay et al., 2008).

Following this final 30 minute period, the muscle was returned to its optimal length and a single twitch was applied to ensure continued viability following CPA exposure. The muscle was then detached from the hook, blotted and the tendons were carefully removed with a scalpel blade. The soleus muscle was then weighted, frozen in liquid nitrogen and stored at -80°C until analysis.

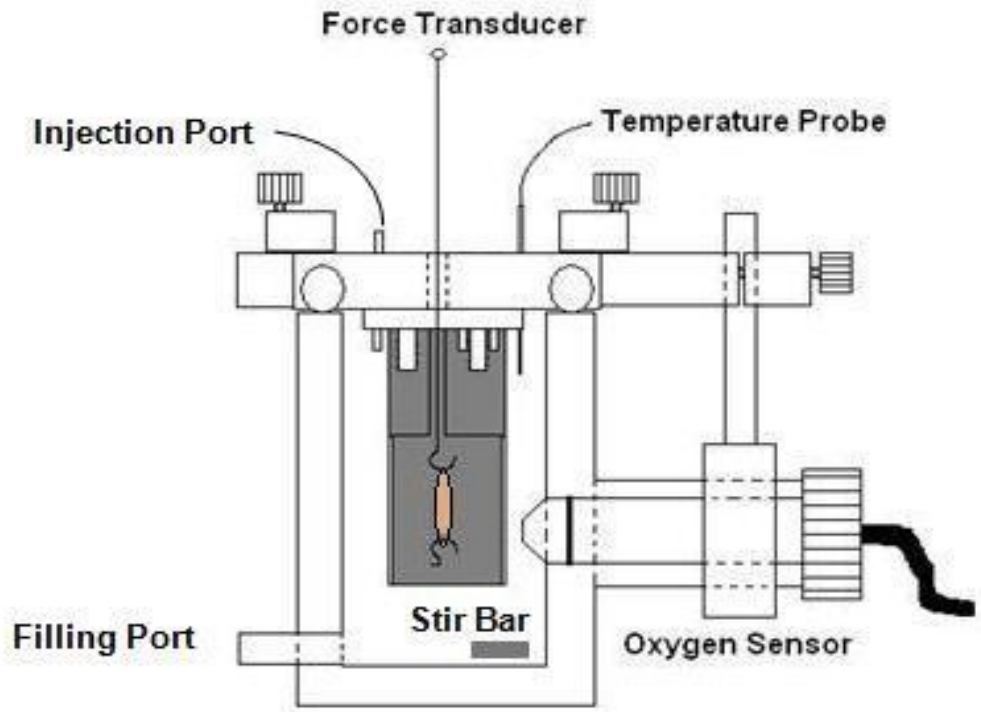

Figure 2.1. Schematic diagram of TIOX tissue bath system (Hugo Sachs Elektronik - Harvard Apparatus).

Calculation of muscle VO_2

The muscle VO_2 was calculated by multiplying the measured drop in partial pressure of oxygen (PO_2) with time by the solubility of oxygen in Ringer's solution at 30ºC and the chamber volume (12.7 ml). The solubility of oxygen at 30ºC was calculated to be 0.001203 M/atm using the following equation:

$$kH = kH_o \times e^{-\frac{\Delta H}{R}(\frac{1}{T}-\frac{1}{T_o})} \qquad \text{Equations 2.3}$$

where kH is the solubility constant of O_2 at experimental temperature, kH_o is the solubility constant of O_2 in pure water at standard temperature of 25ºC (0.0013 M/atm), ΔH is the enthalpy to dissolve O_2 (gas) in water (11.7 kJ/mol), R is the gas constant (0.008312 kJ/mol/K), T is the experimental temperature (30ºC or 303.15 K) and T_o is standard temperature (25ºC or 298.15 K).

In reality, the TIOX system is not completely closed to the atmosphere resulting in leak of oxygen out of the solution. Therefore, in order to account for the oxygen leak, blank trials were done at the beginning and at the end of daily data collection. A blank trial measures the rate of oxygen loss from the oxygenated Ringers solution in an empty chamber (i.e. no muscle). The rate of oxygen loss in the blank trial is then subtracted from the oxygen loss in the presence of the muscle to give the muscle VO_2. A sample PO_2 tracing of a leak, rest, and CPA trial is depicted in Figure 2.2. Muscle VO_2 was expressed relative to muscle wet weight (µl O_2 per g muscle • sec^{-1}).

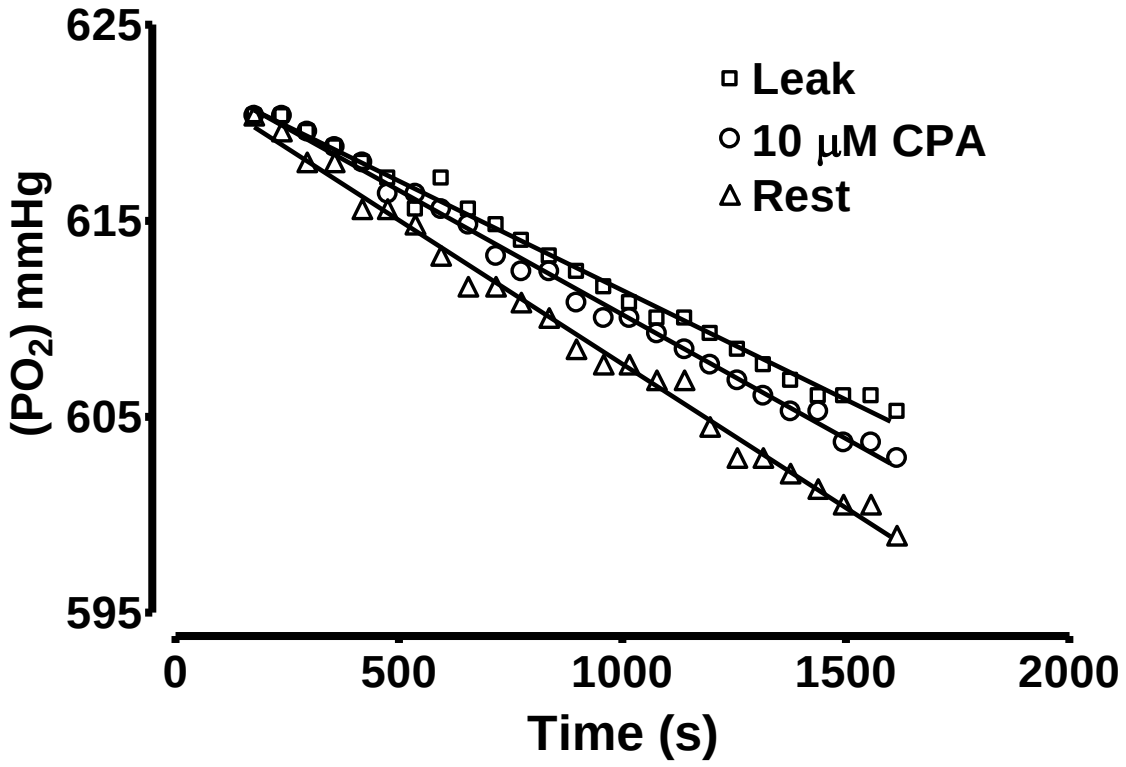

Figure 2.2. Representative raw tracing of PO_2 decline in soleus muscle over a 30 min period at 30°C from the TIOX tissue bath system. Leak represents a trial with no muscle in the bath. Rest corresponds to the decrease in PO_2 in the presence of a soleus muscle. 10 μM CPA represents a trial with the soleus muscle and 10μM of CPA present in the bath. Taken from Norris et al., 2010.

Statistical analysis

One-way ANOVA was used to test for differences between KO and WT mice for CLAMS data, VO_2max, V_{max} and pCa_{50} of Ca^{2+} ATPase activity, Ca^{2+} uptake, coupling ratio, TIOX data and Western blotting data. A two-way ANOVA with repeated measure was used to detect differences between KO and WT mice for submaximal VO_2 and Ca^{2+}-dependent Ca^{2+} ATPase activity. The significance level was set at 0.05, and when appropriate, a Newman-Keuls post hoc test was used to compare specific means. Values are means ± SE.

RESULTS

Endogenous SLN protein content in cardiac, hindlimb and respiratory muscles and BAT

SLN protein levels from cardiac muscles, selected mouse hindlimb muscles, diaphragm and BAT in WT mice were measured using Western blot analysis (Figure 2.3) using a SLN-specific antibody (Babu et al., 2007b). For these analyses, cardiac muscle was analyzed separately as atrial and ventricular tissue to show that SLN is expressed in the atrium, but not in the ventricle in WT mice which is in agreement with previous findings (Babu et al., 2007b). Gastrocnemius muscle was fractionated into red and white portions to show that SLN is expressed in red, but not in white gastrocnemius in WT mice. Comparisons between skeletal muscles from WT mice show that SLN is expressed at relatively high levels in the diaphragm, at medium levels in soleus, red gastrocnemius and tibialis anterior, at low levels in EDL, and not at all in white gastrocnemius, quadriceps and BAT.

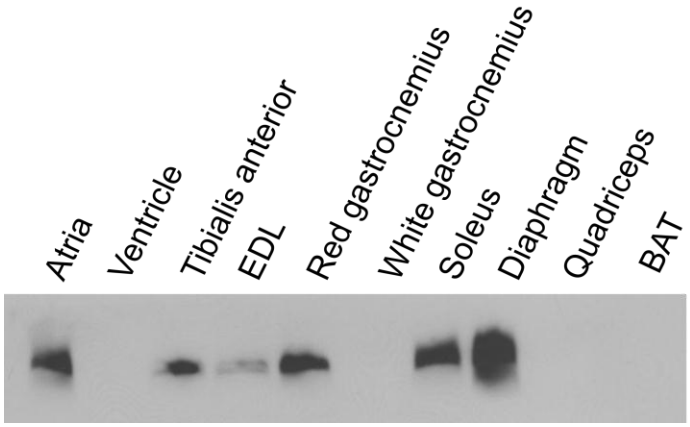

Figure 2.3. Representative Western blot of SLN protein distribution in cardiac and skeletal muscle of wild type (WT) mice. A 16% tricine gel was used to resolve total homogenates from WT mice. Representative Western blot of SR protein in soleus muscle. EDL, extensor digitorum longus; BAT, brown adipose tissue.

***Sln*–null transgenic mice.**

KO mice have already been partially characterized (Babu et al., 2007a), but the effects of SLN ablation on skeletal muscle and whole body metabolism have not been explored in this model. RT-PCR genotyping for the SLN targeting construct and the WT allele is shown in Figure 2.4A. Comparisons between WT and KO mice confirmed the absence of SLN protein in skeletal and cardiac muscles of KO mice (Figure 2.4B).

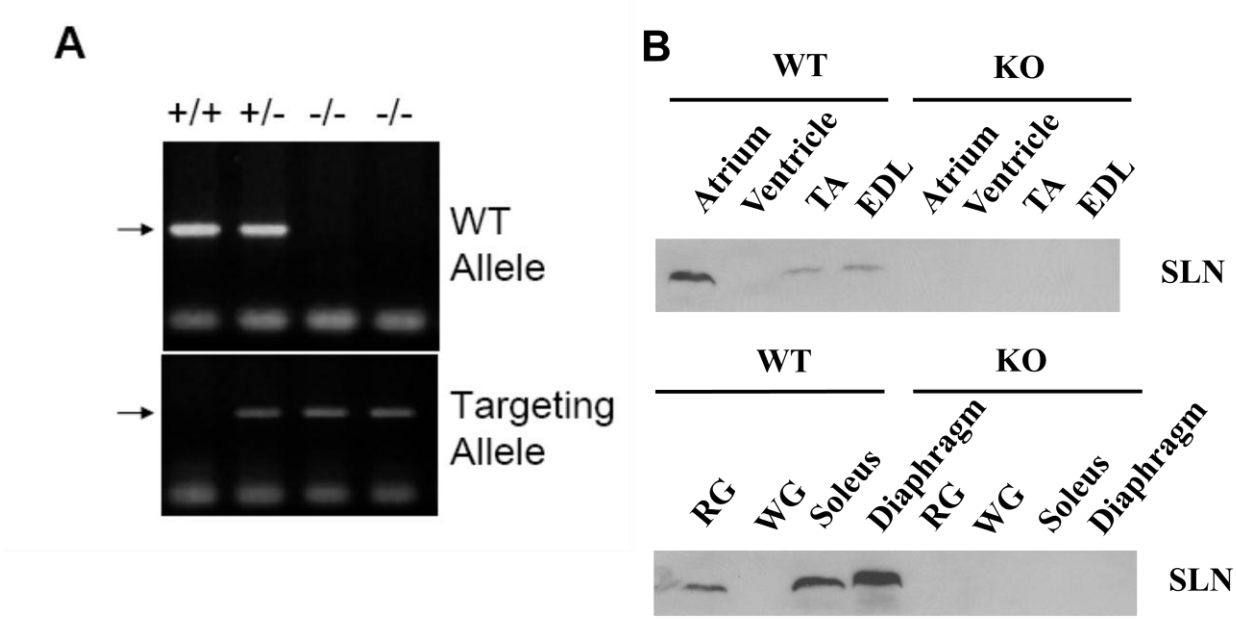

Figure 2.4. Characterization of S*ln*-null (KO) mice. (A) RT-PCR genotyping for the SLN targeting construct and the WT allele. (B) Western blotting analyses of SLN in different skeletal and cardiac muscles from WT and KO littermate mice. A 16% tricine gel was used to resolve total homogenates from both WT and KO mice. Equal quantities of protein were loaded in each well. TA, tibialis anterior; EDL, extensor digitorum longus; RG, red gastrocnemius; WG, white gastrocnemius.

Quantification of SR proteins in wild type and *Sln*-null mice.

To examine potential compensatory changes in the levels of the major Ca^{2+} regulatory proteins in the SR associated with this KO model, semiquantitative Western blotting was performed to determine the relative levels of expression of SERCA1a, SERCA2a, CSQ and PLN in both WT and KO skeletal muscles (soleus, Figure 2.5; white gastrocnemius, Figure 2.6A) and BAT (Figure 2.6B). A comparison of the expression levels of SERCA1a, SERCA2a and PLN in WT and KO mice shows that the loss of SLN induced no compensatory changes in the expression of SERCA1a, SERCA2a, CSQ or PLN in any of the tissues examined. In agreement, Babu et al. (2007a) also found no differences in these Ca^{2+} handling proteins in atria and ventricle from this SLN ablation mouse model. This would suggest any alterations seen in Ca^{2+} handling and potentially muscle metabolism would be a direct result of SLN ablation.

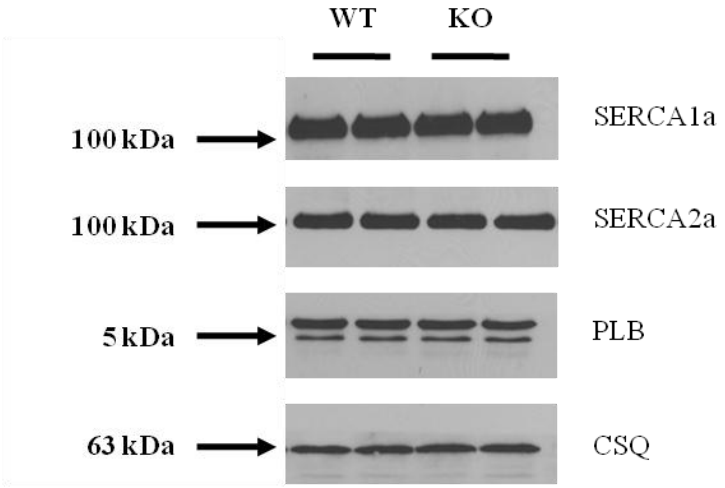

Figure 2.5. Western blot analysis of SR Ca^{2+} regulatory proteins in soleus muscle from wild type (WT) and *Sln*-null (KO) mouse. CSQ was used as a loading control. The loading control sample from only one of the membranes is shown. Different SDS-PAGE gel concentrations (8% for SERCA1a, SERCA2a and CSQ, 15% for PLB) were used to resolve total homogenates from both WT and KO mice. Equal quantity of protein was loaded in each well. PLB,

phospholamban; CSQ, calsequestrin. Representative Western blot of SR protein in soleus muscle.

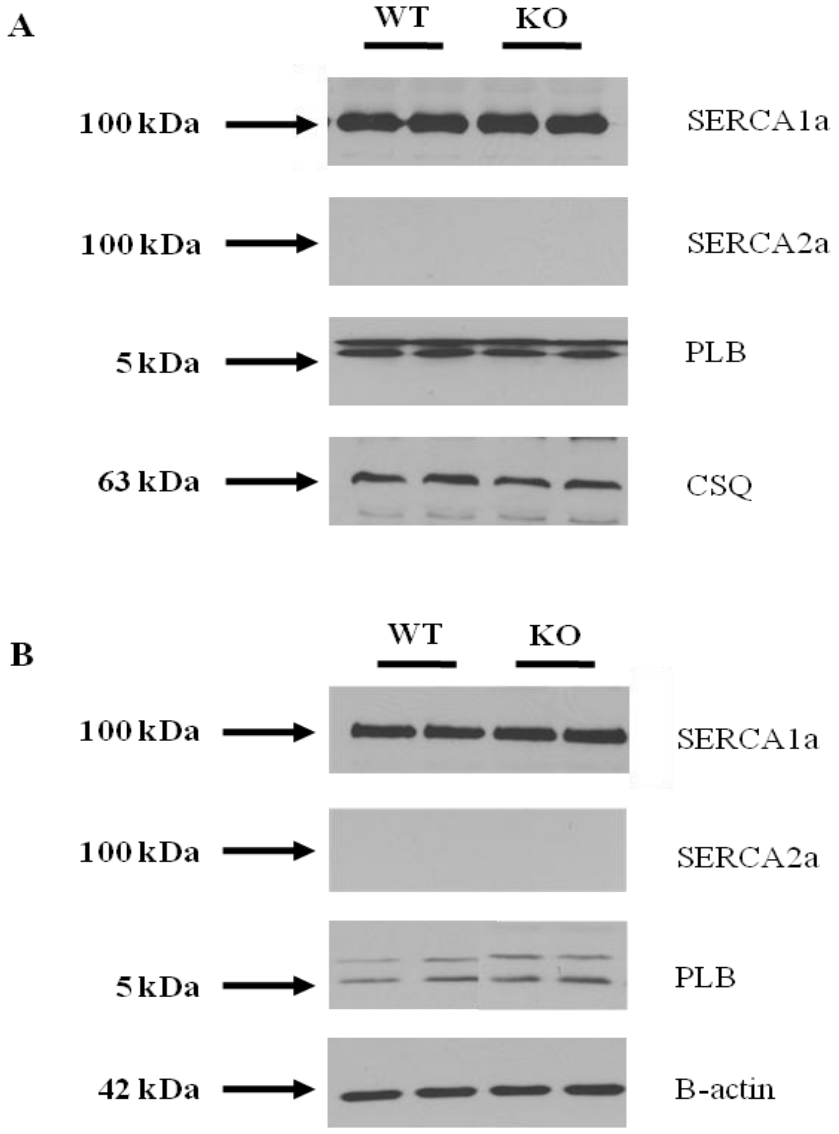

Figure 2.6. Western blot analysis of SR Ca^{2+} regulatory proteins in (A) white gastrocnemius muscle and (B) Brown adipose tissue from wild type (WT) and *Sln*-null (KO) mouse. CSQ and β-actin were used as a loading control respectively. The loading control sample from only one of the membranes is shown. Different SDS-PAGE gel concentrations (8% for SERCA1a, SERCA2a, CSQ and β-actin, 15% for PLB) were used to resolve total homogenates from both WT and KO mice. Equal quantity of protein was loaded in each well. PLB, phospholamban; CSQ, calsequestrin. Representative Western blot of SR protein in soleus muscle.

Ca^{2+}-dependent SR Ca^{2+}-ATPase activity.

Measurements of Ca^{2+}-ATPase activity in soleus and EDL homogenates were made with and without the Ca^{2+} ionophore A23187. In the presence of the ionophore, there is no Ca^{2+} gradient across the SR membrane. In the absence of the ionophore, Ca^{2+} accumulates inside the SR vesicle and causes back-inhibition of SERCA pumps, which is more relevant to the physiological system found in skeletal muscle. When assessed in the absence of a Ca^{2+} gradient, there was an increase in the apparent affinity of SERCA for Ca^{2+} in the soleus muscle of KO mice compared to WT (Figure 2.7A), as indicated by a significant decrease in the pCa_{50} (Table 2.1) and a corresponding leftward shift in plots of the Ca^{2+} dependence of Ca^{2+}-ATPase activity (Figure 2.7A). These effects of SLN ablation on Ca^{2+}-ATPase activity measured with ionophore in soleus were not observed in the EDL muscle (Figure 2.7B; Table 2.1). Maximal SR Ca^{2+} ATPase activity in the absence of a Ca^{2+} gradient was not different between the WT and KO mice in the soleus or EDL muscle (Table 2.1).

In the presence of a Ca^{2+}gradient (without ionophore A23187) Ca^{2+}dependent Ca^{2+}-ATPase in soleus homogenate showed no difference in maximal activity between KO and WT mice (36.0±2.4 μmol per g protein•min^{-1} for KO versus 39.8±2.9 μmol per g protein•min^{-1} for WT). Maximal Ca^{2+} ATPase activity in the EDL muscle was also not different between WT and KO mice (143.5±15.7 μmol per g protein•min^{-1} for KO versus 186.2±21.9 μmol per g protein•min^{-1} for WT). Repeated ANOVA analyses of the Ca^{2+} ATPase activity revealed a rightward shift and lower ($P<0.05$) average activity at any given [Ca^{2+}] in the soleus muscle of KO mice compared with WT mice (Figure 2.8A). Analyses preformed on EDL muscle showed a similar trend but the differences between KO and WT mice were not significant

(P=0.074) (Figure 2.8B). Taken together these data are consistent with the proposal that SLN, by inducing slippage of SERCA pumps, reduces the extent of back-inhibition of Ca^{2+} ATPase activity.

Table 2.1. SERCA activity in the absence of a Ca^{2+} gradient.

Muscle	genotype	Vmax	pCa_{50}	ΔKca
			pCa	
Soleus	WT	201.2±12.0	6.85 ± 0.01	--
	KO	208.7±16.9	6.95 ± 0.03*	0.10
EDL	WT	1052.7±48.6	6.71 ± 0.02	--
	KO	964.6±20.7	6.73 ± 0.01	0.02

Homogenates from wild type (WT) and *Sln*-null (KO) mouse hindlimb muscles and were analyzed for Ca^{2+}-ATPase activity over Ca^{2+} concentrations ranging from pCa 7.4 to pCa 5.5. Vmax is the maximal SR Ca^{2+}ATPase activity expressed as μmol per g pro•min^{-1}. pCa_{50} is the negative logarithm of the Ca^{2+} concentration required to attain the half-maximal Ca^{2+}-ATPase activity rate. * Significantly different ($P<0.05$) than WT. Data are mean ± SE (n=5).

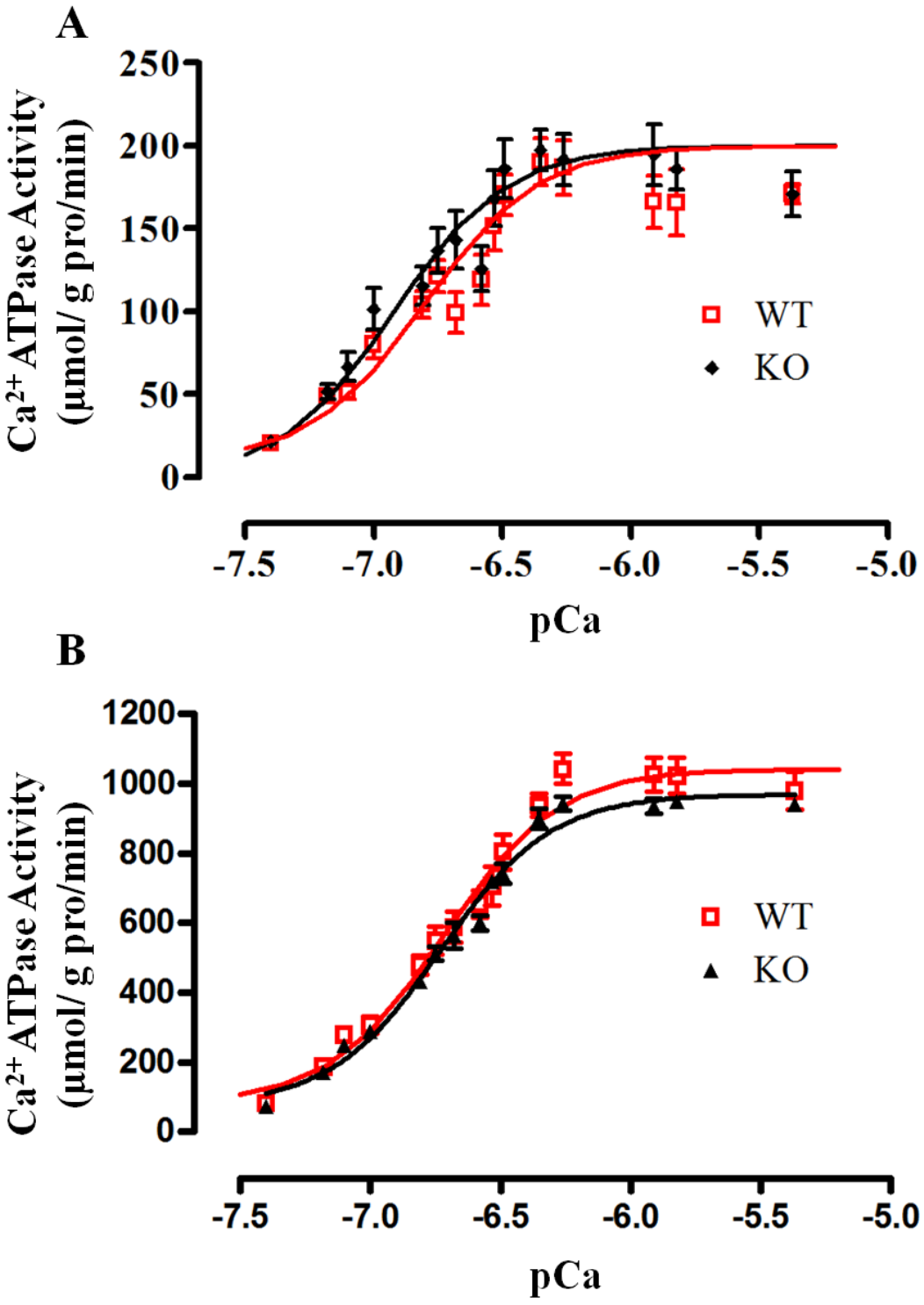

Figure 2.7. Ca^{2+} dependent Ca^{2+}-ATPase activity was assessed in soleus (A) and EDL (B) muscle homogenates from wild type (WT) and *Sln*-null (KO) mice, over Ca^{2+} concentrations ranging from pCa -7.4 to pCa -5.0 in the absence of a Ca^{2+} gradient (with ionophore A23187). Values are means ± SE (n=5).

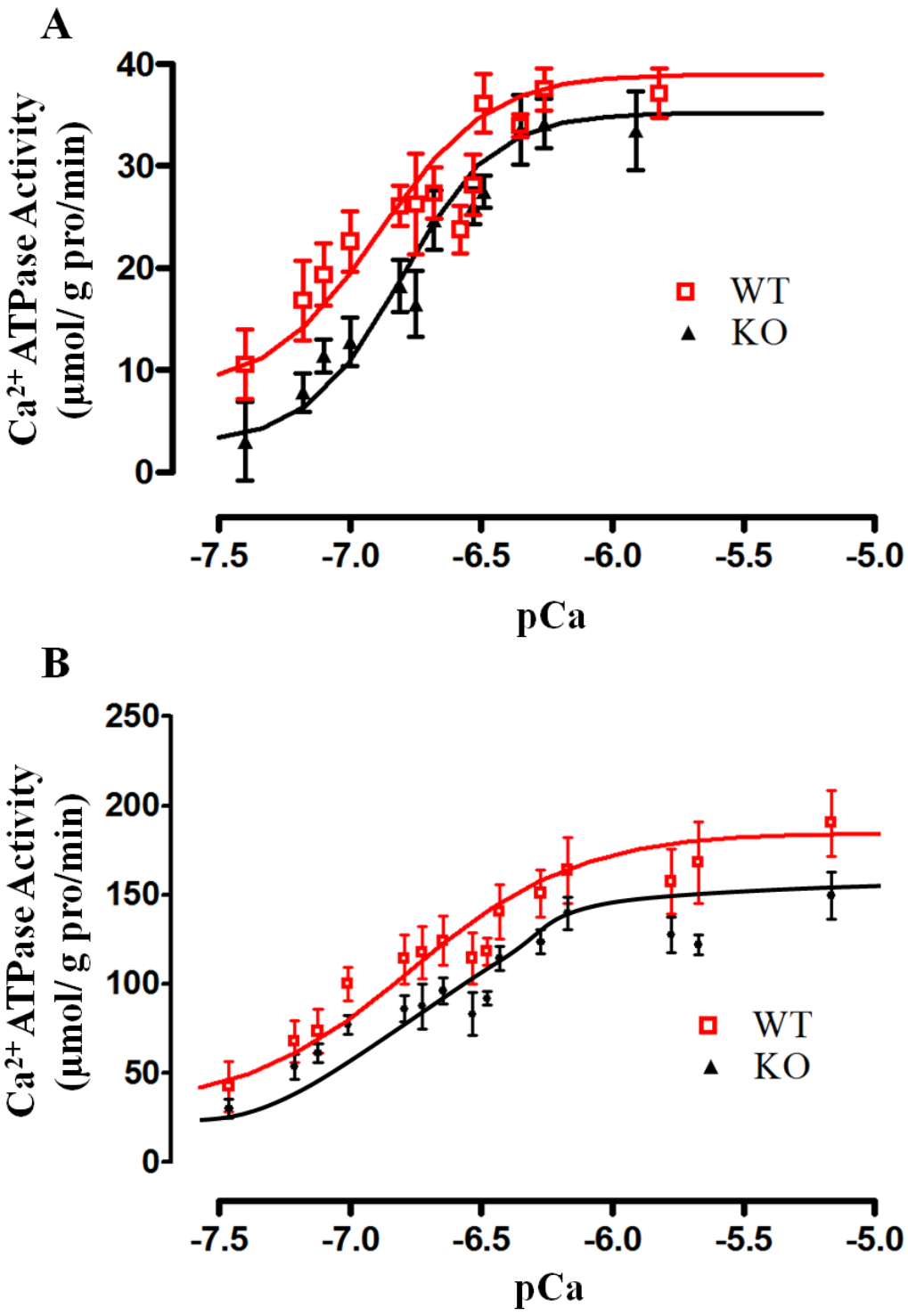

Figure 2.8. Ca^{2+} dependent Ca^{2+}-ATPase activity was assessed in soleus (A) and EDL (B) muscle homogenates from wild type (WT) and *Sln*-null (KO) mice, over Ca^{2+} concentrations anging from pCa -7.4 to pCa -5.0 in the presence of a Ca^{2+}gradient (without ionophore A23187). Main effect ($P<0.05$) of SLN in soleus muscle WT >KO ($P<0.05$). Values are means ± SE (n=5).

The apparent coupling ratio of Ca^{2+} transport into the SR per ATP hydrolyzed.

Measurements of Ca^{2+} uptake rates in soleus and EDL homogenates were made without the Ca^{2+} precipitating anion, oxalate. In the absence of oxalate, Ca^{2+} accumulates inside the SR vesicle and causes back-inhibition of SERCA pumps, which is more relevant to the physiological system found in skeletal muscle. The Ca^{2+} transport efficiency of the SERCA pumps in skeletal muscle was assessed by calculating the stoichiometry (apparent coupling ratio) of SERCA pumps (Ca^{2+} uptake/Ca^{2+}-ATPase activity) in the absence of oxalate and ionophore at a pCa of 7.0. Ca^{2+} uptake in soleus homogenate was not different between KO and WT mice (Figure 2.9A); however, Ca^{2+} ATPase activity was significantly lower ($P<0.01$) in the KO mice compared with WT mice (Figure 2.9B). This resulted in a higher ($P<0.05$) calculated coupling ratio in KO mice suggesting a more efficient Ca^{2+} pumping system, at least at low [Ca^{2+}] (pCa 7.0) and in the presence of a Ca^{2+} gradient across the SR membrane (Figure 2.9C). In EDL, there were no significant differences between KO and WT mice in Ca^{2+} uptake (Figure 2.10A), Ca^{2+} ATPase activity (Figure 2.10B) or the calculated apparent coupling ratio (Figure 2.10C). The higher coupling ratios ($P<0.0001$) found in the soleus homogenate compared to the EDL in both WT and KO mice is in agreement with previous studies showing slow twitch muscle vesicles to be more efficient than fast twitch muscle vesicles by a factor of 3 to 4.5-fold in the presence of a Ca^{2+} gradient (Reis et al., 2002).

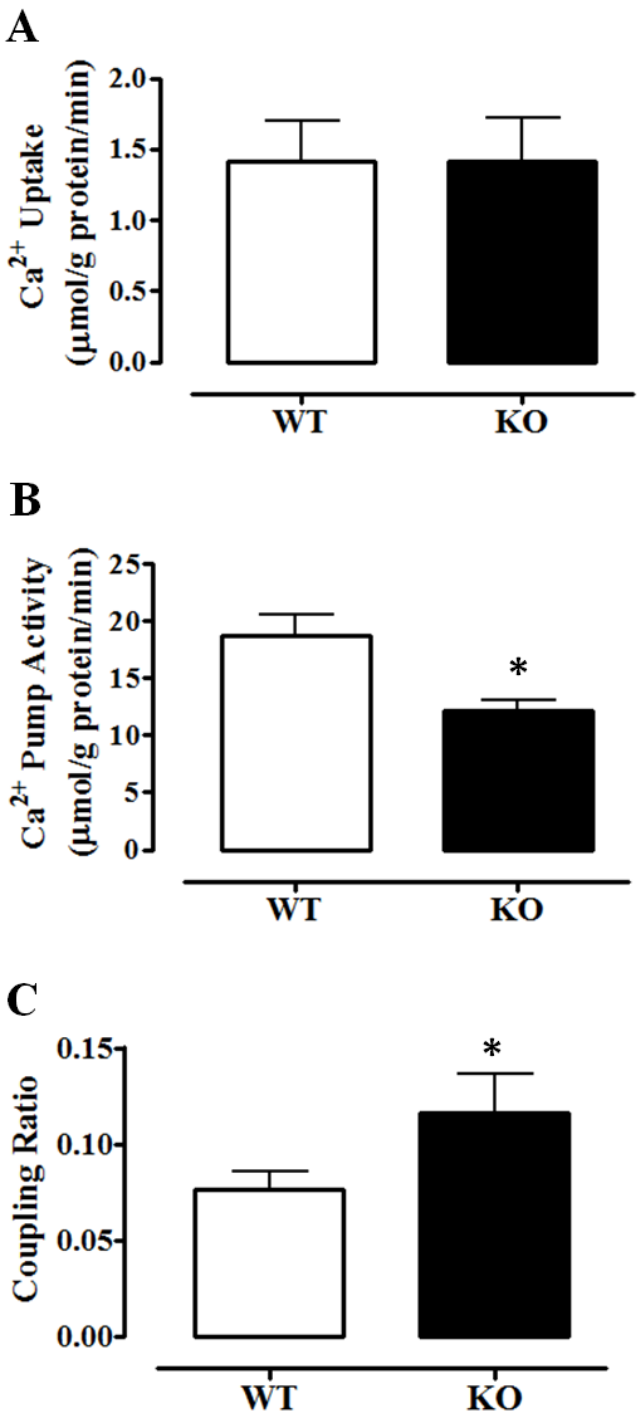

Figure 2.9. Average values in soleus muscle homogenates for Ca^{2+} handling in the presence of a Ca^{2+} gradient at *p*Ca 7.0 from wild type (WT) and *Sln*-null (KO) mice. (A) Ca^{2+} uptake without oxalate; (B) Ca2+-ATPase activity without Ionophore A23187;(C) Apparent coupling ratio (Ca2+ uptake / Ca2+-ATPase activity). * Significantly different ($P<0.05$) than WT. Data are mean ± SE (n=5).

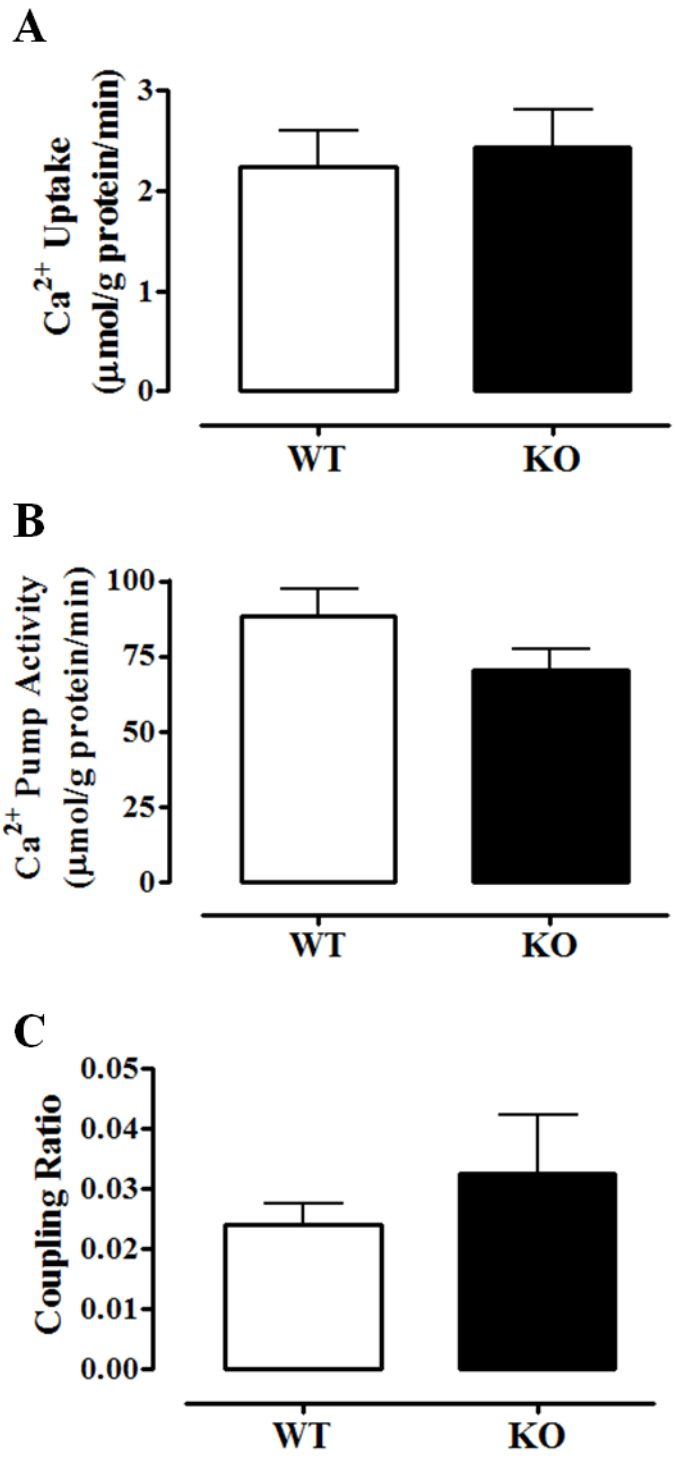

Figure 2.10. Average values in EDL muscle homogenates for Ca^{2+} handling in the presence of a Ca^{2+} gradient at *p*Ca 7.0 from wild type (WT) and *Sln*-null (KO) mice. (A) Ca^{2+} uptake without oxalate; (B) Ca2+-ATPase activity without Ionophore A23187;(C) Apparent coupling ratio (Ca2+ uptake / Ca2+-ATPase activity). Data are mean ± SE (n=5).

Measurement of VO_2 and SERCA contribution to VO_2 in isolated soleus muscle.

The increased efficiency of SERCA pumps observed in soleus muscle homogenate from KO mice suggests that less energy is required by SERCA pumps to accomplish a given amount of SR Ca^{2+} uptake in soleus muscles from KO mice, compared with WT. Furthermore, since SERCA pumps contribute ~50% to resting metabolic rate in mouse soleus (Norris et al., 2010), it was proposed that resting soleus VO_2 would be lower in KO mice, compared with WT. However, resting VO_2 (µl O_2 per g muscle • sec^{-1}) of isolated intact soleus muscles at 30ºC was not significantly different between WT and KO mice (Figure 2.11A). Similar to the Norris et al., study (2010), there were no differences between the rest trial (l_o) and the stretch trial (~1.4 l_o) for either the KO mice (0.427 ± 0.015 µl O_2 per g muscle • sec^{-1} for rest versus 0.425 ± 0.015 µl O_2 per g muscle • $sec^{-1}$for stretch trial) or the WT mice (0.428 ± 0.017 µl O_2 per g muscle • sec^{-1} for rest versus 0.428 ± 0.017 µl O_2 per g muscle • sec^{-1} for stretch trial).

In order to quantify the specific contribution of SERCA pump activity to resting metabolic rate, the change in muscle VO_2 following the addition of cyclopiazonic acid (CPA, 10 µM), a highly specific inhibitor of SERCA pump activity (Goeger and Riley, 1989; Seidler et al., 1989), was measured. Muscle VO_2 in both WT and KO soleus was significantly reduced following CPA treatment but the relative decrease was significantly greater in WT (Figure 2.11A). As a result, the relative contribution of SERCA pumps to resting VO_2 in soleus is lower in KO (~42.7%) compared with WT (~49.5%) mice (Fig. 2.11B). Assuming a caloric expenditure equivalent of 5 kcal per litre of O_2 consumed, then the calculated rate of ATP consumption by SERCA pumps in resting soleus is 125.7 ± 6.0 nmoles per g muscle • sec^{-1} in KO compared with 144.9 ± 5.8 nmoles per g muscle • sec^{-1} in WT.

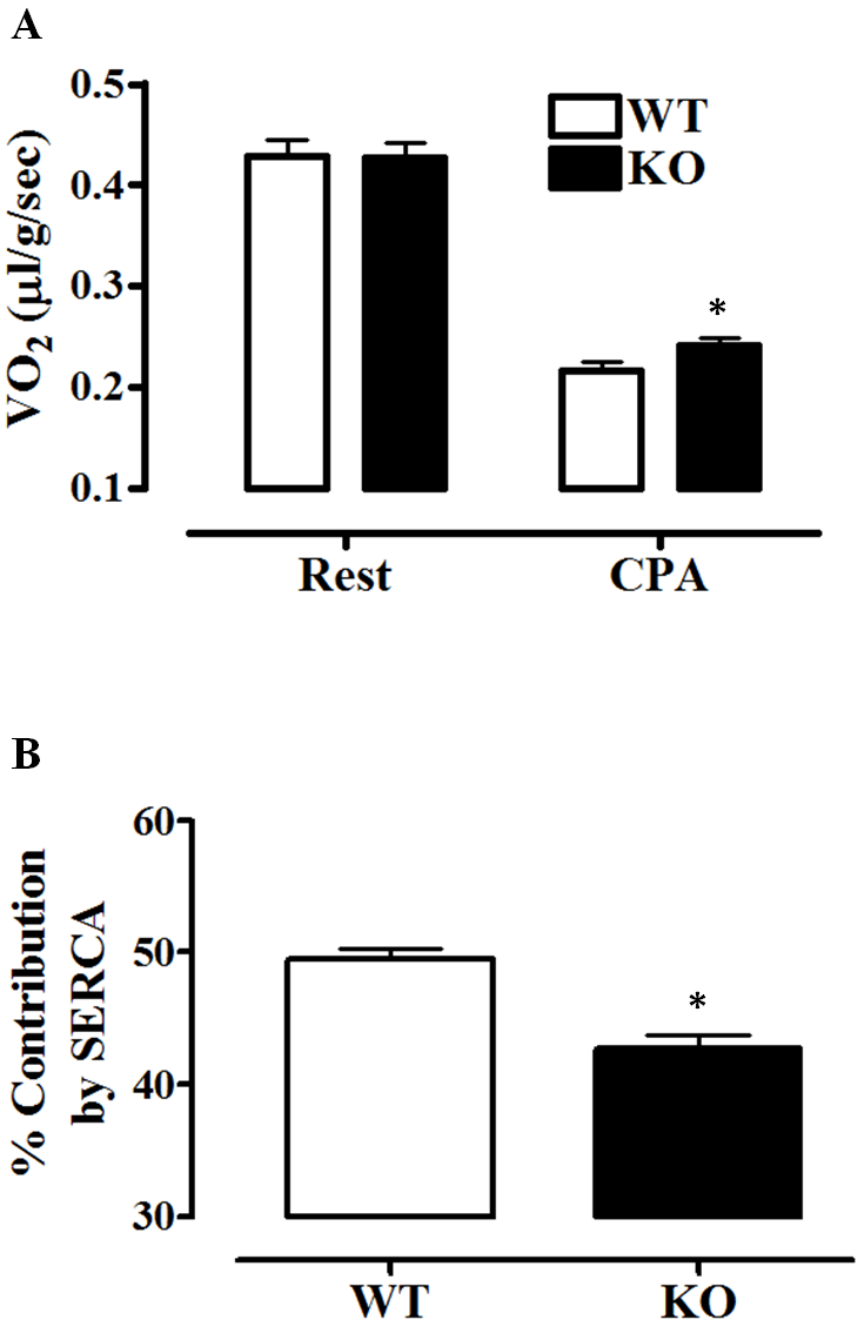

Figure 2.11. Basal oxygen consumption (VO_2) of isolated soleus muscle from wild type (WT) and *Sln*-null (KO) mice in the presence and absence of CPA. (A) Basal VO_2; (B) Contribution of SERCA to basal VO_2. Basal VO_2 showed a main effect ($P<0.0001$) of CPA with Rest>CPA. * Significantly different ($P<0.05$) than WT. Values are means±SE (n=20).

Semiquantitative Western blotting analysis of UCP-3 protein content.

To account for the fact that resting VO_2 in KO soleus is unchanged despite less energy utilization by SERCA pumps compared with WT, it was reasoned that SLN ablation must result in compensatory adaptation(s) that involve one or more other energy consuming processes in muscle. Mitochondrial uncoupling protein 3 (UCP-3), which reduces the proton gradient across the inner mitochondrial membrane, has been shown to increase energy expenditure (Clapham et al., 2000; Schrauwen et al., 2002). Therefore, it was hypothesized that UCP-3 might be increased in KO soleus. As hypothesized, expression levels of UCP-3 in soleus were significantly higher (34%) in KO versus WT mice (Figure 2.12).

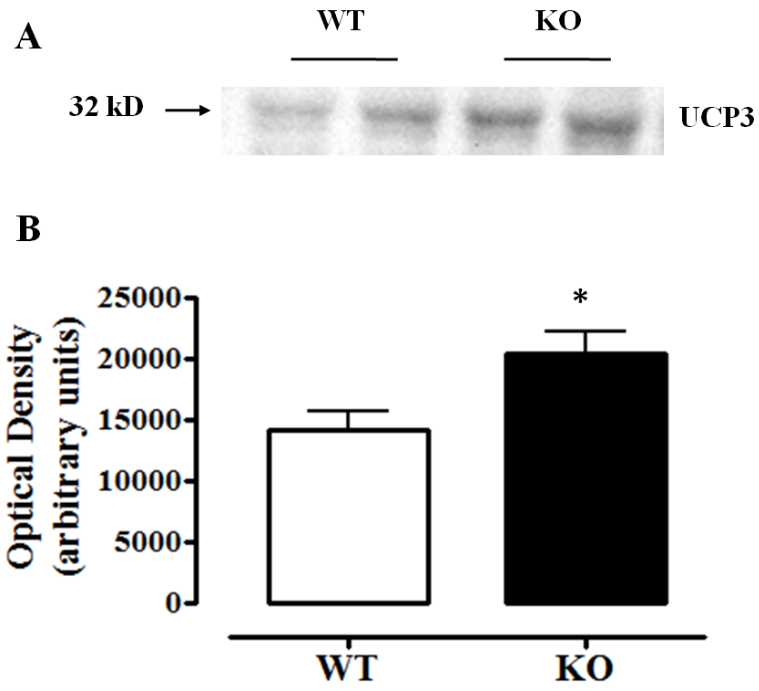

Figure 2.12. Uncoupling protein-3 (UCP-3) content in soleus from wild type (WT) and *Sln*-null (KO) mice. (A) Representative Western blot of UCP3 at 32 kD. (B) Optical density (arbitrary units) of UCP3 band for WT and KO mice. * Significantly different ($P<0.05$) than WT. Values are means ± SE (n=6).

Measurement of whole body metabolism

Total body weight was similar between WT (33.15±0.87g; n=28) and KO (31.94±0.98g; n=28) mice. To determine whether ablation of SLN caused alterations in whole body metabolism, mice were housed in metabolic cages for 3 days. Consistent with the effects of SLN ablation on resting soleus VO_2 and total body weight, no significant differences in whole body metabolic rate, food intake, cage activity or RER were observed between WT and KO mice (Table 2.2). However, dual beam movement tended to be higher ($p<0.09$) in WT mice compared with KO mice.

Table 2.2. Basal metabolic CLAMS measurements for wild type (WT) and *Sln*-null (KO) mice

	WT	**KO**
Weight (g)	33.2±0.9	31.9±1.0
Waking VO_2 (ml O_2/kg/hr)	3065±72.3	3029±56.8
Sleeping VO_2 (ml O_2/kg/hr)	2470±44.3	2489±50.8
Total daily VO_2 (ml O_2/kg/hr)	2865±60.1	2853±50.0
Food Intake (grams)	5.17±0.12	4.90±0.12
Total Activity	10777±509	10211±462
Dual Beam Activity	3001±201	2598±127
Daily VO_2 (ml O_2/Hr)	97.95±1.93	95.34±2.15
Waking RER	1.014±0.0061	1.006±0.0035
Sleeping RER	0.993±0.0099	0.977±0.0063
Total RER	1.012±0.0064	1.003±0.0036

Values are means ± SE (n=28). RER, respiratory exchange ratio.

Sub-maximal and maximal VO_2 during treadmill exercise

The maximal VO_2 measured during progressive treadmill exercise was not different ($P>0.05$) between WT and KO mice (5025±119 ml O_2 /kg/hr for WT versus 5095±127 ml O_2/kg/hr for KO). VO_2 measured in the treadmill at rest was also not different between WT and KO mice (3765±92 ml O_2/kg/hr for WT versus 3762±168 ml O_2/kg/hr for KO, Figure 2.13). There were no significant differences ($P<0.05$) in VO_2 between WT and KO mice measured during sub-maximal treadmill exercise at either 8, 16 or 24 m/min (Figure 2.13); however there was a main effect ($P<0.0001$) of speed on submaximal VO_2.

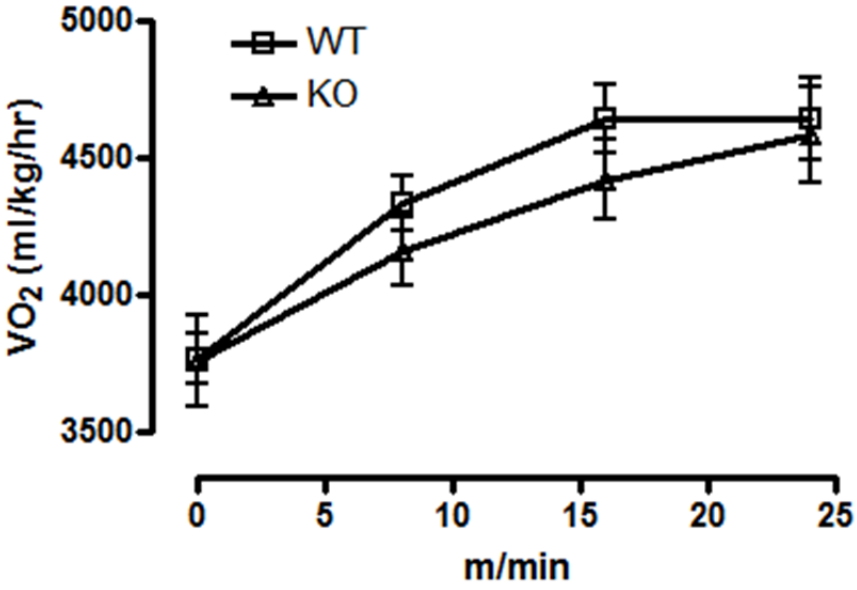

Figure 2.13. Submaximal VO_2 from wild type (WT) and *Sln*-null (KO) mice. Main effect ($P<0.0001$) of speed with 0 (rest) < 8 m/min < 16 and 24 m/min. Values are means ± SE (n=12).

Plasma catecholamines

Concentrations of plasma catecholamines were also measured for an index of altered sympathetic activity, which might also contribute to the maintenance of thermogenesis in KO mice. However no differences ($P>0.05$) were found between KO and WT mice for either NE (2.94 ± 0.486 ng/ml for KO mice versus 2.70 ± 0.65 ng/ml for WT mice) or E (1.35 ± 0.4 ng/ml for KO mice versus 1.91 ± 0.28 ng/ml for WT mice).

DISCUSSION

It is well established that protein-protein interactions between SLN and either SERCA1a or SERCA2a lowers the apparent affinity of the SERCAs for Ca^{2+} (Odermatt et al., 1998; Asahi et al., 2002). It has been demonstrated that the rate of relaxation of force for both cardiac myocytes (Asahi et al., 2004; Gramolini et al., 2006; Babu et al., 2005; Babu et al., 2006) and slow twitch skeletal muscle (Tupling et al., 2002) that overexpress SLN is slower, thus demonstrating that Ca^{2+} removal by the SR limits the rate of muscle relaxation *in vivo.* Although these studies show that increases in SLN expression can result in altered or impaired function, it is also important to determine the effects of loss of SLN on muscle function, given the likelihood that endogenous SLN protein levels are optimal for physiological function. Recently, Babu et al. (2007a) generated a *Sln*-null mouse line and demonstrated that SLN acts as a major regulator of SERCA2a, mediating the β-adrenergic responses in atria, but not in ventricles. Analyses of skeletal muscle function have demonstrated increased SR Ca^{2+} uptake and faster rates of muscle relaxation in the soleus of *Sln*-null mice (Tupling et al. 2008). Thus, it is well established that SLN is a key modulator of SERCA pump function and skeletal muscle relaxation *in vivo*; however, conceptually it is unclear how expression of a SERCA pump inhibitor might be beneficial for skeletal muscle contractile performance. Therefore, the physiological role of SLN in skeletal muscle is still uncertain.

In this study, analyses of the physiological function of SLN were expanded to investigate the metabolic functions of SLN in skeletal muscle using *Sln*-null mice. To test the hypothesis that SLN causes slippage on the Ca^{2+} pump thereby uncoupling ATP hydrolysis from Ca^{2+} transport *in vivo,* SERCA activity and Ca^{2+} uptake were assessed in selected skeletal muscles: the EDL, which is known to express low levels of endogenous SLN (Ottenheijm et

al., 2008), and the soleus, which is known to express relatively high levels of SLN (Babu et al., 2007b; Ottenheijm et al., 2008). To determine whether SLN might contribute to thermogenesis in skeletal muscle, the basal oxygen consumption (VO_2) of soleus muscles isolated from WT and KO mice and the contribution of energy utilized by SERCA was also compared.

Recently, SLN antibodies have been generated in two laboratories (Vangheluwe et al., 2005a; Babu et al., 2007b) and used to examine the level of SLN expression in mouse heart, diaphragm, quadriceps, soleus and EDL. Results using both antibodies are consistent with respect to cardiac muscle. SLN is expressed abundantly in atria, but is low in ventricle; these findings were confirmed in the present study (Figure 2.3 and 2.4). With respect to skeletal muscles, the two antibodies gave slightly different results: SLN was found to be highly expressed in diaphragm and soleus and weakly detectable in EDL using an antibody directed against the 100% conserved C-terminus of SLN (Babu et al., 2007b; Ottenheijm et al., 2008), but was undetectable in either soleus or EDL using an antibody directed against the variable N terminus of SLN (Vangheluwe et al., 2005a). It is likely that the antibody directed against the highly conserved C-terminus is the more sensitive and, therefore, the more reliable antibody. In this study, measurements of the relative levels of expression of SLN in various mouse skeletal muscles were repeated using the antibody directed against the C terminus of SLN (Babu et al., 2007b). It was found that SLN was expressed abundantly in diaphragm, soleus and red gastrocnemius, to a lesser extent in both tibialis anterior and EDL and was absent from white gastrocnemius and quadriceps (Figure 2.3 and 2.4). Compared with soleus, SLN levels were 1.8- and 3.8-fold lower in tibialis anterior and EDL, respectively.

Ca^{2+}-dependent Ca^{2+}-ATPase activity was measured in the absence (with ionophore A23187) of a Ca^{2+} gradient in both soleus and EDL muscle homogenates. As expected, in the

absence of a gradient, an increased affinity of SERCA for Ca^{2+} was observed in soleus as demonstrated by a leftward shift in the Ca^{2+} activity-*p*Ca curves, with no change in Vmax (Table 2.1, Figure 2.7A). By contrast, no changes in SERCA Ca^{2+} affinity or Vmax were detectable with the loss of SLN in EDL, as measured in crude homogenates prepared from EDL (Table 2.1; Figure 2.7B). The different results in soleus and EDL can be explained by differences in endogenous SLN expression between these muscles.

Ca^{2+}-dependent Ca^{2+}-ATPase activity and Ca^{2+} uptake were also measured in the presence (without ionophore A23187 and without oxalate) of a Ca^{2+} gradient in both soleus and EDL muscle homogenates. In the absence of both the ionophore and precipitating anions, Ca^{2+} accumulates inside the SR vesicle and causes back-inhibition of SERCA pumps, which is more relevant to the physiological system found in skeletal muscle (Inesi and de Meis, 1989). Ca^{2+} uptake measured in homogenates at a pCa of 7.0 was not different between WT and KO mice in either the soleus (Figure 2.9A) or the EDL (Figure 2.10A); however, Ca^{2+} ATPase activity was significantly lower in soleus (Figure 2.8A and 2.9B) and tended to be lower in EDL (Figure 2.8B and 2.10B) homogenates from KO mice compared with WT mice. As a result, the calculated coupling ratio in the soleus was 36% higher in KO mice compared with WT (Figure 2.9C) suggesting a more efficient Ca^{2+} pumping system in KO mice, at least at low [Ca^{2+}] (pCa 7.0) and in the presence of a Ca^{2+} gradient across the SR membrane. This is the first study to show that at a physiological SLN:SERCA pump ratio, SLN reduces the stoichiometry of SERCA pumps in skeletal muscle. These findings are in agreement with earlier *in vitro* studies, in which the reconstitution of SLN with Ca^{2+}-ATPase from skeletal muscle SR in sealed vesicles resulted in a lower Ca^{2+} uptake for the same rate of ATP hydrolysis and greater heat production per mol ATP hydrolyzed (Smith et al., 2002; Mall et al.,

2006). Those studies led to the proposal that SLN increases the rate of slippage of the Ca^{2+}-ATPase (reaction 11 in Figure 1.3). Although the increased coupling ratio (33%) measured in EDL homogenates from KO animals was not statistically significant, this finding suggests that even relatively small quantities of SLN in EDL can cause slippage and thereby decrease back inhibition on ATPase activity.

Slippage, an inherent property of P-type pumps, induces an uncoupled catalytic cycle which results in continuously variable coupling ratios from theoretical values down to zero (Berman, 2001). In the absence of precipitating anions, factors that increase slippage should cause sealed SR vesicles to fill more slowly with Ca^{2+} and reduce the extent of back-inhibition of SERCA pump activity. The Ca^{2+} uptake and Ca^{2+}-ATPase activity results in this study can be explained by SLN causing increased slippage and reducing back-inhibition of Ca^{2+} pumps in WT compared with KO SR. First, in the absence of a Ca^{2+} gradient across the SR membrane where slippage should be minimal and back-inhibition of pump activity negligible (Yu and Inesi, 1995), ablation of SLN increases Ca^{2+} uptake (in the presence of oxalate) (Tupling et al., 2008) and Ca^{2+}-ATPase activity (in the presence of Ca^{2+} ionophore A23187) in soleus homogenates at low [Ca^{2+}]. These results are consistent with the well known ability of SLN to act as an inhibitor of SERCA pumps (Odermatt et al., 1998; Asahi et al., 2002). However, in the absence of oxalate, slippage is increased (Yu and Inesi, 1995), but to a greater extent in WT compared with KO, which would decrease the initial rate of Ca^{2+} uptake resulting in less back-inhibition of SERCA pumps in WT compared with KO. Therefore, the similar Ca^{2+} uptake rates between WT and KO when measured without oxalate and the increased Ca^{2+}-ATPase activity in WT compared with KO when measured without Ca^{2+} ionophore reflects the

balance between differences in SLN inhibitory effects on SERCA function, rates of slippage and back-inhibition of SERCA activity between WT and KO.

Based on findings obtained with isolated SR vesicles, slippage likely occurs to a significant extent under physiological conditions in skeletal muscle fibers (Sumbilla et al., 2002). As would be expected with a lower rate of slippage and a higher coupling ratio, the rate of ATP consumption by SERCA pumps in resting soleus was found to be lower in KO mice than WT mice (125.7 ± 6.0 nmol ATP per g muscle•sec^{-1} for KO mice versus 144.9 ± 5.8 nmol ATP per g muscle•sec^{-1} for WT mice). Furthermore, the relative contribution of SERCA pump activity to whole muscle energy expenditure in soleus was ~6.8% lower in KO mice than WT mice (Figure 2.11B). These results obtained in WT mice are consistent with results from an earlier study using C57BL/6 mice (Norris et al., 2010). Importantly, Western blot analyses of soleus homogenates from KO and WT mice revealed that loss of SLN induced no compensatory changes in the expression of SERCA1a, SERCA2a, PLN or CSQ, SR proteins which are known to influence SR Ca^{2+} content, Ca^{2+} leak and the coupling ratio of SERCA pumps (Reis et al., 2002; de Meis et al., 2005; Murphy et al., 2009). Therefore, the lower absolute and relative energy consumption by SERCA pumps in KO versus WT soleus is most likely due to a direct effect of SLN ablation on slippage of the SERCA pumps.

It has already been established that SERCA pumps play an important role in thermogenesis (Block, 1994; de Meis, 2001b). These data from the present study strongly suggest that SLN is a novel regulator of the thermogenic function of SERCA pumps in skeletal muscle. Therefore, the findings that resting soleus and whole body VO_2 were not different between WT and KO mice were unexpected. After blocking SERCA pump activity with CPA, muscle VO_2 was significantly higher in KO compared with WT soleus (Figure 11A), indicating

that the contribution of one or more non-SERCA mediators of resting skeletal muscle metabolism is increased in KO soleus. The increase in UCP-3 content in KO soleus could potentially account for the increase in SERCA-independent VO_2 in those muscles. Although controversial, there are several lines of evidence showing that UCP-3 is an uncoupler of oxidative phosphorylation in skeletal muscle and increases energy expenditure under various conditions (Rousset et al., 2004; Krauss et al., 2005; Brand and Esteves, 2005). Other experimental perturbations which have demonstrated increases in UCP-3 protein and mRNA content include high fat diets and acute cold exposure, both resulting in an increased metabolic rate and heat production (reviewed by Schrauwen and Hesselink, 2002). Therefore, it is proposed that an adaptive increase in UCP-3 expression compensates for the absence of SLN which provides further support for the view that SLN is important for the regulation of thermogenesis.

There could also be other compensatory adaptations in skeletal muscle and/or other metabolically active organs such as BAT that could account for the increase in non-SERCA dependent skeletal muscle and whole body energy expenditure in KO mice. NE and E are two key hormones in the regulation of thermogenesis and metabolism (Webber and Macdonald, 2000); elevated levels would suggest potential compensation for the lack of SLN resulting in higher VO_2 in both isolated muscle and whole body. Plasma catecholamine concentrations however were not different between WT and KO mice suggesting that adrenergic activity was not altered in KO mice. Furthermore, SLN protein was not detected in BAT and there were no effects of SLN ablation on the expression of other Ca^{2+} regulatory proteins (Figure 2.6B) in BAT. However, the potential involvement of other cellular processes such as protein turnover, ion cycling or substrate cycling, in contributing to the increase in SERCA-independent VO_2 in

KO soleus, cannot be ruled out. Given the similarities in body weights and whole body energy expenditure between KO and WT mice, it was to be expected that food intake, RER and total cage activity were also similar between KO and WT mice.

During exercise, skeletal muscle metabolism accounts for up to 90% of the increased whole body metabolic rate above resting metabolism (Rolfe and Brown, 1997). Recently, Zhang et al. (2006) demonstrated that SERCA pumps might consume 80% of the energy used by skeletal muscle during sub-maximal contractions. Therefore, it was hypothesized that differences in metabolism between KO and WT mice would be greater during exercise than during rest. Interestingly, during sub-maximal exercise at the lower running speeds (8 and 16 m/min) VO_2 was approximately 4-5% higher in WT mice compared with KO mice, accounting for 175 and 229 ml O_2 per Kg $\bullet hr^{-1}$ respectively, but this was not significant due to the high variability found between mice. These differences were not seen at the higher running speeds (25m/min and VO_2 max), potentially due to a higher degree of phosphorylation and dissociation of SLN from SERCA via activation of Ca^{2+}/calmodulin-dependent protein kinase (CAMKII) (Bhupathy et al., 2009). The higher ($P<0.005$) resting VO_2 values found with the treadmill system is believed to be due to a greater stress response, as mice were only acclimated for 30 min in the treadmill as opposed to 24 hrs in the CLAMS.

In the heart, SLN regulates SERCA2a activity and plays a significant role in controlling the rate of atrial relaxation and atrial contractility through β-adrenergic signalling (Babu et al., 2007a). It is also clear that SLN is an inhibitor of skeletal muscle Ca^{2+} pumps causing slowed relaxation rates of skeletal muscle and that inhibitory function of SLN is relieved in response to repeated muscle contractions (Tupling et al., 2008) possibly due to (CAMKII) signalling and phosphorylation of SLN at Thr^5 (Bhupathy et al., 2009). However, unlike the heart,

conceptually it is unclear how this might be beneficial for skeletal muscle contractile performance which raised the question of the physiological role of SLN in skeletal muscle forming the basis of this study. It is proposed that the primary physiological function of SLN in skeletal muscle is regulation of thermogenesis. In quiescent skeletal muscle, where cytosolic [Ca^{2+}] is low and SR lumenal [Ca^{2+}] is high, SLN would be dephosphorylated and bound to SERCAs causing an increased rate of slippage and heat production by SERCAs. In working skeletal muscle, SLN inhibitory function must be removed so that SERCAs can be activated maximally to pump Ca^{2+} from the cytoplasm into the SR both rapidly and efficiently. Therefore, the design of this thermogenic system in skeletal muscle involving SLN enables SERCA pumps to contribute significantly to thermogenesis in resting skeletal muscle without compromising their Ca^{2+} pumping function in working skeletal muscle. Further supporting this notion, large mammals which possess relatively little BAT, which is the major thermogenic organ in small mammals, have significantly higher levels of SLN in all muscles that have been examined to date (Babu et al., 2007b). Of note, comparisons between wild type and *Pln*-null mice have shown that PLN, like SLN, also decreases the Ca^{2+}:ATP coupling ratio of SERCA pumps, specifically at low $[Ca^{2+}]_f$ (Frank et al., 2000). The role of PLN in skeletal muscle thermogenesis remains to be evaluated.

In summary, using *Sln*-null mice it was shown that SLN reduces the coupling ratio of SERCA pumps thereby increasing the amount of energy consumed by SERCA pumps in resting skeletal muscle without altering muscle VO_2. An increase in UCP-3 content in soleus was observed in KO mice and this is proposed to act as a compensatory mechanism for maintenance of resting metabolic rate. These data strongly suggest that the primary physiological function of SLN in skeletal muscle is to regulate thermogenesis by SERCA

pumps. Thus, SLN represents a potential control point for energy balance regulation and a potential target for metabolic alterations to oppose obesity and other metabolic disorders.

CHAPTER III

EFFECTS OF SARCOLIPIN ABLATION ON SUSCEPTIBILITY TO OBESITY AND INSULIN RESISTENCE

OVERVIEW

Physiological levels of sarcolipin (SLN) uncouple ATP hydrolysis from sarcoplasmic reticulum (SR) Ca^{2+} uptake in skeletal muscle resulting in a lower contribution of Ca^{2+} handling to basal metabolism (VO_2). Through the use of transgenic *Sln*-null (KO) mice, SLN was determined to be a key regulator of ATP utilization by sarco(endo)plasmic reticulum Ca^{2+}-ATPase (SERCA) pumps and hence energy metabolism in skeletal muscle. To investigate the hypotheses that SLN ablation will increase susceptibility to diet-induced obesity and insulin resistance, KO mice and their wild type (WT) littermates were placed on a "Western" style high fat diet (HFD; 42% of kcal derived from fat with 0.2% cholesterol) for a period of 8 weeks. Whole body metabolic rate (mlO_2/kg/hr), weight gain (g), whole body glucose tolerance and insulin tolerance were measured before and after the HFD. Following the HFD, fat pads, skeletal muscles, pancreas, liver and plasma samples were also collected from WT and KO mice for biochemical analyses. For comparison, at matched time points, tissues and blood were also collected from littermates that were fed a standard chow diet (control). Intact soleus muscles were isolated from some animals and were used to determine basal VO_2 and relative (%) contribution of Ca^{2+} handling to basal VO_2 via the TIOX system. The comprehensive laboratory animal monitoring system (CLAMS) revealed no differences in whole body metabolic rate, food intake, respiratory exchange ratio (RER) or activity levels between KO and WT mice pre HFD; however, KO mice had a lower ($P<0.05$) metabolic rate than WT mice post HFD. Interestingly, RER was also lower ($P<0.01$) in KO mice compared with WT mice post HFD indicating a greater reliance on fat oxidation. KO mice gained more ($P<0.05$) weight over the 8 week HFD period and had a higher ($P<0.02$) adiposity index and epididymal/inguinal fat pad weight post HFD compared to WT mice. Not surprisingly, KO

mice also became extremely glucose intolerant ($P<0.03$) post HFD compared to WT mice who also demonstrated glucose intolerance ($P<0.001$) compared to the pre diet values. Unexpectedly, neither WT nor KO mice were insulin resistant following the HFD based on similar IT responses compared with pre diet values. Compared with control mice, both KO and WT mice displayed elevated serum glucose levels ($P<0.001$), insulin levels ($P<0.001$), and had elevated ($P<0.001$) leptin and cholesterol (LDL and HDL) levels post HFD. Planned comparisons further revealed elevated ($P<0.05$) non-esterified fatty acids (NEFA) and LDL levels in the KO mice compared to the WT mice post HFD. Plasma norepinephrine (NE) and epinephrine (E) levels were also higher ($P<0.01$) in KO mice compared with WT mice following the HFD and compared with control KO and WT mice. Western blotting analysis revealed SLN protein content to be 3.8 fold higher ($P<0.05$) in soleus of WT mice post HFD compared to control WT mice and phospholamban (PLN), a homologue of SLN, was found to be 2.1 fold higher ($P<0.05$) in brown adipose tissue (BAT) in both WT and KO mice post HFD. These adaptive increases in SLN and PLN expression following the HFD suggest that PLN, SLN and hence Ca^{2+} handling may play a role in adaptive thermogenesis. Soleus UCP-3 expression was significantly ($P<0.03$) higher in control KO mice compared to the other three groups. The basal VO_2 of isolated soleus muscle was higher ($P<0.006$) post HFD in both WT and KO mice; however, compared with control mice, the metabolic cost of Ca^{2+} handling was lower ($P<0.001$) post HFD in both WT and KO mice. The relative contribution of SERCA pump activity to resting soleus VO_2 was 14.4 % lower in KO mice ($P<0.001$) than WT mice post HFD; this was significantly ($P<0.01$) greater than the 8.9% difference found between KO and WT control mice. The decrease ($P<0.0001$) in the % contribution of SERCA to basal VO_2 in both KO and WT mice post HFD reveals the complexity of this model and the many

adaptations which occur in skeletal muscle with a HFD. Moreover, even with a 3.8 fold increase in SLN content there were no differences in resting energy expenditure of soleus muscles between WT and KO mice following the HFD. These results can be accounted for by diet-induced increases in catecholamines, NE and E, found in KO mice as well as other adaptive responses leading to increased energy expenditure of soleus in both high fat fed WT and KO mice. Therefore, differences in whole body energy expenditure and obesity between WT and KO mice following a HFD do not seem to be associated with SLN effects on thermogenesis in skeletal muscle. Interestingly, soleus and EDL muscle weights (expressed as % body weight) were decreased ($P<0.04$) in high fat fed KO mice but not WT mice, compared with control. Therefore, lower lean body tissue mass may explain the lower whole body metabolic rate and increased susceptibility to obesity in KO mice compared with WT mice. It is concluded that SLN increases resistance to diet-induced obesity and glucose intolerance in mice through mechanisms that are independent from thermogenic adaptations and in skeletal muscle..

INTRODUCTION

Obesity is the accumulation of excess adipose tissue as a result of a chronic energy imbalance with energy (food) intake being greater than energy expenditure. Due to its cumulative nature, obesity can occur with a very small imbalance in the energy equation (3.1) over an extended period of time. In 2004, approximately 6.8 million Canadian adults between the ages of 20 to 64 years were overweight, and an additional 4.5 million were obese (Statistics Canada, 2004). Over the past decades, obesity has become a worldwide problem with an estimated 315 million people being obese (James, 2004). Obesity is often associated with insulin resistance and hypertension all of which form the major symptoms of metabolic syndrome leaving individuals more susceptible to cardiovascular disease and diabetes (Kahn, 2008). It is important to understand the molecular pathways and physiological systems underlying the regulation of energy balance if we are to develop successful prevention and/or treatment strategies for obesity and its co-morbidities which would have a significant impact on the health of an ever growing population segment.

The first law of thermodynamics dictates energy balance in mammals, which can be expressed as this simple equation:

Energy intake = energy expenditure + energy storage (3.1)

Excess food (energy) intake will be converted to and stored as lipids, as they are more energy efficient and easier to store than carbohydrates or proteins. However, this equation (3.1) is over simplified in assuming: 1) caloric absorption in the gut is 100% efficient; 2) the body's response to altered energy intake or expenditure is static. Energy expenditure can be broken down into 4 major components: (1) obligatory metabolism, cellular and organ functions for basal maintenance; (2) physical activity (voluntary and involuntary); (3) thermic effect of food,

cost of digestion; and (4) adaptive thermogenesis, the body's response to positive energy balance (Rosen and Spiegelman, 2006).

Adaptive thermogenesis refers to increased metabolism/heat production in response to alterations in environmental temperature or more relevantly to dietary intake. This function is believed to protect mammals from cold exposure as well as maintaining homeostasis in energy balance with altered dietary intake (Lowell and Spiegelman, 2000). Increasing dietary intake has been repeatedly shown to increase metabolic rate due to the thermic effect of food but more importantly through adaptive thermogenesis as well (for review see Cannon and Nedergaard, 2000). In support of these effects of dietary intake on adaptive thermogenesis and metabolism, the inverse, a decrease in metabolic rate, has also been demonstrated by the implementation of a starvation diet in pigs, rats and humans (Chwalibog et al., 2005; Goldsmith et al., 2010). Adaptive thermogenesis has been predominately ascribed to uncoupling protein 1 (UCP-1) found in brown adipose tissue (BAT) where high mitochondrial density and UCP-1 content are activated with elevated levels of plasma catecholamines (norepinephrine (NE) and epinephrine (E)) during periods of high energy intake and cold exposure (Matthias et al., 2000).

It has been demonstrated repeatedly that altering energy intake in humans by as little as 10% in either direction results in changes in basal metabolism and energy expenditure to offset the altered dietary intake (Goldsmith et al., 2010; Leibel et al., 1995; Rosenbaum et al., 2003). Larger mammals, including humans, have relatively little BAT in the adult stage of the life cycle suggesting that other mechanisms may be responsible for the adjusted metabolism that occurs with altered energy intake. It has been speculated that skeletal muscle may play an integral part in adaptive thermogenesis as it is a highly metabolically active tissue contributing

up to 40% of body weight and 20-30% of daily energy expenditure (Zurlo et al., 1990; Rolfe and Brown, 1997).

Currently, there are several possible mechanisms proposed to be involved in energy "wasting" during periods of high caloric intake in skeletal muscle. UCP-3 in skeletal muscle was originally thought to have a similar adaptive thermogenic function as its homologue, UCP-1, as consumption of a high fat diet resulted in increased UCP-3 mRNA and protein content in skeletal muscle of mice (Kontani et al., 2005; Gong et al., 1999) and UCP-3 mRNA in humans (Schrauwen et al., 2001). However, there are currently many conflicting ideas as to the exact function of UCP-3 in skeletal muscle. Counter-intuitive to its function in adaptive thermogenesis, UCP-3 mRNA expression has been found to increase in both rats (Boss et al., 1998) and humans (Millet et al, 1997) following starvation. As well, studies have shown decreases in UCP-3 mRNA and/or no change in UCP-3 protein content following prolonged cold exposure (Boss et al., 1998; Lin et al., 1998; Schrauwen et al., 2002). Other potential mechanisms for adaptive thermogenesis in skeletal muscle include a futile fatty acid synthesis/oxidation cycle (Solinas et al., 2004), increased protein degradation/synthesis (Rolfe and Brown,1997), protein and metabolite dephosphorylation/phosphorylation and lastly ion (Na^+, K^+ and Ca^{2+}) leak (Lowell and Spiegelman, 2000).

Ca^{2+} cycling in skeletal muscle has recently received growing attention in its contribution to both resting and sub-maximal metabolism. Zhang et al. (2006) found that sarco(endo)plasmic reticulum Ca^{2+} ATPase (SERCA) pumps consume approximately 80% of the ATP hydrolyzed in rat extensor digitorum longus (EDL) during sub-maximal contractions. More recently, Norris et al. (2010) demonstrated that maintaining the Ca^{2+} gradient between the lumen of the sarco-plasmic reticulum (SR) and the cytosol in both mouse fast (EDL) and

slow (soleus) twitch skeletal muscle constituted 50% of the energy utilized during resting metabolism (Norris et al., 2010). These two studies suggest that Ca^{2+} handling in muscle has been highly underestimated in its contribution to muscle metabolism and, consequently, whole body metabolism considering values that have been published previously (Rolfe and Brown, 1997; Chinet et al., 1992; Hasselbach and Oetliker; 1983). Two other examples highlighting the role of Ca^{2+} handling in skeletal muscle in thermogenesis are: 1) malignant hyperthermia, a genetic disorder resulting in excessive Ca^{2+} release from the ryanodine receptor (RYR) during periods of stress that results in increased heat production due to activation of both myosin ATPase and SR Ca^{2+} ATPase (Denborough, 1998); and 2) the heater organ of deep diving fish, which is comprised of specialized muscle cells containing no contractile proteins and an extensive SR membrane network (Morrisette et al., 2003). Therefore, decreasing the efficiency of the SERCA pumps and increasing the cost of transporting a given amount of Ca^{2+} into the SR may be a potential mechanism by which adaptive thermogenesis occurs in skeletal muscle, especially in larger mammals which possess minimal BAT.

Reconstitution experiments have shown that SLN uncouples ATP hydrolysis from Ca^{2+} transport by SERCA pumps (Smith et al., 2002) and increases the amount of heat released per mol of ATP hydrolyzed (Mall et al., 2006). These results could be explained by SLN causing an increased rate of slippage of the SERCA pump (Figure 1.3, reaction 11; Mall et al., 2006) which would decrease the fraction of energy released during ATP hydrolysis that is converted into work and increase the amount of heat released (de Meis, 2001b; de Meis, 2002). The greater levels of heat produced at higher SLN:SERCA ratios found in the reconstitution experiments (Mall et al., 2006) demonstrate the potential for increased SLN expression contributing to adaptive thermogenesis *in vivo*. Importantly, analyses of skeletal muscles from

Sln-null (KO) mice (presented in Chapter II), have now established that at a physiological SLN:SERCA pump ratio, SLN reduces the stoichiometry of SERCA pumps in skeletal muscle *in vivo* by ~36%. As would be expected with a higher coupling ratio, the rate of ATP consumption by SERCA pumps in resting soleus muscle is also significantly lower in KO mice than wild type (WT) mice. Thus, SLN appears to be a novel regulator of the thermogenic function of SERCA pumps in skeletal muscle. Although, SLN ablation does not reduce resting skeletal muscle or whole body metabolic rate and does not cause obesity in chow fed mice, it is possible that KO mice could be more susceptible to obesity and related complications (i.e. glucose intolerance) in response to high fat feeding if SLN expression in skeletal muscle from WT mice is induced by high fat feeding resulting in increased skeletal muscle and whole body energy expenditure compared to KO mice. In order to investigate these hypotheses, WT and KO mice were fed *ad libitum*, either a high-fat diet (HFD) with 42% kcal derived from fat (product 8728CM, Harlan Teklad) for 8 weeks, or were maintained on a standard chow diet (product 8728CM, Harlan Teklad). The Comprehensive Lab Animal Monitoring System (CLAMS) was used to monitor whole body metabolic rate ($mlO_2/kg/hr$), food intake (g) and activity level of WT and KO mice pre and post HFD. Weight gain, whole body glucose tolerance (GT) and insulin tolerance (IT) were also measured in WT and KO mice before and after the 8 wk HFD. Fat pads, skeletal muscles and plasma samples from chow fed control and post HFD mice were collected for biochemical analyses. Lastly, polaragraphic measurements of oxygen consumption (VO_2) from isolated soleus muscle at 30 ºC using the TIOX tissue bath system were also used to determine basal VO_2 and % contribution of Ca^{2+} handling to basal VO_2.

METHODS

Transgenic mice colony

Transgenic mice, *Sln*-null, donated by Dr. Muthu Periasamy, Ohio State University, were utilized to establish a continuous breeding colony at the University of Waterloo. Breeding of the heterozygous *Sln*-null mice produced wild type (+/+; WT), heterozygous (+/-) and homozygous (-/-; KO) mice. At 3-4 weeks of age all mice were ear notched and tagged. Genotyping was performed as previously described in Chapter 2.

Once the animals had been genotyped, the WT and KO mice were separated into individual cages. Animals were housed in an environmentally controlled room with a standard 12:12 light/dark cycle and allowed access to food (Tekland 22/5 Rodent Diet, Harland-Tekland, Madison, WI) and water *ad libitum.* The study was approved by the Animal Care Committee at the University of Waterloo and all procedures were performed in accordance with the Canadian Council on Animal Care.

Experimental design and high fat diet

A total of 32 sexually mature (~4-5 months) male KO mice and an equal number of WT littermates were further divided into a HFD group (n=20 KO and WT) while the remaining mice were used as a standard chow fed control group (n=12 KO and WT). Mice in the HFD group were fed a high-fat diet containing 42% of its kcal derived from fat with 0.2% cholesterol (product TD 88137, Harlan Teklad, Madison, WI; product sheet in Appendix A) *ad libitum* for a period of 8 weeks. Mice in the control group were fed standard rodent chow (Teklad 22/5 Rodent Diet, Harland-Teklad, Madison, WI; product sheet found in Appendix B) *ad libitum* for the duration of the study. Animal body weights were monitored weekly in WT

and KO mice on the HFD for a period of 8 wks. The time-line of the measurements made during the experiment can be found in Appendix C.

Indirect calorimetry of whole-body basal metabolic rate

Whole body metabolic rate, food consumption, RER and cage activity were measured before and after the HFD, in WT and KO mice, using a 12-chamber Comprehensive Lab Animal Monitoring System (CLAMS) (Oxymax series; Columbus Instruments, Columbus, OH) as previously described in chapter 2. Each mouse was acclimated to single housed clear mesh bottom cages for a period of one week prior to initiating pre-diet CLAMS trials. Following 3 separate pre-diet CLAMS trials, which were performed over a period of 3 weeks, mice in the HFD group started consuming the high fat diet. The first CLAMS trail was routinely discarded as individual data were variable and VO_2 values were considerably higher than proceeding trials. Following the 8 week diet period, CLAMS measurements were repeated during 3 separate trials. In total, 3 WT and 4 KO mice could not be used as their CLAMS data were very erratic resulting in either loss of weight or hyper-activity during all of the final three trials. These 7 mice were not used for any other analyses.

Glucose tolerance tests

Glucose tolerance tests (GTT) were performed after an overnight fast, pre and post HFD, in WT (n=16) and KO (n=14) mice. A total of 5 – 10 μl of blood was drawn from the tail and assayed for glucose using a blood glucose meter (Accu-Chek Aviva, Roche Diagnostics) at 0, 30, 60 and 120 min following an intraperitoneal injection of 10% D-glucose at a dose of 1 g / kg body weight (Li et al., 2000).

Insulin tolerance tests

Insulin tolerance tests (ITT) were performed after a 4 hour fast, pre and post HFD, in WT (n=10) and KO (n=10) mice. A total of 5 – 10 μl of blood was drawn from the tail and assayed for glucose using a blood glucose meter (Accu-Chek Aviva, Roche Diagnostics) at 0, 30, 60 and 120 min following an intraperitoneal injection of insulin (Humulin, Eli Lilly, Toronto, ON) at a dose of 0.75 U / kg body weight (Li et al., 2000).

Tissue and serum collection

All mice (post HFD and control) were fasted for 4 hrs prior to being anaesthetized using 0.65mg of somnitol per kg body weight. Blood was collected from the left ventricle (700 μl) and spun down at 5000g for 8 min. The resulting serum was collected and stored at -80°C until analysis. Soleus, EDL and white portions of the gastrocnemius muscles, along with BAT were excised from the mice, cleaned of extraneous and connective tissues, weighed and then stored at -80°C for Western blotting analyses. The liver and epididymal/inguinal and retroperitoneal fat pads were also removed and weighed.

Adiposity index

Adiposity was determined from the weights of the epididymal/inguinal and retroperitoneal fat pad and calculated as an adiposity index defined as 100 x (sum of fat pad weights) / body weight (Taylor and Phillips, 1996).

Serum parameters

Serum concentrations of glucose, insulin, leptin, non-esterified fatty acids (NEFA), cholesterol (HDL, LDL, total) and triacylglycerols (TAGs) were measured in WT and KO mice post HFD and in the standard chow fed control group. Glucose was measured using a blood glucose meter (Accu-Chek Aviva, Roche Diagnostics); insulin concentrations were determined by radioimmuno-assay techniques (COAT-A-COUNT, Siemens, Malvern, PA); an enzyme-immunoassay was used for leptin (EIA, ALPCO Diagnostics, Salem, NH); and assay kits were used for triacylglycerols (TG SL-ASSAY, Genzyme Diagnostics, Charlottetown, PE), cholesterol (Total serum cholesterol/HDL-ADVANCE ASSAY, Diagnostic Chemicals Limited, Charlottetown, PE) and NEFA (NEFA C, WAKO Chemicals GmbH, Neuss, Germany). Catecholamines, NE and E, were determined using high-performance liquid chromatography and electrochemical detection as described by Weicher et al. (1984) and modified by Green et al. (1991).

Muscle homogenate and Western blotting analysis

Soleus muscles from WT and KO mice, from chow fed control and HFD groups, were diluted 10:1 (vol/wt) in ice cold PMSF buffer and homogenized as previously described in chapter 2 for Western blotting analysis. BAT and white gastrocnemius muscle from WT and KO mice, from control and HFD groups, were also homogenized in PMSF buffer to determine SR protein (SLN, SERCA1a, SERCA2a, PLN and calsequestrin (CSQ)) content using Western blotting analysis. Total protein concentration of the homogenates was measured by the method of Lowry, as modified by Schacterle and Pollock (Schacterle & Pollock, 1973).

Oxygen consumption of isolated intact mouse soleus muscles

A total of 11 KO and 11 WT mice from both chow fed control and post HFD groups were anesthetized using 65 mg/kg sodium pentobarbital and the soleus muscles were carefully removed from both hind limbs with tendons intact. The isolated soleus muscle was mounted in the TIOX tissue bath system (Figure 2.1; Hugo Sachs Electronik-Harvard Apparatus, Germany) for the measurement of resting muscle oxygen consumption (VO_2) and contribution of Ca^{2+} handling to basal metabolic rate as previously described in Chapter 2.

Statistical analyses

Two-way ANOVAs were used to test for differences between KO and WT mice in both control and HFD groups for physical and serum parameters and TIOX data. A two-way ANOVA with repeated measures was used to detect differences in CLAMS data between KO and WT mice at pre and post time points for the HFD group. Three-way ANOVAs with repeated measures were used to test for differences between the means for glucose and insulin tolerance test data of KO and WT mice at pre and post time points for different times (0, 30, 60 and 120 min) for HFD group. Planned comparisons were also utilized to examine the independent effects of SLN on CLAMS data, physical and serum parameters using student's t-test. The significance level was set at 0.05, and when appropriate, a Newman-Keuls post hoc test was used to compare specific means. Values are means ± SE.

RESULTS

Body weight

At the time of sacrifice, HFD mice (46.7 ± 1.2 g for WT versus 47.9 ± 1.5 g for KO) weighed significantly ($P<0.001$) more than the standard chow fed control mice (37.0 ± 1.2 g for WT versus 35.3 ± 1.4 g for KO). The changes in body weight that occurred over the 8 week HFD period for WT and KO mice are plotted in Figure 3.1. Both WT and KO mice that were fed the HFD for 8 weeks gained ($P<0.0001$) weight with KO mice gaining more ($P<0.05$) than WT mice over the last 6 weeks (13.36±0.86 g for WT versus 16.02±0.92 g for KO).

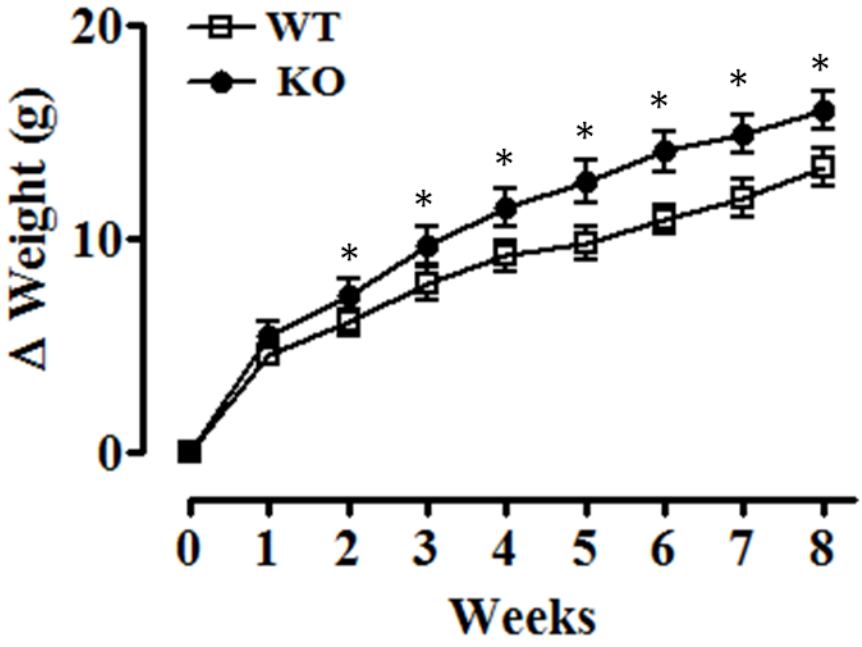

Figure 3.1. Average weight gain of wild type (WT) and *Sln*-null (KO) mice during an 8 wk HFD. * Significantly different ($P<0.05$) from WT mice. Values are means ± SE (n=17, KO; n=16, WT).

Anthropometric parameters

The HFD resulted in larger fat pads and higher adiposity index in both WT and KO mice as shown by the main effect ($P<0.0001$) of diet on epididymal/inguinal fat, retroperitoneal fat, BAT and adiposity index (Figure 3.2). Closer examination of the different fat pads and adiposity index post HFD reveal interactions with higher epididymal/inguinal fat pad weight (Figure 3.2A) ($P<0.02$) and adiposity index (Figure 3.2D) ($P<0.005$) in KO mice compared to WT mice. There were also trends for higher retroperitoneal fat pad ($P<0.09$) (Figure 3.2 B) and BAT ($P<0.09$) (Figure 3.2C) weights in KO mice compared with WT mice post HFD.

Soleus weights showed interesting trends ($P<0.06$), being heavier in HFD compared to chow fed control mice and heavier in WT mice ($P<0.08$) than KO mice (Figure 3.3A). There were no effects of diet or genotype on EDL muscle weights (Figure 3.3B). However, both soleus and EDL make up a smaller ($P<0.0006$) percentage of body weight in HFD mice compared with chow fed control mice (Figure 3.3 C and D). For the soleus, an interaction was found, with WT soleus making up a greater ($P<0.04$) percentage of body weight than KO soleus post HFD. EDL did not show an interaction but planned comparisons revealed WT EDL to make up a greater ($P<0.05$) proportion of body weight than KO EDL post HFD. Liver weights were not different between WT and KO mice either in the control (1.50±0.08 g for WT versus 1.34±0.05 g for KO) or HFD (2.92±0.3 g for WT versus 2.75±0.4 g for KO) groups; however a main effect ($P<0.0001$) was seen with HFD livers being heavier than chow fed control.

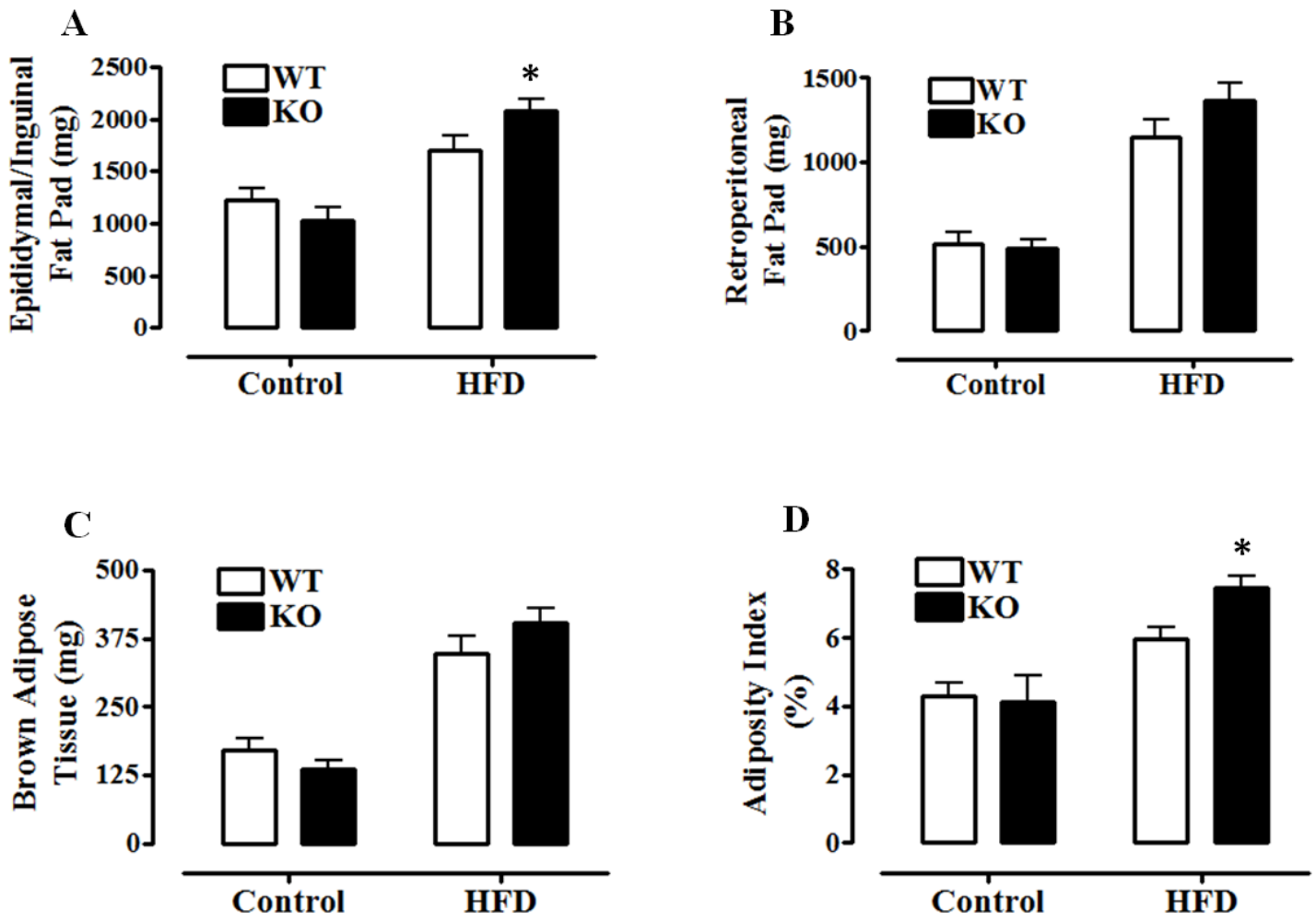

Fgure 3.2. Fat pad weights, brown adipose tissue (BAT) weight and adiposity index for chow fed control and HFD, wild type (WT) and *Sln*-null (KO) mice. (A) epididymal and inguinal fat pad weight; (B) retroperitoneal fat pad weight; (C) BAT weight;(D) adiposity index. All showed a main effect ($P<0.0001$) of diet with HFD>control. * Significantly different ($P<0.05$) than WT. Values are means±SE (n=11 for WT control; n=12 for KO control; n=17 for WT HFD and n=16 for KO HFD).

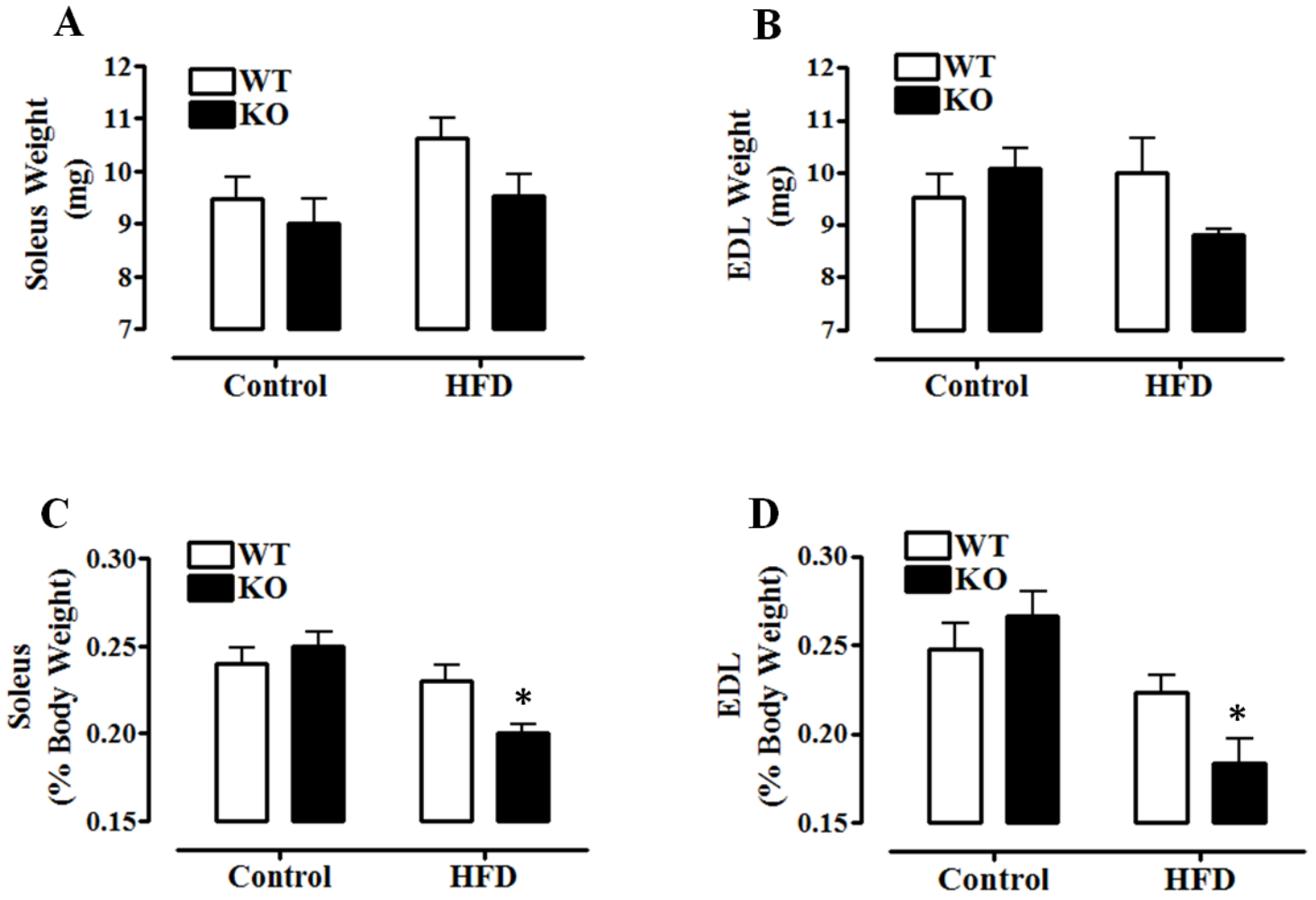

Fgure 3.3. Skeletal muscle (soleus and EDL) weights for chow fed control and HFD, wild type (WT) and *Sln*-null (KO) mice. (A) Soleus weight; (B) EDL weight; (C) soleus % body weight; (D) EDL % body weight. Soleus and EDL % body weight showed a main effect ($P<0.0006$) of diet with HFD<control. * Significantly different ($P<0.05$) than WT. Values are means±SE (n=11 for WT control; n=12 for KO control; n=17 for WT HFD and n=16 for KO HFD).

CLAMS measurements

All CLAMS data for WT and KO mice pre and post HFD are found in Table 3.1. All three relative VO_2 measurements demonstrated a main effect ($P< 0.0001$) of time with post values being less than pre diet values. Planned comparisons revealed that post waking and total daily VO_2 were higher ($P<0.05$) in WT mice compared to KO mice. Unlike relative VO_2, absolute daily VO_2 was higher post HFD compared with pre diet but only a main effect ($P<0.0001$) was observed with no differences between KO and WT mice. Food intake (g) also demonstrated a main effect ($P<0.0001$) of time with post HFD intake being lower than pre diet, and there was a tendency for higher ($P<0.08$) food intake at post HFD in WT mice compared with KO mice. The smaller quantity (g) of high fat food eaten by both WT and KO mice post HFD was calculated to have the same amount of metabolizable energy as the standard rodent chow eaten during pre CLAMS measurement (3.11 kcal/g for standard chow versus 4.5 kcal/g for the HFD). The tendency for lower food intake by KO mice compared to WT post diet could potential be explained by alterations in food consumption during the later stage of the HFD in KO mice as a consequence of elevated fatty acid oxidation and serum NEFA levels both which are known to diminish appetite (Scharrer, 1999; Friedman and Halaas, 1998). There were no differences in either total or dual beam activity counts between KO and WT mice either pre or post HFD. A main effect ($P<0.0001$) of time was also found for all three respiratory exchange ratio (RER) values with pre values being higher than post HFD values. Planned comparisons revealed that both total and waking RER post HFD were higher ($P<0.008$) in WT mice compared with KO mice, with a similar trend ($P<0.056$) observed for sleeping RER.

Table 3.1. Basal metabolic CLAMS measurements from wild type (WT) and *Sln*-null (KO) mice at pre and post HFD.

	PRE		POST	
	WT	**KO**	**WT**	**KO**
Body Weight (g)	33.3±0.9	31.8±0.8	46.7±1.2*	47.9±1.5*
Waking VO_2 (ml O_2/kg/hr)	3237±84	3147±63	2894±97*	2708±61*#
Sleeping VO_2 (ml O_2/kg/hr)	2552±60	2597±58	2358±59*	2254±65*
Total daily VO_2 (ml O_2/kg/hr)	3000±71	2965±52	2708±71*	2553±57*#
Food Intake (grams)	5.09±0.16	4.76±0.17	3.65±0.17*	3.21±0.17*
Total Activity	11327±745	10670±623	10150±822	8984±563
Dual Beam Activity	3262±302	2723±146	3253±393	2674±255
Daily VO_2 (ml O_2/Hr)	96.4±2.81	92.1±2.4	121.6±3.39*	119.7±3.3*
Waking RER	1.020±0.008	1.009±0.004	0.915±0.01*	0.892±0.007*#
Sleeping RER	0.999±0.014	0.979±0.008	0.895±0.011*	0.871±0.011*
Total RER	1.016±0.007	1.006±0.004	0.913±0.009*	0.889±0.007*#

Main effect of time (Pre > Post) for Body Weight ($P<0.0001$), Waking, Sleeping and Total VO_2 ($P<0.0001$), Food Intake ($P<0.0001$), Total Activity ($P<0.007$), and Waking, Sleeping and Total RER ($P<0.0001$). Main effect of time (Pre < Post) for Daily VO_2 ($P<0.0001$). * Significantly different ($P<0.05$) from Pre. # Significantly different ($P<0.05$) than WT. VO_2, oxygen consumption; RER, respiratory exchange ratio. Values are means ± SE (n=17 for WT and n=16 for KO).

Western blotting analysis

Semiquantitative Western blotting was used to examine potential compensatory changes in levels of the major Ca^{2+} regulatory proteins in the SR of the soleus and white gastrocnemius muscles and BAT, in response to the HFD in both KO and WT mice. UCP-3 content was also assessed in soleus muscle. There were no effects of diet on the expression levels of SERCA1a, SERCA2a, CSQ or PLN in the soleus muscle and there were no differences between KO and WT mice in either group (Figure 3.4). Comparisons between HFD and control chow fed mice show that SLN in the soleus muscle of WT mice was elevated ($P<0.02$) by 379% in response to the HFD (Figure 3.4). The white gastrocnemius also showed no differences in SERCA1a, CSQ and PLN between any of the 4 groups; SERCA2a and SLN were not detectable (Figure 3.5A). In BAT, no differences in SERCA1a were found between any of the groups; SERCA2a and SLN were also not detectable. Of interest, PLN content in BAT of WT and KO mice was 213.5% higher ($P<0.003$) in the HFD group than the chow fed control group (Figure 3.5B). UCP-3 content in soleus was not different ($P>0.05$) between control and HFD WT mice; however control KO mice had significantly higher ($P<0.025$) UCP-3 content compared to HFD KO mice (Figure 3.6).

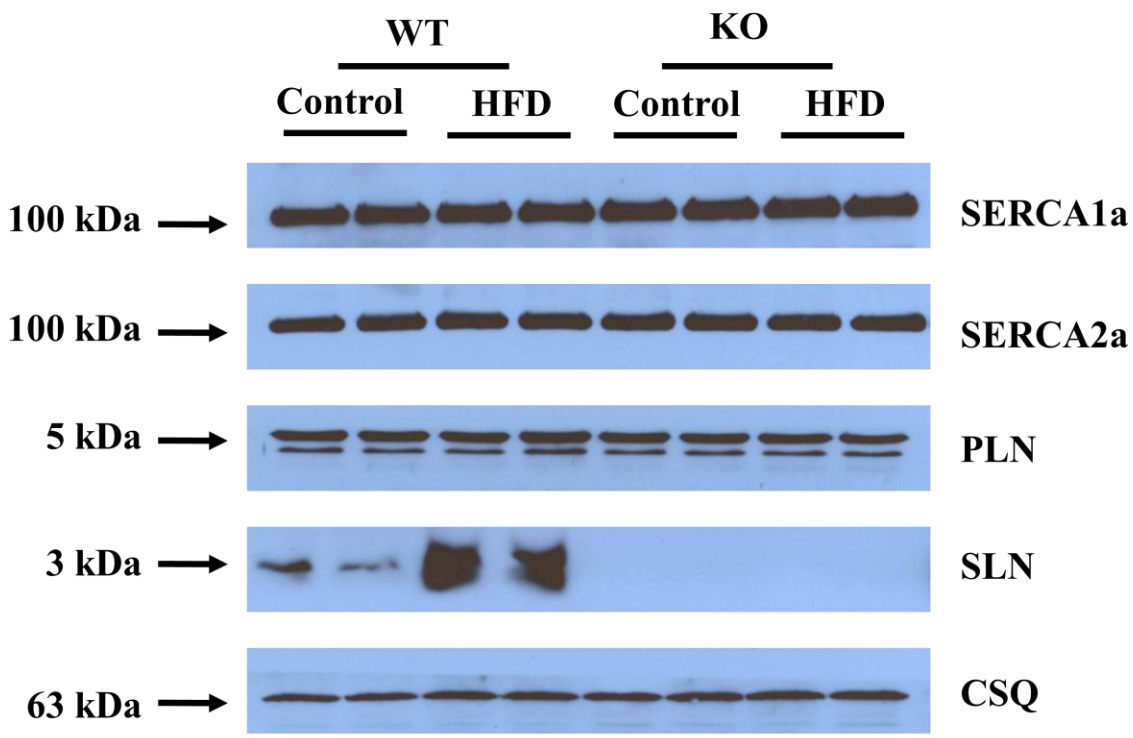

Figure 3.4. Representative Western blot analysis of SR Ca^{2+} regulatory proteins in soleus muscle from chow fed control and HFD, wild type (WT) and *Sln*-null (KO) mice. CSQ was used as a loading control. The loading control sample from only one of the membranes is shown. Different SDS-PAGE gel concentrations (8% for SERCA1a, SERCA2a and CSQ, 15% for PLN or 16% tricine gel for SLN) were used to resolve total homogenates from both WT and KO mice. Equal quantity of protein was loaded in each well. PLN, phospholamban; CSQ, calsequestrin.

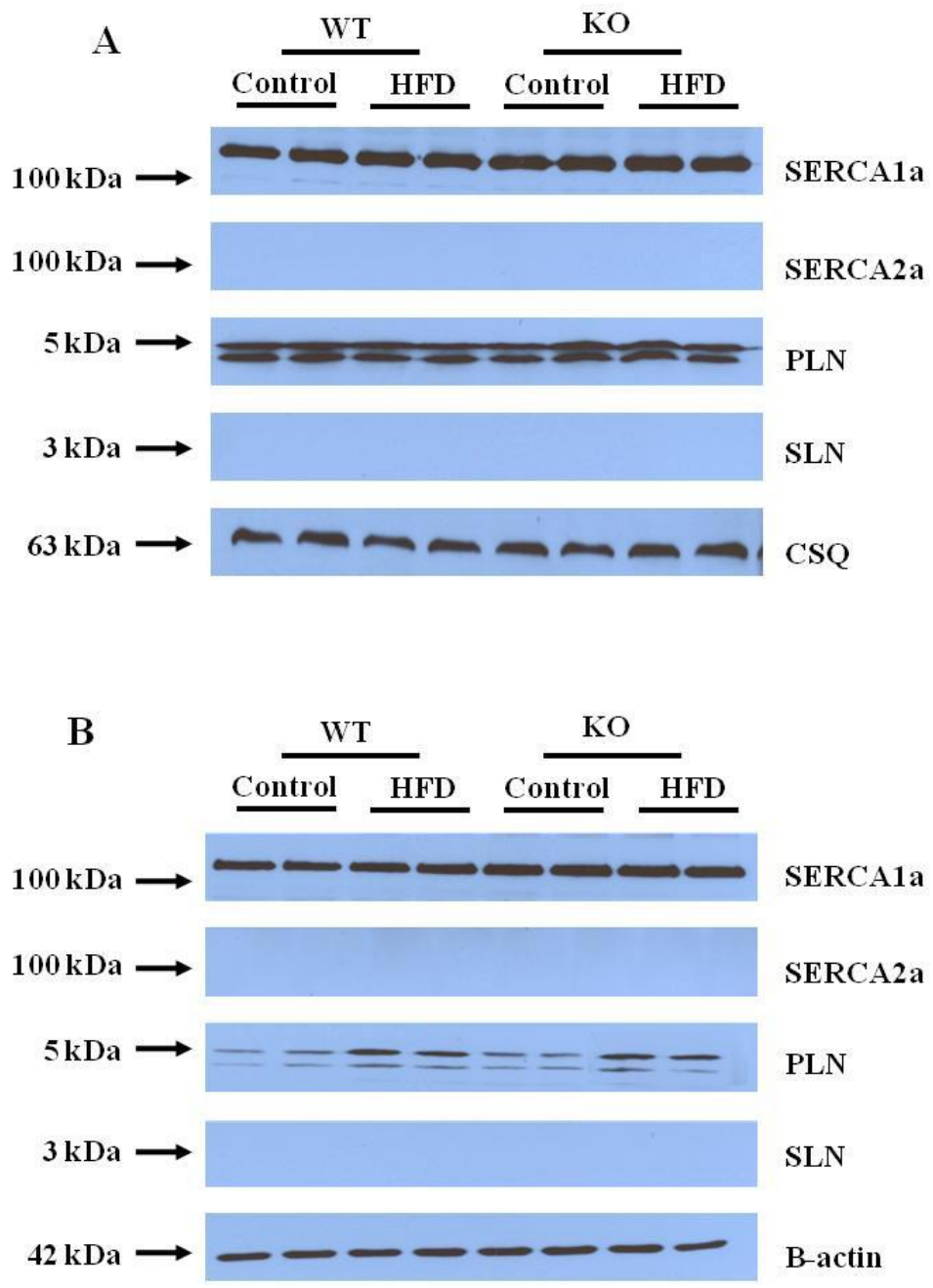

Figure 3.5. Representative Western blot analysis of SR Ca^{2+} regulatory proteins in white gastrocnemius muscle and brown adipose tissue (BAT) from chow fed control and HFD, wild type (WT) and *Sln*-null (KO) mice. (A) White gastrocnemius; (B) BAT. CSQ and β-actin were used as a loading control respectively. The loading control sample from only one of the membranes is shown. Different SDS-PAGE gel concentrations (8% for SERCA1a, SERCA2a and CSQ, 15% for PLN or 16% tricine gel for SLN) were used to resolve total homogenates from both WT and KO mice. Equal quantity of protein was loaded in each well. PLN, phospholamban; CSQ, calsequestrin.

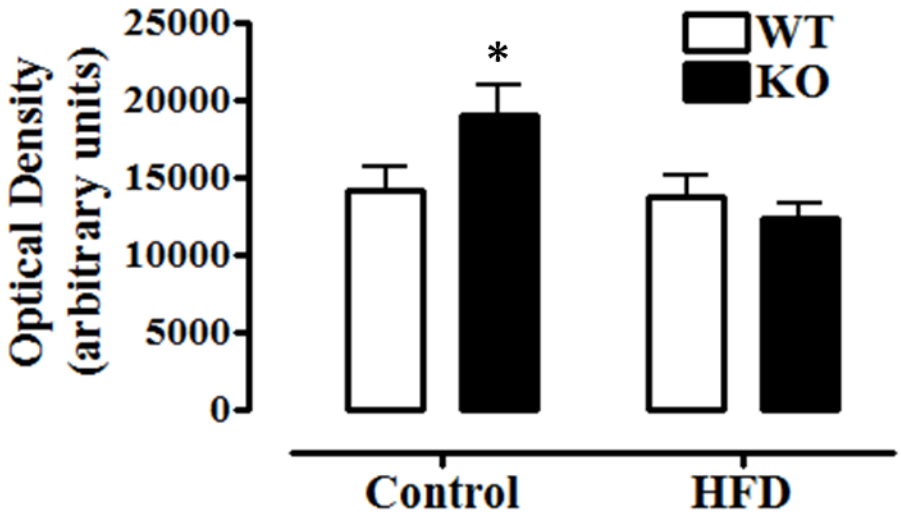

Figure 3.6. Uncoupling protein-3 (UCP-3) content in soleus from chow fed control and HFD, wild type (WT) and *Sln*-null (KO) mice. Optical density (arbitrary units) of UCP-3 bands for WT and KO mice. * Significantly different ($P<0.05$) than all other values. Values are means ± SE (n=6).

Glucose and insulin tolerance tests

GTT were performed on WT and KO mice pre and post HFD (Figure 3.7). There were large differences between pre and post diet responses with the glucose values being lower ($P<0.0001$) at all time points during pre diet tests compared with post diet tests in both WT and KO mice (Figure 3.7). In addition, a significant interaction ($P<0.03$) was found showing greater glucose intolerance (higher glucose levels) post HFD in KO mice compared with WT mice. Main effects were also found for genotype ($P<0.02$), with WT mice having lower blood glucose concentrations than KO mice, and for time ($P<0.0001$), where glucose was lowest at 0 min, followed by 120 min, 60 min and 30 min.

ITT were also performed on WT and KO mice pre and post HFD (Figure 3.8). There was a main effect ($P<0.0001$) of diet with higher glucose levels observed post HFD in both WT

and KO mice (Figure 3.8). There was also a main effect ($P<0.0001$) of time where glucose levels were found to be highest at 0 min, followed by 120 min and 60 min, which was not different than 30 min. There were no differences between WT and KO mice at any time point either pre or post HFD.

Blood parameters

Fasted serum glucose and insulin levels demonstrated a main effect ($P<0.001$) of HFD with chow fed control values being lower than HFD (Figure 3.9). Planned comparisons showed that insulin levels tended ($P<0.08$) to be higher in the KO mice compared to WT mice post HFD (Figure 3.9B). NEFA levels after a 4 hr fast tended ($P<0.07$) to show an interaction and further planned comparisons revealed higher ($P<0.03$) NEFA levels in KO mice compared to WT mice post HFD (Figure 3.10A). There were no effects of HFD or genotype on serum TAGs (WT, 59 ± 7.4 mg/dl for control versus 49.7 ± 6.1 mg/dl for HFD; KO, 61.4 ± 4.9 mg/dl for control versus 50.9 ± 5.8 mg/dl for HFD). As expected, there was a main effect ($P<0.0001$) of HFD on leptin levels, with higher levels found in the HFD group compared with chow fed control; however, there were no differences between WT and KO mice (Figure 3.10B). Plasma NE and E levels were elevated ($P<0.01$) post HFD but only in the KO mice and there were no differences between WT and KO mice in the chow fed control group (Figure 3.11). Total serum cholesterol and its two major components, low density lipoproteins (LDL) and high density lipoproteins (HDL), all demonstrated a main effect ($P<0.0001$) of diet with higher levels in HFD compared to chow fed control mice (Figure 3.12). Planned comparisons

revealed higher ($P<0.05$) levels of LDL in KO mice compared to WT mice post HFD (Figure 3.12A). Total cholesterol also tended ($P<0.07$) to be higher in KO mice compared to WT mice post HFD (Figure 3.12C).

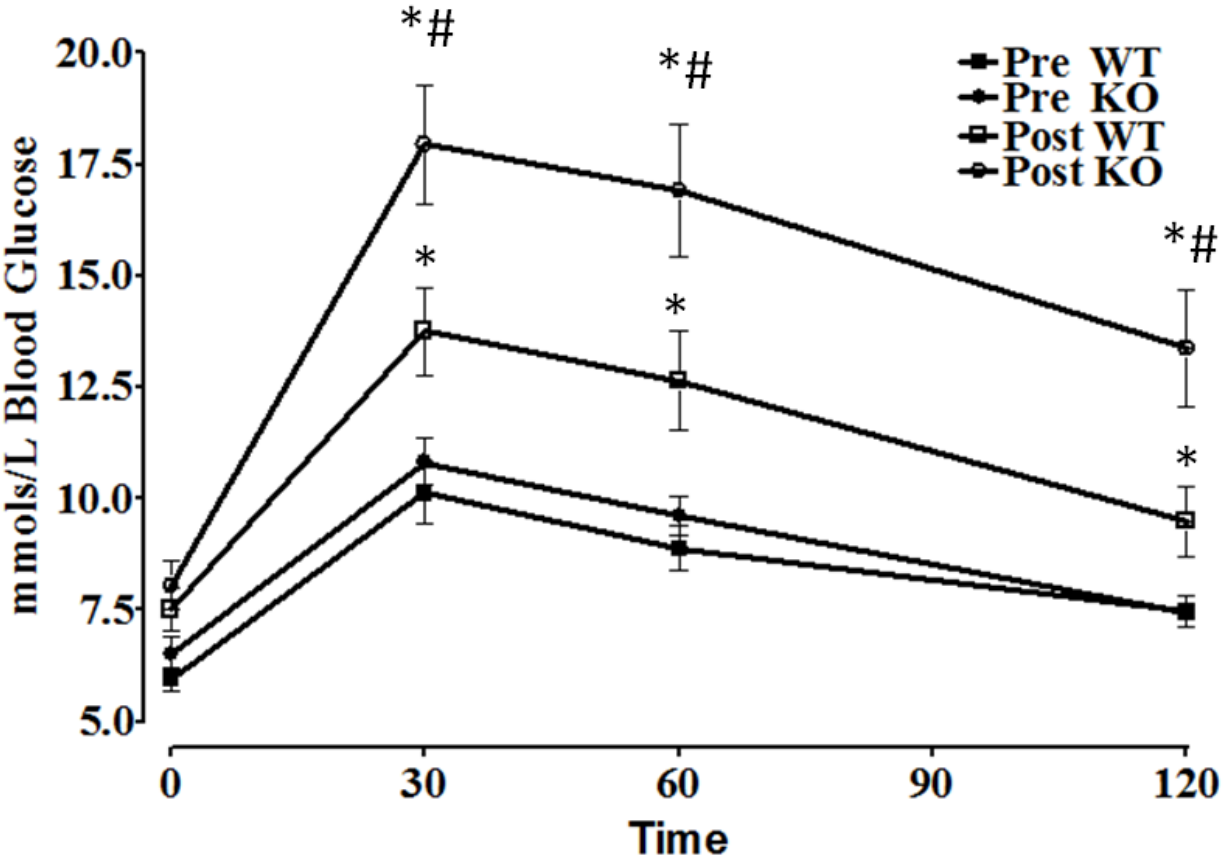

Figure 3.7. Glucose tolerance responses for wild type (WT) and *Sln*-null (KO) mice pre and post 8 week HFD. Main effect ($P<0.0001$) of time, 0 <120<60<30; main effect ($P<0.0001$) of HFD, Pre< Post; main effect ($P<0.02$) of SLN, KO>WT. * Significantly different ($P<0.05$) from Pre. # Significantly different ($P<0.05$) than WT. Values are means ± SE. (n=16 for WT; n=14 for KO).

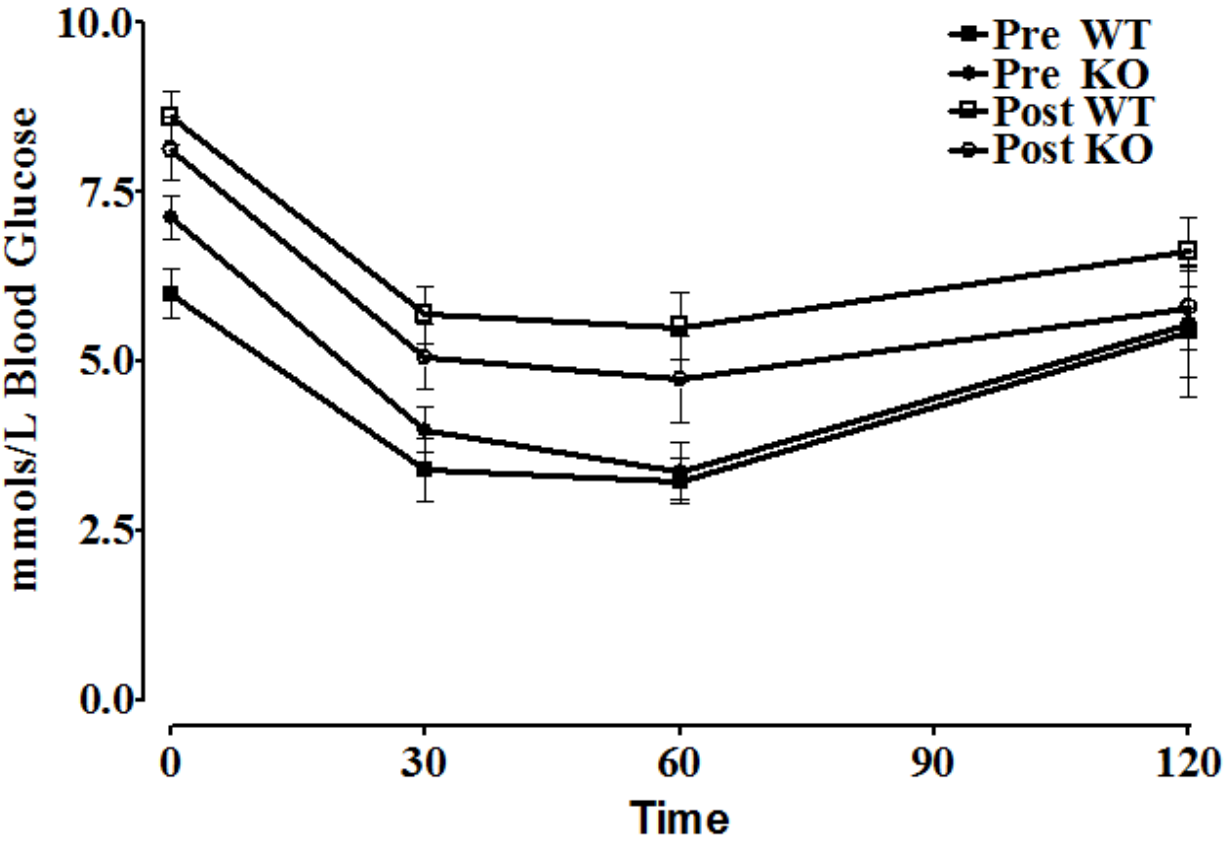

Figure 3.8. Insulin tolerance responses for wild type (WT) and *Sln*-null (KO) mice pre and post 8 week HFD. Main effect ($P<0.0001$) of time, 0 >120>60+30; main effect ($P<0.0001$) of HFD, Pre< Post. Values are means±SE. (n=10).

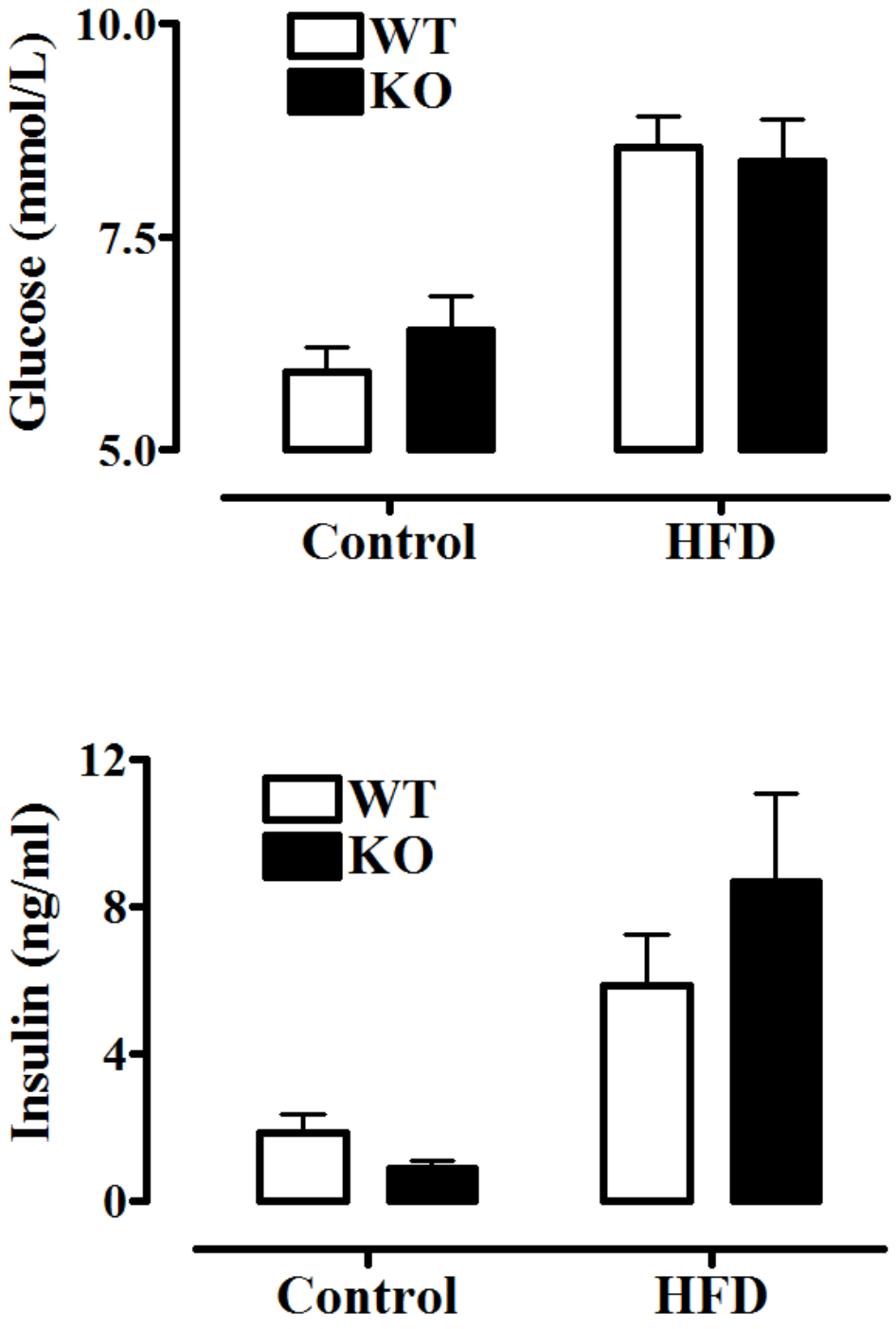

Figure 3.9. Serum glucose and insulin levels post 4 hr fast for chow fed control and HFD, wild type (WT) and *Sln*-null (KO) mice. (A) Serum glucose; (B) Serum insulin. Glucose and insulin levels showed a main effect ($P<0.001$) of diet with HFD>control. Values are means±SE (n=6 for WT control; n=6 for KO control; n=11 for WT HFD and n=11 for KO HFD).

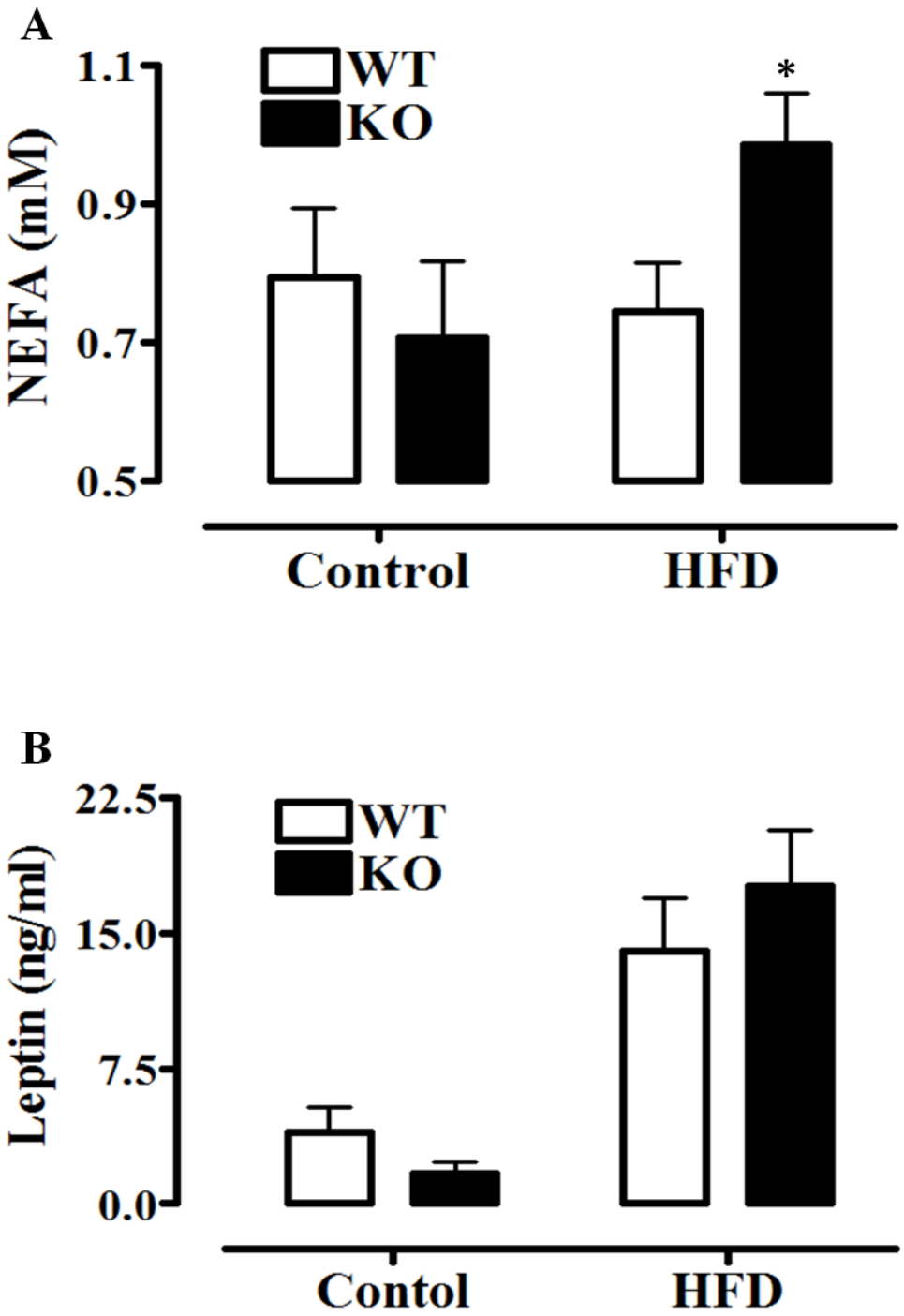

Figure 3.10. Serum NEFA and leptin levels post 4 hr fast for chow fed control and HFD, wild type (WT) and *Sln*-null (KO) mice. (A) Serum non-esterified fatty acid (NEFA); (B) Serum leptin. Leptin levels showed a main effect ($P<0.0001$) of diet with HFD>control. * Significantly different ($P<0.05$) than WT. Values are means±SE (n=6 for WT control; n=6 for KO control; n=11 for WT HFD and n=11 for KO HFD).

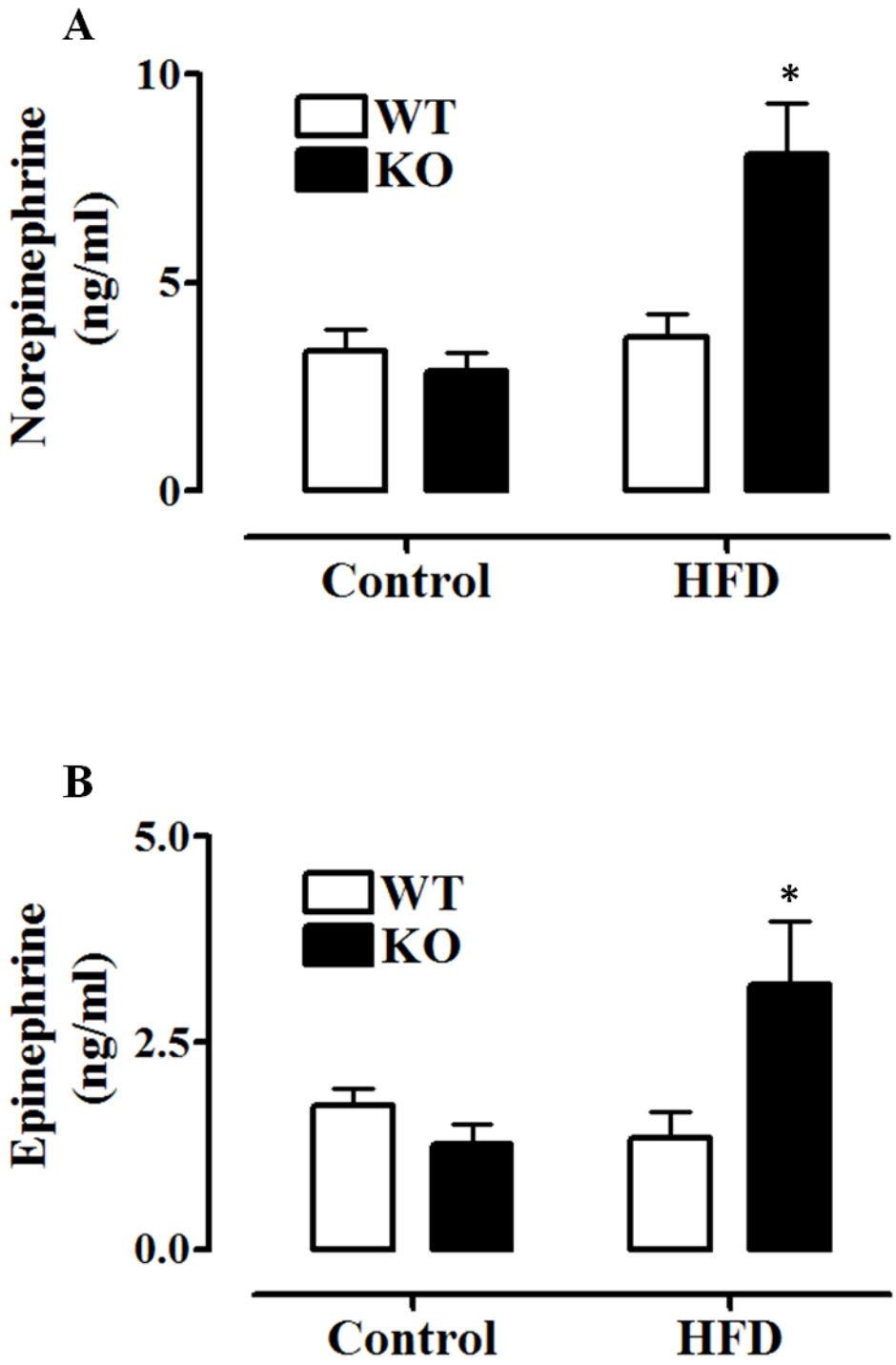

Figure 3.11. Serum norepinephrine (NE) and epinephrine (E) levels post 4 hr fast for chow fed control and HFD, wild type (WT) and *Sln*-null (KO) mice. (A) Serum NE; (B) Serum E. * Significantly different ($P<0.01$) than all other values. Values are means±SE. (n=10 for WT control; n=10 for KO control; n=10 for WT HFD and n=10 for KO HFD).

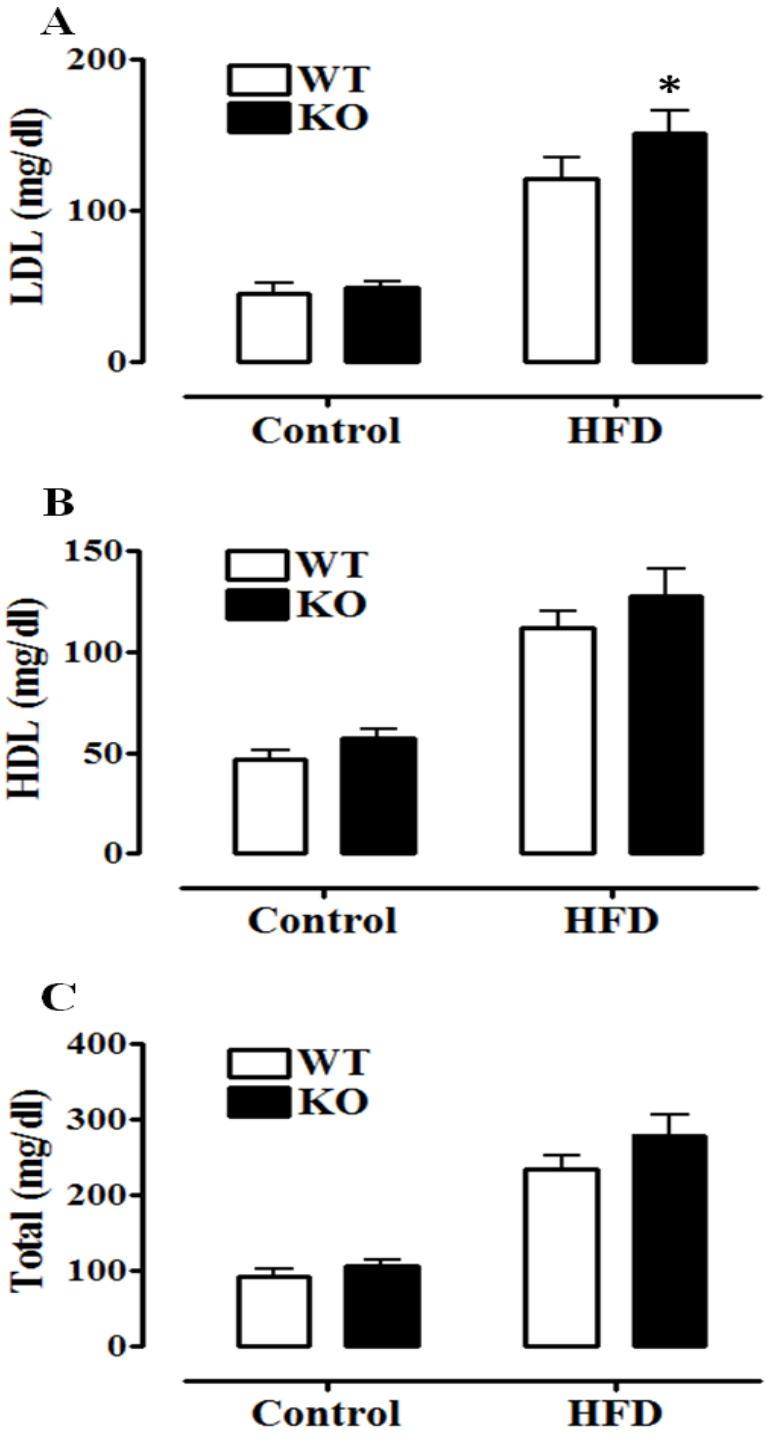

Figure 3.12. Serum LDL, HDL and total cholesterol levels post 4 hr fast for chow fed control and HFD, wild type (WT) and *Sln*-null (KO) mice. (A) Serum LDL; (B) Serum HDL; (C) Serum total cholesterol. All levels showed a main effect ($P<0.0001$) of diet with HFD>control. * Significantly different ($P<0.05$) than WT. Values are means±SE (n=6 for WT control; n=6 for KO control; n=11 for WT HFD and n=11 for KO HFD).

Measurement of VO_2 and SERCA contribution to VO_2 in isolated soleus muscle.

In agreement, with Chapter 2, isolated soleus muscles from both WT and KO mice of the chow fed control group had the same resting VO_2 (Figure 3.13A, left panel). Surprisingly, this was also true for mice in the HFD group where there were no differences in resting VO_2 between WT and KO mice (Figure 3.13A, right panel). There was a main effect ($P<0.006$) of diet with higher soleus VO_2 in HFD mice compared with control. The addition of 10 μM CPA was used to determine the % contribution of SERCA activity to resting muscle VO_2 (Figure 3.12B). There were main effects ($P<0.0001$) of diet and genotype ($P<0.0001$) with SERCA activity from HFD and KO mice contributing a smaller percentage of VO_2. Planned comparisons showed that the difference between WT and KO mice with respect to the percent contribution of SERCA activity to resting muscle VO_2 was larger in HFD mice compared with control mice.

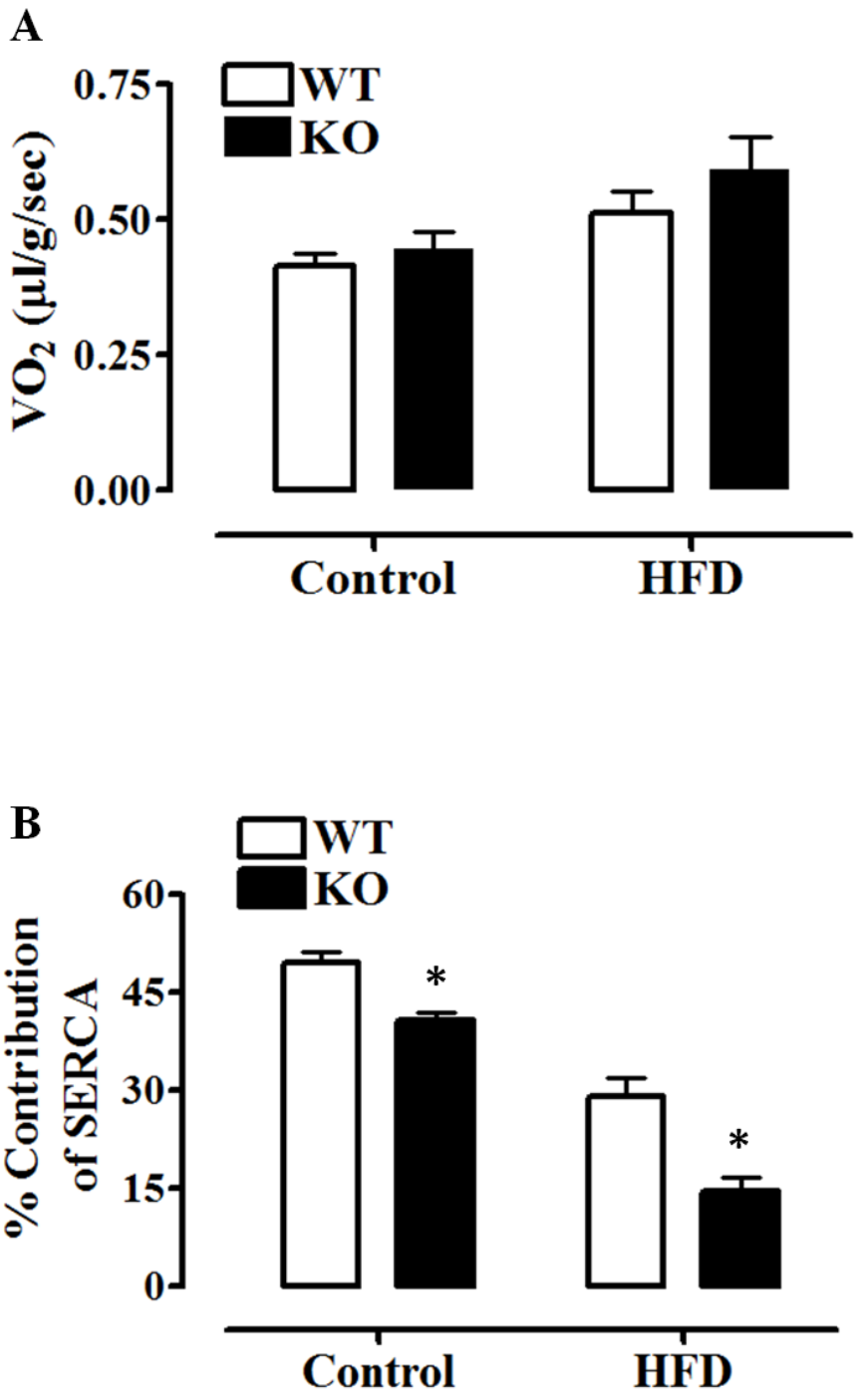

Figure 3.13. Basal oxygen consumption (VO_2) of isolated soleus muscle of chow fed control and HFD, wild type (WT) and *Sln*-null (KO) mice. (A) Basal VO_2; (B) Contribution of SERCA to basal VO_2. Basal VO_2 showed a main effect ($P<0.006$) of diet with HFD>Control. % contribution of SERCA showed a main effect ($P<0.0001$) of diet with HFD<control and a main effect ($P<0.0001$) of SLN with KO<WT. * Significantly different ($P<0.05$) than WT.
alues are means±SE (n=11 for control; n=11 for HFD).

DISCUSSION

This study produced many novel and exciting findings. First, SLN protein content in soleus muscle was highly up-regulated in WT mice and PLN content was also up-regulated in BAT of both KO and WT mice following 8 weeks of high fat feeding, demonstrating for the first time that proteins in skeletal muscle (SLN) and BAT (PLN), other than UCP-1 or UCP-3, may play a role in adaptive thermogenesis. Secondly, the relative contribution of SERCA activity to soleus resting metabolic rate was higher in WT mice than KO mice and, consistent with diet-induced increases in soleus SLN content, this was found to be significantly enhanced by high fat feeding. Third, WT mice were more resistant against diet-induced obesity and glucose intolerance than KO mice likely due to differences in whole body daily metabolic rate, which was higher in WT mice than KO mice following the HFD. Lastly, non-esterified fatty acids (NEFA), low density lipoproteins (LDL), norepinephrine (NE) and epinephrine (E) were all found to be higher in KO mice post HFD which could increase chronic disease risk.

The high fat feeding model is associated with a chronic net positive energy balance where energy intake is greater than energy expenditure resulting in elevated lipid deposits in the fat depots/pads with the ultimate outcome being obesity and associated complications (glucose intolerance and high blood pressure) (for review see Buettner et al., 2007). This has been demonstrated in a variety of species with varying types and different amounts of fat administered to the diet (for review see West and York, 1998). The HFD (TD 88137; Harlan Teklad, Madison, WI) used in this study is regarded as a "Western Diet" containing 0.2% cholesterol and a high portion of fat (42% of kcal derived from fat), the majority (~60%) of which consisted of saturated fats (see Appendix B), which are known to be associated with obesity and related complications (Li et al., 2000).

In this study, it was hypothesized that ablation of SLN would result in blunted adaptive thermogenesis and increased susceptibility to diet-induced obesity and glucose intolerance in mice. The body weights of the WT and KO mice were not different pre or post HFD; however, as hypothesized, the KO mice gained 20% more weight over the 8 week period, demonstrating a higher rate of weight gain from the second week into the HFD until the end of the dietary period (Figure 3.1). The average weight gains observed with 8 weeks of high fat feeding in WT and KO mice are in accordance with other studies using similar high fat diets (Li et al., 2000; Collins et al., 2004). Consistent with data presented in Chapter 2, there were no differences in body weight between WT (37.0±1.2g) and KO (35.3±1.4g) mice that were fed a standard chow rodent diet 22/5 (86540; Harlan Teklad, Madison, WI) and used as controls in this study. The body weights of the control mice were also similar to the pre HFD body weights.

Increased deposit of TAGs into the fat depots is a hallmark of progressive obesity (West and York, 1998) and can be seen in this study with approximately 1.5-3 fold higher fat pad weights in both WT and KO mice post HFD compared to the chow fed control mice (Figure 3.2). Liver weights were also significantly greater post HFD in both WT and KO mice as would be expected, due to greater deposit of lipids during the dietary period (Kontani et al., 2005; DeLanny and West, 2000), but there were no differences between WT and KO mice. As hypothesized, KO mice had a greater quantity of epididymal/inguinal fat compared to WT mice post HFD. Similarly, retroperitoneal fat and BAT weights were also higher (16% and 18%, respectively) in KO mice post HFD but the differences between KO and WT were not statistically significant. Nevertheless, the calculated adiposity index was significantly higher in KO mice, demonstrating a higher degree of obesity in these mice when compared to WT mice.

These data clearly demonstrate higher storage of fats in KO mice due to a greater positive energy balance in these mice compared with WT mice, which is safe to conclude based on the observed differences in weight gain. Not surprisingly, there were no differences in fat pad weights or adiposity index between WT and KO control mice (Figure 3.2), since body weights, food intake and energy expenditure (CLAMS data from Chapter 2) were also not different between these mice.

CLAMS experiments revealed that the differences in energy balance between KO and WT mice that were fed a HFD, which ultimately resulted in greater weight gain and adiposity in KO mice, were due to lower average whole body daily energy expenditure in KO mice than WT mice. Importantly, there were no differences in food intake or cage activity (movement) between WT and KO mice pre or post HFD. In fact, energy intake tended ($P<0.08$) to be lower in KO mice than WT mice post HFD. The lower relative waking and total daily VO_2 ($mlO_2/kg/hr$) observed in KO mice post HFD compared to WT mice, which was not observed in control mice (see Chapter 2), supports the hypothesis that diet-induced adaptive thermogenesis would be blunted in KO mice compared with WT mice, a secondary hypothesis that was related to the primary hypothesis that high fat feeding would result in increased SLN expression and increased energy expenditure in WT skeletal muscle. However, although SLN content in soleus from WT mice was increased 3.8-fold following the HFD (Figure 3.4), which suggests that SLN is an important component of adaptive thermogenesis, energy expenditure in resting soleus from WT mice following the HFD was not higher compared with KO. Therefore, it appears that differences in whole body metabolic rate and obesity observed between WT and KO mice following the HFD are not likely related to adaptive thermogenesis mechanisms in skeletal muscle involving SLN.

Unexpectedly, the contribution of SERCA pump activity to resting metabolism was significantly lower in isolated soleus from both WT and KO mice that were fed the HFD compared with controls. Even though SLN content was approximately 3.8 fold higher in soleus from high fat fed WT mice, ATP consumption by SERCA pumps was actually lower compared with chow fed WT mice (HFD, 110.3±15.5 nmol ATP per g muscle • sec^{-1} versus control, 140.3±8.12 nmol ATP per g muscle • sec^{-1}). This finding is completely paradoxical given that SLN was shown to decrease the coupling ratio of SERCA pumps and increase the ATP consumption by SERCA pumps in resting soleus muscle of chow fed mice (see Chapter 2). However, if there were no increases in SLN expression in WT soleus in response to the HFD, then the decrease in energy consumption by SERCA pumps would have been even greater as was seen in KO mice (HFD, 65.2±12.9 nmol ATP per g muscle • sec^{-1} versus control, 123.5±9.7 nmol ATP per g muscle • sec^{-1}).

Basically 2 main factors could account for the reduction in ATP turnover rate by SERCA pumps in resting muscle that was observed in both WT and KO mice following the HFD: 1) reduced rate of Ca^{2+} leakage out of the SR and/or 2) increased stoichiometry of Ca^{2+} uptake by SERCA pumps (i.e. Ca^{2+}/ATP ratio). Considering that there were no differences in the expression of SERCA isoforms or PLN between WT or KO mice that were fed a HFD and that SLN was increased in soleus from WT mice that were fed a HFD, it could be concluded that the SERCA pump coupling ratio in soleus was likely unaltered in KO mice and decreased in WT mice in response to the HFD. Therefore, to account for the reductions in ATP turnover rates by SERCA pumps in high fat fed mice, Ca^{2+} leakage out of the SR must have been reduced in both WT and KO mice following the HFD. The HFD contained a significant amount of cholesterol and was composed of predominately saturated fatty acids (approx. 60%)

which has been shown to alter phospholipid composition of skeletal muscle membranes and more specifically increase the percent of saturated fatty acids found in the phospholipids of membranes (Janovska et al., 2010). An alteration in the phospholipid membrane composition of the SR, namely increases in saturated fatty acids and cholesterol, has been shown to lower the membrane fluidity and hence reduce the rate of Ca^{2+} leak from the SR/ER (Vangheluwe et al., 2005b).

Despite lower energy consumption by SERCA pumps in resting soleus, basal metabolic rate was increased by 23% ($P<0.08$) in WT mice and 33% ($P<0.03$) in KO mice that were fed a high fat diet. This clearly indicates that other adaptive thermogenic mechanisms were upregulated in soleus from both WT and KO mice post HFD, with these contributing significantly more in KO mice as energy consumption by SERCA pumps was lower in these mice. UCP-3 expression was found to be higher in soleus of KO mice (See Chapter 2) and has been demonstrated to possess similar adaptive thermogenic function as its homologue UCP-1 (Kontani et al., 2005; Gong et al., 1999). Surprisingly, UCP-3 content in soleus muscle was not different between control and HFD WT mice, and was actually lower in the KO mice post HFD compared to chow fed control KO mice (Figure3.6). A similar response has been demonstrated previously, where UCP-3 content in BAT of UCP-1 null mice was lower following consumption of a HFD (42% Kcal from fat) (Kontani et al., 2005). The elevated levels of NEFA found in KO mice post HFD would be expected to accumulate in peripheral non-adipose tissues such as liver and skeletal muscle resulting in increased intracellular TAGs and accompanying lipid signalling molecules, such as long chain acyl CoAs, diacylglycerols (DAGs) and ceramides (for review see Muoio and Newgard, 2009; Bonen et al., 2006). Yang et al. (2009) found that ceramides directly induce elevated expression of suppressor of cytokine

signalling-3 (SOC-3) in adipose tissue, which inhibits UCP-3 gene transcription. A decrease in UCP-3 transcription could potentially explain the lower UCP-3 protein expression found in KO mice following HFD compared to control KO values.

Potentially, an increase in substrate cycling between *de novo* lipogenesis and lipid oxidation could account for the non-SERCA dependent increases in resting VO_2 that were observed following the HFD in both WT and KO mice. The higher fatty acid oxidation in both WT and KO mice post diet as demonstrated by the lower RER values (Table 3.1) accompanied with the higher serum leptin levels (Figure 3.10), which has been shown to induce thermogenesis through substrate cycle (Solinas et al., 2004), support this possibility (Dullo et. al., 2004; Summermatter et al., 2008). In addition, the more pronounced decrease in waking and total RER of KO mice compared to WT mice suggest an even greater dependence on fatty acid oxidation as a fuel source, which has been shown to decrease appetite and hence food intake (Scharrer, 1999) as well as enhance thermogenesis, both leading to enhanced resistance to obesity (for review see Biddinger et al., 2006).

NE and E are both markers of sympathetic nervous system (SNS) activity and it is well established that increased SNS activity augments energy metabolism and thermogenesis (Maickel et al., 1967; Cannon and Nedergrad, 2003). The catecholamine (NE and E) levels in WT mice post HFD were not different from the chow fed control group which is consistent with previous work by Chan et al., (2005) and Chen and Li (2005) who also did not see an increase in plasma NE or E in rats after a 7 week HFD. However, NE and E were found to be 2.2-2.4 fold higher in HFD KO mice compared to both WT and KO control mice (Figure 3.11A and B). Hindlimb perfusion experiments in rats (Shiota and masumi, 1988) and Muscovy duckling (Marmonier et al., 1997) have both demonstrated NE to stimulate skeletal

muscle VO_2 potentially through increased activity of the Na^+-K^+ ATPase (Clausen, 1986; Shiota and Masumi, 1988). It has also been postulated that catecholamines may augment the fat lipolysis/*de novo* synthesis futile cycle through AMPK activation in skeletal muscle (Dulloo et al., 2004). The elevated levels of serum catecholamines are also known to activate Gs-coupled receptors in adipocytes, stimulating adenylyl cyclase which gives rise to elevated cyclic AMP, ultimately activating hormone sensitive lipase resulting in elevated levels of serum NEFA (For review see Amhadian et al., 2007). The elevated SNS activation witnessed in KO mice would explain the higher NEFA plasma levels and the elevated fatty acid oxidation (lower RER) seen in KO mice post HFD. Therefore the higher catecholamine levels found in KO mice post HFD could partly account for the similar basal muscle VO_2 between WT and KO mice post HFD even though ATP consumption by SERCA pumps was lower in KO mice.

Since skeletal muscle basal metabolism is not different and therefore cannot account for the differences seen in whole body daily energy expenditure and susceptibility to diet-induced obesity and glucose intolerance between WT and KO mice, other potential factors must be considered. Interestingly, soleus and EDL weights both tended to be lower (Soleus, $P<0.08$; EDL, $P<0.1$) in KO mice post HFD which became significant when muscle weights were expressed as a % of body weight (Figure 3.3C and D). Taken with the adiposity data (Figure 3.2), it is clear that the greater weight gain in KO mice was associated with greater fat deposits and not an increase in lean body mass. More importantly, this lower proportion of skeletal muscle may explain the lower whole body metabolic rate in KO mice post HFD, as skeletal muscle is a highly metabolically active tissue and has been shown to make up a considerable portion of daily energy expenditure (Zurlo et al., 1990; Rolfe and Brown, 1997). The lower skeletal muscle weights (% of body weight) post HFD in the KO mice could be due to lower

cytosolic $[Ca^{2+}]_f$ in KO mice compared to WT mice given that SLN increases slippage of SERCA pumps, potentially causing increased cytosolic $[Ca^{2+}]_f$ in WT muscle. Ca^{2+} is a potent signalling molecule in skeletal muscle that activates Ca^{2+}/calmodulin-dependent kinases (CAMKs) and the Ca^{2+}-dependent phosphatase (i.e. calcineurin) which are both implicated in the activation of transcription factors involved in skeletal muscle hypertrophic growth, development and regeneration (for reviews see Chin, 2005 and Mallinson et al., 2009).

The greater differences between WT and KO mice found in waking compared to sleeping whole body metabolism post HFD in addition to the greater (5%; not significant) VO_2 measured during low running speeds in WT mice (See Chapter 2) suggest that the elevated level of SLN found in the WT mice post diet could have a greater effect on skeletal muscle energy expenditure during sub-maximal contractions. This is one reason not to dismiss the importance of SLN in adaptive thermogenesis as a potential mechanism underlying the increased resistance to obesity in WT mice. The cost of ATP utilization by SERCA pumps in isolated soleus subjected to sub-maximal electrical stimulation in WT and KO mice following the HFD may provide some important insight into the lower basal metabolic rate found in KO mice post diet.

The influence of SLN on energy expenditure of other metabolically active organs including the brain, liver and kidney (Rolfe and Brown, 1997) and their contribution to whole body energy expenditure can not be ignored given that measurable quantities of mRNA have been detected in these organs (European Molecular Biology Laboratory-European Bioinformatics Institute EMBL-EBI, 2010). The role of UCP-1 in BAT should also not be dismissed as it is a powerful thermogenic agent that has been demonstrated to be implicated in adaptive thermogenesis (Lowell and Spiegelman, 2000). UCP-1 protein was not measured in

this study, however, for the first time to the author's knowledge, another protein other than UCPs was shown to be elevated in BAT as a consequence of high fat feeding. PLN was found to be 2.1 fold higher in BAT of both WT and KO mice post HFD (Figure 3.5B) suggesting that PLN may be involved in adaptive thermogenesis in BAT. PLN, a homologue of SLN, has the similar capacity to uncouple Ca^{2+} transport from ATP hydrolysis in SERCA (Frank et al., 2000). The elevated SLN content in skeletal muscle and PLN in BAT following a HFD demonstrates that modulation of Ca^{2+} handling is important to energy expenditure and could potentially play a role adaptive thermogenesis in BAT and skeletal muscle. This notion is supported by the finding of Ukropec et al., (2006) who found elevated PLN levels in white adipose tissue as well as SERCA2a following cold exposure in UCP-1 null transgenic mice. Further supporting this notion is the previously stated thermogenic effects of Ca^{2+} handling seen in malignant hyperthermia (Denborough, 1998) and in the heater organ of deep sea fish (Morrisette et al., 2003).

Regardless of the precise mechanisms underlying the lower total whole body metabolic rate in KO mice, the fact still remains that KO mice become more obese and glucose intolerant compared to littermate WT mice when placed on a HFD. Glucose tolerance responses in WT and KO mice were not different pre HFD. Both WT and KO mice demonstrated glucose intolerance following the HFD; however, as hypothesized, KO mice showed a greater severity of glucose intolerance than the WT mice post HFD (Figure 3.7). These results are in agreement with a previous high fat feeding study which also demonstrated glucose intolerance following a HFD using the same 'western' diet (TD 88137) as in the present study (Li et al., 2000). These data suggest impaired glucose uptake by skeletal muscle and hence insulin resistance, both of which are conditions seen in the pre-stage of type 2 diabetes (Petersen and

Shulman, 2002; Bonen et al., 2006). Accordingly, fasted serum glucose and insulin values were elevated post HFD in both WT and KO mice (Figure 3.9) which has been repeatedly demonstrated in other HFD studies (Ste Marrie et al., 2005; Kus et al., 2008; Janovska et al., 2010). Serum insulin levels were 48% higher in the KO mice compared to WT post HFD but did not show significance ($P<0.08$), insinuating greater insulin resistance in skeletal muscle of the KO mice.

Insulin tolerance tests (ITT) were performed to assess the effects of the HFD on whole body insulin sensitivity in KO and WT mice. Surprisingly, there were no differences between KO and WT mice in ITT responses either pre or post HFD; however, pre diet values were lower in both WT and KO mice than post HFD as would be expected with elevated glucose levels associated with obesity (Figure 3.8) (Shanik et al., 2008). This is not the first study to find dissociation between GTT and ITT responses in mice fed a HFD (Hojman et al., 2009). Another study by Bruning (1998) found normal ITT response in transgenic mice lacking (>95% reduction) muscle insulin receptors; however, upon further examination using the hyperinsulinemic-euglycemic clamp technique, these mice showed severe insulin resistance. The ITT does not provide precise estimates of insulin sensitivity or tissue specific glucose disposal and compensatory homeostatic mechanisms may have also confounded the current results (Muniyappa et al., 2008). A better approach to measuring insulin sensitivity is the hyperinsulinemic-euglycemic clamp technique which is considered the "gold standard" (Kim, 2009; Muniyappa et al., 2008); however, these tests could not be performed at our facility due to lack of infrastructure and expertise. Pancreatic dysfunction, specifically failure of β-cells, is another possible explanation for the greater whole body glucose intolerance observed in high fat fed KO mice given that Ca^{2+} cycling is known to be intimately involved in the insulin

secretion process (Henquin, 2009) and that SLN mRNA has been found in high quantities in the pancreas (European Molecular Biology Laboratory-European Bioinformatics Institute EMBL-EBI, 2010). Accordingly, KO mice may be more susceptible to diet-induced "β-cell failure" which could contribute to the development of glucose intolerance in high fat fed KO mice. Further assessment of peripheral insulin sensitivity and insulin secretion from pancreas in KO and WT mice before and after consuming a HFD would provide critical information on the role of SLN in diet-induced glucose intolerance.

The greater glucose intolerance found in KO mice post HFD (Figure 3.7B) accompanied with higher NEFA (Figure 3.10A) and insulin levels ($P<0.08$; Figure 3.9B) in the fasted serum samples would suggest a greater impairment in glucose uptake by skeletal muscle as a result of impaired insulin signalling and decreased translocation of glucose transporter, GLUT 4. It has been shown that acute intralipid-heparin infusion in humans induces skeletal muscle insulin resistance through inhibition of GLUT 4 translocation (Boden et al., 1994; Roden et al., 1996; Dresner et al., 1999). As previously stated, elevated levels of NEFA found in KO mice post HFD would be expected to result in increased intracellular TAGs, DAGs, ceramides and long chain acyl CoAs (for review see Muoio and Newgard, 2009; Bonen et al., 2006). The accumulation of DAGs within skeletal muscle has been shown to activate protein kinase C (PKC) thereby blunting tyrosine phosphorylation of insulin receptor substrate (IRS)-1 thus decreasing the activation of phosphatidylinositol (PI)-3 kinase (Griffin et al., 1999; Moro et al., 2009); while ceramides have been shown to inhibit the activation of Akt, downstream of PI-3-kinase (Chavez et al., 2003). Both of these actions ultimately lead to a decrease in GLUT 4 translocation and glucose transport into skeletal muscle and liver, the primary glucose depots (Okada et al., 1994; Hegarty et al., 2003).

Other potential mechanisms which may explain the greater glucose intolerance found in KO mice compared to WT mice post HFD include: 1) lower levels of adiponectin, an insulin sensitizing agent (Dyck et al., 2006) associated with greater obesity (Arita et al., 1999) and/or 2) greater inflammation of adipose tissue associated with hypertrophy of adipocytes resulting in elevated levels of circulating TNF-α and other cytokines (Guilherme et al., 2008). The greater adiposity index found in KO mice following HFD would suggest that both of these mechanisms may be implicated in the greater glucose intolerance, as both of these mechanism have been shown to decrease glucose uptake (for reviews see Dyck et al., 2006 and Guilherme et al., 2008).

The greater susceptibility to diet-induced obesity and glucose intolerance found in the KO mice make it an interesting model for examining type 2 diabetes. The accompanying higher fasted serum NEFA and LDL level (38% and 24% respectively) found in KO mice post HFD compared to WT mice (Figure 3.10A and 3.12A) place the KO mice at greater risk of coronary heart disease. Moreover, the chronically elevated catecholamine levels found in KO mice following the HFD, results in over-stimulation of the SNS which increases the risk of hypertension (for review see Reaven et al., 1996). The data from the present study indicate that the *Sln*-null transgenic mice may be a novel model for examining metabolic syndrome as it possesses many of the pathophysiological symptoms found with this disease (Kennedy et al., 2010)

One of the major limitations of this study was the inability to continuously monitor the mice on the CLAMS throughout the entire high fat dietary period. This would have allowed for a more in-depth examination of food consumption (i.e. energy intake) and energy expenditure during the early portion of the study. More importantly, early metabolic measures may have

revealed greater differences between WT and KO mice as the upregulation of SLN in skeletal muscle may have preceded adaptations in other thermogenic processes. This is another reason why the importance of SLN in adaptive thermogenesis and increasing resistance to obesity should not be discounted. Future studies should examine the time course of these adaptive thermogenic processes by employing shorter high fat dietary periods.

In summary *Sln*-null (KO) mice gained more weight and became more obese potentially due to the lower daily energy expenditure found in KO mice compared to WT mice after consuming the HFD. Western blotting analyses revealed SLN protein content to be 3.8 fold higher in WT soleus post HFD and PLN to be 2.1 fold higher in BAT of both WT and KO mice post HFD. Collectively, these results suggest that PLN and SLN may play a role in adaptive diet-induced thermogenesis. On the other hand, compared with chow fed control mice, the metabolic cost of Ca^{2+} handling in soleus muscle was significantly reduced post HFD in both WT and KO mice, although to a greater extent in KO mice than WT mice. Moreover, there were no differences in resting energy expenditure of soleus muscles between WT and KO mice following the HFD. Therefore, differences in whole body metabolic rate and obesity between WT and KO mice post HFD do not appear to be due to adaptive thermogenic mechanisms in resting skeletal muscle involving SLN. Lower percent of lean body mass in KO mice post diet as implied by the lower EDL and soleus weights (% body weight) may explain the lower metabolic rate and associated obesity found in KO mice. Overall, it can be concluded that SLN increases resistance to diet-induced obesity and glucose intolerance in mice but the precise mechanisms involved remain to be determined.

CHAPTER IV

GENERAL DISCUSSION, CONCLUSION AND FUTURE DIRECTIONS

DISCUSSION

The primary objectives of the research in this thesis were to first determine if physiological levels of sarcolipin (SLN) results in "slippage" of the sarco(endo)plasmic reticulum Ca^{2+} ATPase (SERCA) pumps in skeletal muscle *in vivo* through the use of a *Sln*-null (KO) mouse model**.** Specifically, it was hypothesized that the efficiency (Ca^{2+} transported into lumen per ATP hydrolyzed) of the SERCA pumps measured in skeletal muscle homogenates from wild type (WT) mice, under conditions in which a Ca^{2+} gradient was preserved across the SR vesicles, would be lower compared with KO mice. A secondary aim was to examine the hypotheses that a decrease in SERCA pump efficiency would result in greater energy utilization at rest by isolated soleus muscle and increased whole body metabolism. Lastly, WT and KO mice were fed *ad libitum* a "Western" style high-fat diet (HFD) with 42% of kcal derived from fat and 0.2% cholesterol (product 8728CM, Harlan Teklad) for 8 weeks, to examine the involvement of SLN and Ca^{2+} handling in adaptive thermogenesis and diet-induced obesity and associated health complications (i.e. glucose intolerance). Even if SLN ablation did not reduce resting skeletal muscle or whole body metabolic rate in chow fed mice, it was postulated that KO mice could be more susceptible to diet-induced obesity and glucose intolerance in response to high fat feeding if SLN expression in skeletal muscle from WT mice is induced by high fat feeding resulting in increased skeletal muscle and whole body energy expenditure compared to KO mice.

SLN was found predominately in highly oxidative skeletal muscles (ie. soleus, red gastrocnemius and diaphragm) which are known to be highly active during waking hours. The lack of SLN protein in brown adipose tissue (BAT) was somewhat surprising as SLN mRNA is fairly abundant in BAT (unpublished data, European Molecular Biology Laboratory-European

Bioinformatics Institute EMBL-EBI, 2010). The research focus of the thesis was to examine the metabolic function of SLN in skeletal muscle and more specifically soleus muscle as it contains a relatively high amount of SLN protein and could be isolated to measure basal metabolism. The major differences between WT and KO mice observed in this thesis appear to be due to ablation of SLN specifically, since there were no compensatory adaptations in other major SR proteins involved in Ca^{2+} handling, specifically SERCA1a, SERCA2a, calsequestrin and phospholamban (PLN), as a result of SLN ablation. Consistent with these results, Babu et al. (2007a) also found SLN ablation to have no effect on other Ca^{2+} handling proteins in the ventricle and atria of *Sln*-null mice.

The uncoupling of Ca^{2+} uptake from ATP hydrolysis has been demonstrated in membranes reconstituted with SLN and SERCAs at ratios as low as 2:1, potentially due to increased rates of "slippage" (Mall et al., 2006; Smith et al., 2002). The decrease in efficiency of the SERCA pumps results in the production of heat as dictated by the first law of thermodynamics which is believed to be a mechanism of maintaining thermal homeostasis within skeletal muscle. SLN is deemed to invoke "slippage" by decreasing the affinity of the SERCA pumps for Ca^{2+}; as it directly binds with SERCA pumps at two of the four transmembrane helixes making up the Ca^{2+} binding sites (Morita et al., 2008; Bhupathy et al., 2007; Odermatt et al., 1998). This is supported by measurements of Ca^{2+} dependent Ca^{2+}-ATPase activity in the absence of a Ca^{2+} gradient, where the pCa_{50} for SERCA activity in soleus homogenates of WT mice was lower compared to KO mice demonstrating that more Ca^{2+} was needed to reach 50% of Vmax in WT mice. This was not observed in the EDL, as SLN protein content is much lower in EDL and has a much smaller effect in the absence of a Ca^{2+} gradient.

This is the first study to show that at a physiological SLN:SERCA pump ratio and in the presence of a Ca^{2+} gradient across the SR, SLN reduces the stoichiometry of SERCA pumps in skeletal muscle at low [Ca^{2+}]. The presence of a gradient allows one to examine the Ca^{2+} pumps under more physiologically relevant conditions. In skeletal muscle there is a 1:10,000 Ca^{2+} gradient across the SR membrane (Rasmussen, 1986) and back inhibition is an important factor affecting SERCA activity, Ca^{2+} uptake and Ca^{2+} leak (Inesi and de Meis, 1989). In the presence of a Ca^{2+} gradient, the coupling ratio (Ca^{2+} uptake / Ca^{2+}-ATPase activity) was higher in soleus homogenates and tended ($P<0.08$) to be higher in EDL homogenates from KO mice. This demonstrates the potent effect of back inhibition on SERCA activity as even the low levels of SLN found in EDL muscle have a tendency to make a difference in the presence of a Ca^{2+} gradient which must be considered when interpreting data from the present and previous studies.

Once it was established that the Ca^{2+} ATPase coupling ratio was higher in soleus homogenates from KO mice, the hypotheses that the basal metabolism (VO_2) of isolated soleus muscles and whole body metabolism (basal, sub-maximal and maximal) would be lower in KO mice compared with WT mice were examined. These hypotheses were not supported based on the findings that there were no differences in resting soleus VO_2 or whole body VO_2, measured at rest or during sub-maximal or maximal treadmill exercise, between KO and WT mice. However, when % contribution of Ca^{2+} handling to basal metabolism was determined using CPA, energy requirements by SERCA pumps were significantly lower (6.8%) in the KO soleus compared to WT, clearly demonstrating the potential influence of SLN as a regulator of energy metabolism in skeletal muscle. The lack of difference in VO_2 suggests other energy consuming processes in the muscle were compensating for the lack of SLN potentially to

maintain muscle temperature. Western blotting analysis revealed higher (34%) mitochondrial uncoupling protein 3 (UCP-3) content in soleus from the KO mice compared to WT mice. It is proposed that an adaptive increase in UCP-3 expression compensates for the absence of SLN which provides further support for the view that SLN is important for the regulation of thermogenesis. However it should be note that other adaptations may have also been a factor in elevating basal metabolism of the isolated soleus muscles in the KO mice.

Phenotypic differences in transgenic mouse models often become more apparent when mice are examined under more extreme conditions that challenge the homeostasis of a number of physiological systems (i.e. HFD, cold exposure, aging, etc). For example, the ablation of UCP-1 protein in mice results in little or no phenotypic differences between KO and WT littermates if mice are fed a standard chow diet; however, these same mice are considerably more susceptible to diet-induced obesity when placed on a HFD (41.9% kcal derived from fat; Kontani et al., 2005). Similar results have also been found with UCP-3 knockout mice (Vidal-Puig et al., 2000). Therefore, to further investigate the function of SLN in skeletal muscle, its role in adaptive thermogenesis and its implications on diet-induced obesity, WT and KO mice were placed on a HFD (42% kcal derived from fat) for an 8 wk period. As was hypothesized, KO mice displayed lower whole body basal metabolic rates when compared to WT littermates post HFD. In accordance with the energy balance equation (3.1), this led to greater energy storage which was demonstrated by the greater weight gain over the 8 wk period, higher epididymal/inguinal fat pad weights and a higher adiposity index in the KO mice post HFD. Surprisingly, KO mice also tended ($P<0.08$) to have a lower caloric intake post diet which potentially could be explained by decreases in food consumption during the later stage of the HFD due to the observed increased fatty acid oxidation and NEFA levels in KO mice, both of

which are known to diminish appetite (Scharrer, 1999; Friedman and Halaas, 1998). Unfortunately, food consumption was not measured during the 8 wk dietary period and, therefore, the latter possibility could not be addressed; future studies should examine this possibility through continuous food monitoring during the dietary period.

The higher adiposity index found in KO mice was accompanied by a greater glucose intolerance compared to WT mice post HFD who also demonstrated glucose intolerance compared to pre HFD values; however, whole body insulin resistance was not observed in either WT or KO mice, at least when assessed by the insulin tolerance test (ITT). The ITT is often criticized as it does not provide precise estimates of insulin sensitivity or tissue specific glucose disposal and compensatory homeostatic mechanisms may also confound results (Muniyappa et al., 2008). A better procedure to use for assessment of whole body insulin sensitivity would have been the hyperinsulinemic-euglycemic clamp technique as it allows for a more direct assessment of insulin sensitivity for a given tissue, limits compensatory homeostatic mechanisms and is considered the "gold standard" (Kim, 2009; Muniyappa et al., 2008). The elevated fasted glucose and insulin levels accompanied with greater glucose intolerance found in both KO and WT mice post HFD support this idea of greater insulin resistance and suggest that the mice were in the pre-stage of type 2 diabetes. The greater dyslipidemia (elevated serum NEFA levels) and insulin levels (48%; $P<0.08$) observed in KO mice accompanied with greater glucose intolerance post HFD compared to WT mice suggest a greater metabolic disturbance and susceptibility to diet-induced obesity and diabetes.

It was hypothesized that KO mice may be more susceptible to diet-induced obesity and glucose intolerance if SLN expression in skeletal muscle from WT mice is induced by high fat feeding and if, as a result of increased SLN expression, skeletal muscle and whole body energy

expenditure were also increased in WT mice compared with KO mice. In agreement with the first postulate, Western blotting analysis revealed a 3.8 fold increase in SLN content of soleus muscle in WT mice following the HFD. Interestingly, there was also a 2.1 fold increase in PLN levels in BAT in both WT and KO mice induced by the HFD. To the author's knowledge, this is the first study to show a diet-induced increase in the content of proteins (SLN and PLN), other than mitochondrial uncoupling proteins, that have been shown to uncouple energy consuming processes in muscle (Mall et al., 2006; Frank et al., 2000), a response which could serve as a potential mechanism for maintaining energy homeostasis. The large increase in SLN protein content of skeletal muscle and PLN in BAT post HFD in WT mice suggests that futile Ca^{2+} cycling in both BAT and skeletal muscle may be enhanced in response to a HFD, which could provide a novel mechanistic basis for adaptive thermogenesis.

Surprisingly, despite increased SLN expression in WT soleus post HFD and in contrast to what was hypothesized, there were no differences in resting VO_2 of isolated soleus muscles between KO and WT mice post HFD. This would suggest that other adaptive thermogenic mechanisms are activated to a greater extent in KO muscle compared with WT muscle in response to the HFD. Elevated serum levels of norepinephrine (NE) and epinephrine (E) found in KO mice post HFD, are known to enhance skeletal muscle VO_2 (Shiota and Masumi, 1988; Marmonier et al., 1997) potentially through increased ion leak resulting in a Na^+/K^+ futile cycle (Clausen, 1986; Shiota and Masumi, 1988). Other potential adaptive compensatory mechanisms in skeletal muscle which may have been responsible for maintaining VO_2, particularly in KO mice, include a fat lipolysis/de novo synthesis futile cycle (Summermatter et al., 2008), increased protein degradation/synthesis (Rolfe and Brown,1997) and protein and metabolite dephosphorylation- phosphorylation (Lowell and Spiegelman, 2000). These energy

"wasting" processes were not investigated in this thesis and remain to be examined in future HFD studies with this transgenic KO mouse model.

Another surprising finding was that the energy expenditure of SERCA pumps contributed significantly less to the basal metabolic rate of isolated soleus muscle from both WT and KO mice post HFD. It is possible that the SR membrane lipid composition was altered by the HFD (i.e. increased saturated fatty acids and cholesterol content) resulting in significantly lower Ca^{2+} leak from the SR (Vangheluwe et al., 2005b). However, the relative contribution of SERCA pumps to basal metabolism was reduced to a much greater extent in KO mice compared to WT mice post HFD which is consistent with the effects of SLN on the SERCA pump coupling ratio.. Therefore, the higher SLN content found in soleus muscle of WT mice post HFD may be viewed as a compensatory mechanism to increase energy expenditure by SERCA pumps in order to help maintain energy homeostasis within the muscle.

Finally, it was also hypothesized that whole body metabolic rate would be higher in WT mice than KO mice following the HFD, specifically because it was assumed that SLN expression and energy expenditure of skeletal muscle would be increased in WT mice following the HFD. Given that basal VO_2 of isolated soleus muscles was not different between WT and KO mice following the HFD, it is somewhat surprising that whole body metabolism was in fact lower in KO mice than WT mice post HFD. The significantly lower weights of soleus and EDL muscle when expressed as % body weight found in KO mice post HFD could potentially account for the lower total whole body metabolism as skeletal muscle is a highly metabolically active tissue which contributes significantly (~20-30%) to whole body energy expenditure (Rolfe and Brown, 1997; Zurlo et al., 1990). Another possibility worth examining is that the energy expenditure in contracting muscle from WT mice may be elevated compared

with KO post HFD due to the higher SLN expression in WT muscle. The greater difference in waking compared to sleeping whole body metabolism found between WT and KO mice post HFD and the greater (5%; not significant) VO_2 measured during low running speeds in WT mice support this possibility. Lastly, a shorter period of high fat feeding should be investigated as earlier metabolic CLAMS measures may reveal greater differences between WT and KO mice as the upregulation of SLN in skeletal muscle may have preceded adaptations in other thermogenic processes.

The many physiological adaptations that occur with high fat feeding make this model extremely complex and can often confound results, leading to misinterpretation of data and inaccurate conclusions. The examination of acute SLN overexpression through tetracycline induced transcription would limit confounding and compensatory adaptations allowing for a better understanding of the role of SLN in energy expenditure and adaptive thermogenesis in skeletal muscle. Future studies using an SLN overexpression mouse model may be able to determine the optimal level of SLN protein in skeletal muscle where the functional capacity of the muscle is maintained and Ca^{2+}pumping efficiency is decreased, presenting interesting implications for genetic therapy in the treatment of obesity.

Taken together, these studies are the first to demonstrate that SLN increases energy expenditure by SERCA pumps in isolated skeletal muscle in both standard chow fed and high fat fed mice. However, due to other thermogenic adaptations in standard chow fed mice (i.e. elevated UCP-3 protein content) and high fat fed mice (i.e. elevated NE and E), SLN ablation did not cause a reduction in the absolute VO_2 of skeletal muscle or whole body VO_2. Therefore, the metabolic and adiposity differences found between WT and KO mice post HFD do not appear to be due to adaptive thermogenesis mechanisms in skeletal muscle involving

SLN. However, SLN does increase resistance to diet-induced obesity and glucose intolerance in mice through mechanisms which are currently unidentified.

CONCLUSION

The results obtained from the major studies completed for this thesis, reveal for the first time that SLN is a key regulator of both ATP utilization in Ca^{2+} handling and of overall energy metabolism in skeletal muscle. The first study demonstrates that at a physiological SLN:SERCA ratio, SLN uncouples ATP hydrolysis from SR Ca^{2+} uptake in skeletal muscle resulting in a lower contribution of Ca^{2+} handling to basal muscle VO_2. However, KO mice fed standard rodent chow did not demonstrate lower isolated soleus resting VO_2 or resting whole body metabolism, even though homogenates from soleus of KO mice where more efficient in Ca^{2+} handling. Elevated expression of UCP-3 protein found in the soleus muscle of KO mice could, potentially, provide compensation, resulting in higher basal VO_2 in KO mice than expected. These data support the view that the primary physiological function of SLN in skeletal muscle is regulation of thermogenesis.

When placed on a "Westernized" HFD (42% of kcal derived from fat with 0.2% cholesterol) for a period of 8 weeks, KO mice were found to have a lower whole body metabolic rate resulting in greater weight gain, adiposity index and glucose intolerance compared with WT mice. The 3.8 fold increase in SLN protein found in soleus muscle from WT mice placed on a HFD and the lower ATP consumption by SERCA in isolated soleus of KO mice post diet compared to WT mice suggests that SLN may also play an important role in adaptive thermogenesis. However, even though whole body metabolic rate was higher in WT mice than KO mice following the HFD, induction of SLN expression by high fat feeding in WT soleus did not translate into increased energy expenditure in soleus compared to KO mice owing to greater adaptive thermogenesis through other mechanisms in KO muscle. Collectively, these results suggest that SLN may exert effects on other cellular processes

independent of thermogenesis, that imparts resistance against diet-induced obesity and glucose intolerance. Overall, this work has revealed that the KO mouse represents a novel model of obesity and type II diabetes which could provide new insights into the mechanisms linking obesity with insulin resistance.

FUTURE DIRECTIONS

These studies are the first to demonstrate several key components in defining the function of SLN as an important regulatory protein involved in a futile Ca^{2+} cycle where Ca^{2+} is prematurely released into the cytoplasm from SERCA resulting in greater hydrolysis of ATP for a given amount of Ca^{2+} taken into the SR. This protein has been shown under physiological conditions to alter the cost of Ca^{2+} handling in resting muscle and to reduce susceptibility to diet-induced obesity and potentially the accompanying complications associated with metabolic syndrome (ie. type 2 diabetes and hypertension). However, due to the novelty of the *Sln*-null mouse model used for the studies in this thesis with regard to adaptive thermogenesis, energy utilization by SERCA and susceptibility to diet-induced obesity, there are still many questions of interest which remain to be examined.

The significantly lower weights of soleus and EDL muscle when expressed as % body weight found in KO mice post HFD could potentially account for the lower total whole body metabolism seen in KO mice post HFD, as skeletal muscle has been shown to make up a considerable portion of daily energy expenditure (Zurlo et al., 1990; Rolfe and Brown, 1997). Since cytosolic $[Ca^{2+}]$ is known to be a potent signalling molecule involved in skeletal muscle hypertrophic growth, development and regeneration (for reviews see Chin, 2005 and Mallinson et al., 2009), future studies should examine the effects of a HFD on cell growth signalling pathways and determine whether intracellular free Ca^{2+} concentration is altered in skeletal muscle of KO mice. The accurate determination of lean body mass in WT and KO post HFD by dual energy X-ray absorptiometry (DXA) should also be a high priority for future studies.

The higher (5%; not significant) sub-maximal VO_2 found in WT mice compared to KO during the lower running speeds (8 and 16 m/min) should also be exploited via running wheels

to explain and potentially exacerbate the differences witnessed in waking whole body metabolism in WT and KO mice. As the greatest differences in metabolic rates were seen during the waking periods post HFD, the incorporation of free access to running wheels during the high fat dietary period should result in significantly greater metabolism in the WT mice and hence even lower susceptibility to obesity compared to KO mice.

The greater severity of glucose intolerance accompanied with elevated levels of NEFA and potentially ($P<0.08$) insulin found in the fasted serum of KO mice post HFD suggests diminished GLUT 4 translocation potentially as a result of elevated intramuscular triacylglycerols (TAGs) and accompanying lipid metabolites (diacylglycerols (DAGs) and ceramides). To confirm this as the potential mechanism, future studies should examine intramuscular TAGs, DAGs and ceramides as well as the insulin signalling pathways responsible for the translocation/activation of GLUT4. Further investigation of leptin levels (as the sample number in this study was limited) and adipokines particularly adiponectin may have merit as both of these have been implicated in the pathophysiology of diet-induced obesity as well as glucose and fat oxidation. Lastly, inflammatory response in these mice post HFD may provide further insight into the greater glucose intolerance witnessed in KO mice as greater fat deposition has been associated with increase in cytokine and TNF-α release from macrophages in white adipose tissue which have been shown to decrease glucose uptake in skeletal muscle (for review see Guilherme et al., 2008).

The chronically elevated levels of serum NE and E found in the KO mice post HFD would suggest that these mice may also be more susceptible to hypertension as previous studies have demonstrated the sympathetic nervous system to be highly implicated in vasoconstriction and hypertension (for review see Reaven et al., 1996). Studying the

vasoconstrictive properties of vessels in peripheral tissue and their relation to the potential development of hypertension in this *Sln*-null mouse model placed on a HFD may provide important mechanistic information on the development of hypertension, as well as provide a new model for examining metabolic syndrome and its potential prevention.

The data presented in this thesis demonstrates an elevated susceptibility of KO mice to diet-induced obesity suggesting that an important function of SLN and more importantly Ca^{2+} handling efficiency is in energy homeostasis of skeletal muscle and whole body metabolism. One avenue of interest to be examined is the overexpression of SLN in skeletal muscle and its influence on metabolic rate and more importantly diet-induced obesity and accompanying complication; however care must be taken not to alter functional capacity of the skeletal muscles at the cost of an elevated metabolic rate. Further work to systematically increase SLN protein levels in skeletal muscles to optimal levels without altering muscle function still remains to be examined as this may have very important clinical implications.

PLN and other substances (fluoride, capsaicin, fatty acids/cholesterol) have also been previously found to alter Ca^{2+} uptake, Ca^{2+} ATPase activity and Ca^{2+} leak out of the SR, all of which could influence the efficiency or coupling ratio of SERCA/Ca^{2+} handling (Frank et al., 2000; Hawkins et al., 1994; Mahmmoud, 2008; Vangheluwe et al., 2005b). As Ca^{2+} handling efficiency has been shown to be important in skeletal muscle metabolism and more specifically whole body metabolism, working with PLN and these other substances may provide other avenues for decreasing SERCA efficiency and increasing metabolic rate under conditions of high fat feeding without altering muscle function. This may be of particular benefit to larger mammals which have relatively little or no BAT to induce adaptive thermogenesis during periods of elevated energy intake. The large relative presence of BAT in mice may have

lessened the impact of SLN on adaptive thermogenesis in these studies, which could be substantially much greater in larger mammals possessing higher concentrations of SLN in skeletal muscle (Babu et al., 2007b).

Another interesting aspect revealed in the second study was the lower RER values and higher fasted serum NEFA values found in the KO mice following post HFD implying higher reliance on fatty acid oxidation by skeletal muscle. Examination of fibre type distribution, metabolic pathways through enzymatic analysis and fuel utilization pre and post HFD will help to further characterize this mouse model and potentially clarify some of the results found in these studies. Due to the novelty of this mouse model (Babu et al., 2007a), further work is clearly needed to determine the role of SLN and Ca^{2+} cycling on other processes within skeletal muscle and whole body metabolism.

.

REFERENCES

Ahmadian M, Duncan RE, Jaworski K, Sarkadi-Nagy E and Sul HS. Triacylglycerol metabolism in adipose tissue. *Future Lipidol*. 2: 229-237, 2007.

Arita Y, Kihara S, Ouchi N, Takahashi M, Maeda K, Miyagawa J, Hotta K, Shimomura I, Nakamura T, Miyaoka K, Kuriyama H, Nishida M, Yamashita S, Okubo K, Matsubara K, Muraguchi M, Ohmoto Y, Funahashi T and Matsuzawa Y. Paradoxical decrease of an adipose-specific protein, adiponectin, in obesity. *Biochem. Biophys. Res. Commun.* 257: 79-83, 1999.

Arruda AP, daSilva WS, Carvalho DP and deMeis L. Hyperthyroidism increases the uncoupled ATPase activity and heat production by the sarcoplasmic reticulum Ca^{2+} ATPase. *Biochem. J.* 375: 753-760, 2003.

Asahi M, Kurzydlowski K, Tada M and MacLennan DH. Sarcolipin inhibits polymerization of phospholamban to induce superinhibition of sarco(endo)plasmic reticulum Ca2+-ATPases (SERCAs). *J. Biol. Chem.* 277: 26725-26728, 2002.

Asahi M, Sugita Y, Kurzydlowski K, de Leon S, Tada M, Toyoshima C and MacLennan DH. Sarcolipin regulates sarco(endo)plasmic reticulum Ca^{2+}-ATPase (SERCA) by binding to transmembrane helices alone or in association with phospholamban. *Proc. Natl. Acad. Sci.* 100: 5040-5045, 2003.

Asahi M, Otsu K, Nakayama H, Hikoso S, Takeda T, Gramolini AO, Trivieri MG, Oudit GY, Morita T, Kusakari Y, Hirano S, Hongo K, Hirotani S, Yamaguchi O, Peterson A, Backx PH, Kurihara S, Hori M and MacLennan DH. Cardiac-specific overexpression of sarcolipin inhibits sarco(endo)plasmic reticulum Ca^{2+}ATPase (SERCA2a) activity and impairs cardiac function in mice. *Proc. Natl. Acad. Sci.* 101: 9199-9204, 2004.

Babu GJ, Bhupathy P, Petrasheversuskaya NN, Wang H, Raman S, Wheeler D, Jagatheesan G, Wieczorek D, Schwartz A, Janssen PM, Ziolo MT and Periasamy M. Targeted overexpression of sarcolipin in the mouse heart decreases sarcoplasmic reticulum calcium transport and cardiac contractility. *J. Biol. Chem.* 281: 3972-3979, 2006.

Babu GJ, Zheng Z, Natarajan P, Wheeler D, Janssen PM and Periasamy M. Overexpression of sarcolipin decreases myocyte contractility and calcium transient. *Cardiovas. Res.* 65: 177-186, 2005.

Babu GJ, Bhupathy P, Timofeyev V, Petrasheversuskaya NN, Reiser PJ, Chiamvimonvat N and Periasamy M. Ablation of sarcolipin enhances sarcoplasmic reticulum calcium transport and atrial contractility. *Proc. Natl. Acad. Sci*. 104: 17867-17872, 2007a.

Babu GJ, Bhupathy P, Carnes CA, Billman GE and Periasamy M. Differential expression of sarcolipin protein during muscle development and cardiac pathophysiology. *J. Mol. Cell. Cardiol.* 42: 215-222, 2007b.

Barclay CJ. Mechanical efficiency and fatigue of fast and slow muscles of the mouse. *J. Physiol.* 497: 781-794, 1996.

Barclay CJ. Modelling diffusive O_2 supply to isolated preparations of mammalian skeletal and cardiac muscle. *J. Muscle. Res. Cell. Motil.* 26: 225-235, 2005.

Barclay CJ, Woledge RC and Curtin NA. Energy turnover for Ca^{2+} cycling in skeletal muscle. *J. Muscle. Res. Cell. Motil.* 28: 259-274, 2007.

Barclay CJ, Lichtwark GA and Curtin NA. The energetic cost of activation in mouse fast-twitch muscle is the same wether measured using reduced filament overlap or N-benzyl-p-toluenesulphonamide. *Acta. Physiol.* 193: 381-391, 2008.

Berchtold MW, Brinkmeier H and Muntener M. Calcium ion in skeletal muscle: Its crucial role for muscle function, plasticity, and disease. *Physiol. Rev.* 80: 1215-1265, 2000.

Berman MC. Slippage and uncoupling in P-type cation pumps; implications for energy transduction mechanisms and regulation of metabolism. *Biochem. Biophys. Acta.* 1513: 95-121, 2001.

Bhupathy P, Babu GJ and Periasamy M. Sarcolipin and phospholamban as regulators of cardiac sarcoplasmic reticulum Ca^{2+}ATPase. *J. Mol. Cell. Cardio.* 42: 903-911, 2007.

Bhupathy P, Babu GJ and Periasamy M. Threonine-5 at the N-terminus can modulate sarcolipin function in cardiac myocytes. *J. Mol. Cell. Cardiol.* 47: 723-729, 2009.

Biddinger SB, Miyazaki M, Boucher J, Ntambi JM and Kahn CR. Leptin suppresses strearoyl-CoA desaturase I by mechanisms independent of insulin and sterol regulatory element-binding protein 1c. *Diabetes.* 55: 2032-2041, 2006.

Block BA. Thermogenesis in muscle. *Annu. Rev. Physiol.* 56: 535-577, 1994.

Boden G, Chen X, Ruiz J, White JV and Rossetti L. Mechanisms of fatty acod-induced inhibition of glucose uptake. *J. Clic. Invest.* 93: 2438-2446, 1994.

Bonen A, Dohm GL and van Loon LJ. Lipid metabolism, exercise and insulin action. *Essays Biochem.* **42:** 47-59, 2006.

Boss O, Samec S, Kuhne F, Bijlenga P, Assimacopoulos-Jeannet F, Seydoux J, Muzzin P and Giacobina JP. Uncoupling protein-3 expression in rodent skeletal muscle is modulated by food intake but not by changes in environmental temperature. *J. Biol. Chem.* 273: 5-8, 1998.

Brand MD and Esteves TC. Physiological functions of the mitochondrial uncoupling proteins UCP2 and UCP3. *Cell. Metab.* 2: 85-93, 2005.

Buettner R, Schölmerich J and Bollheimer LC. High-fat diets: modeling the metabolic disorders of human obesity in rodents. Obesity. 15: 798-808, 2007.

Calle EE, Thun MJ, Petrelli JM, Rodriguez C and Heath CW. Body-mass index and mortality in a prospective cohort of U.S. adults. *N. Engl. J. Med.* 341: 1097-1105, 1999.

Cannon B and Nedergard J. Brown Adipose Tissue: Function and physiological significance. *Physiol. Rev.* 84: 277-359, 2003.

Chan LLY, Chen Q, Go A, Lam E and LI E. Reduced adiposity in bitter lemon (Momordica charantia)-fed rats is associated with increased lipid oxidative enzyme activities and uncoupling protein expression. *J. Nutr.* 135: 2517-2523, 2005.

Chavez JA, Knotts TA, Wang LP, Li G, Dobrowsky RT, Florant GL and Summers SA. A role for ceramides , but not diacylglycerol, in the antagonism of insulin signal transduction by saturated fatty acids. *J. Biol. Chem.* 278: 10279-10303, 2003.

Chen Q and Li ET. Reduced adiposity in bitter melon (momordica charantia) fed rats is associated with lower tissue triglyceride and higher plasma catecholamines. *Br. J. Nutr.* 93: 747-754, 2005.

Chin ER. Role of Ca^{2+}/calmodulin-dependent kinases in skeletal muscle plasticity. *J. Appl. Physiol.* 99: 414-423, 2005.

Chinet A, Decrouy A and Even PC. Ca^{2+}-dependent heat production under basal and near-basal conditions in the mouse soleus muscle. *J. Physiol.* 455: 663-678, 1992.

Chwalibog A, jakobsen K, Tauson AH and Thorbek G. Energy metabolism and nutrient oxidation in young pigs and rats during feeding, starvation and re-feeding. *Comp. Biochem. Physiol. A. Mol. Integr. Physiol.* 140: 299-307, 2005.

Clapham JC, Arch JRS, Chapman H, Haynes A, Lister C, Moore GBT, Piercy V, Carter SA, Lehner I, Smith SA, Beeley LJ, Godden RJ, Herrity N, Skehel M, Changani KK, Hockings PD, Reid DG, Squires SM, Hatcher J, Trail B, Latcham J, Rastan S, Harper AJ, Cadenas S, Buckingham JA, Brand MD and Abuin A. Mice overexpressing human uncoupling protein-3 in skeletal muscle are hyperphagic and lean. *Nature.* 406: 415-418, 2000.

Clausen T. Regulation of active Na^{+}-K^{+} transport in skeletal muscle. *Physiol. Rev.* 66: 542-580, 1986.

Clausen T, Van Hardeveld C and Everts ME. Significance of cation transport in control of energy metabolism and thermogenesis. *Physiol. Rev.* 71: 733-774, 1991.

Collins S, Martin TL, Surwit RS and Robidoux J. Genetic vulnerability to diet-induced obesity in the C57BL/6J mouse: physiological and molecular characteristics. *Physiol. Behav.* 81: 243-248, 2004.

Cusin I, Zakrzewska KE, Boss O, Muzzin P, Giacobino JP, Ricquier D, Jeanrenaud B and Rohner-Jeanrenaud F. Chronic central leptin infusion enhances insulin-stimulated glucose metabolism and favors the expression of uncoupling proteins. *Diabetes*. 47: 1014-1019, 1998.

deLany JP and West DB. Changes in body composition with conjugated linoleic acid. *J. Am. Coll. Nutr.* 19: 487S-493S, 2000.

de Meis L and Vianna AL. Energy interconversion by the Ca^{2+} ATPase transport ATPase of sarcoplasmic reticulum. *Annu. Rev. Biochem.* 48: 275-292, 1979.

de Meis L. Control of heat produced during ATP hydrolysis by the sarcoplasmic reticulum Ca^{2+}-ATPase in the absence of a Ca^{2+} gradient. *Biochem. Biophys. Res. Commun.* 243: 598-600, 1998.

de Meis L. ATP synthesis and heat production during Ca^{2+} efflux by sarcoplasmic reticulum Ca^{2+}-ATPase. *Biochem. Biophys. Res. Commun.* 276: 35-39, 2000.

de Meis L. Uncoupled ATPase activity and heat production by the sarcoplasmic reticulum Ca^{2+}-ATPase: Regulation by ADP. *J. Biol. Chem.* 276: 25078-25087, 2001a.

de Meis L. Role of the sarcoplasmic reticulum Ca^{2+}-ATPase on heat production and thermogenesis. *Biosci. Rep.* 21: 113-137, 2001b.

de Meis L. Ca^{2+}-ATPases (SERCA): Energy transduction and heat production in transport ATPases. *J. Membr. Biol.* 188: 1-9, 2002.

de Meis L, Oliveira GM, Arruda AP, Santos R, da Costa RM and Benchimol M. The thermogenic activity of rat brown adipose tissue and rabbit white muscle Ca^{2+}-ATPase. *IUBMB. Life.* 57: 337-345, 2005.

Denborough M. Malignant hyperthermia. *Lancet.* 352: 1131-1136, 1998.

Dresner A, Laurent D, Marcucci M, Griffin ME, Dufour S, Cline GW, Slezak LA, Andersen DK, Hundal RS, Rothman DL,Petersen KF and Shulman GI. Effects of free fatty acids on glucose transport and IRS-1 associated phosphatidylinositol 3-kinase activity. *J. Clin. Invest.* 103: 253-259, 1999.

Duhamel TA, Green HJ, Stewart RD, Foley KP, Smith IC and Ouyang J. Muscle metabolic, SR Ca^{2+}-cycling responses to prolonged cycling, with and without glucose supplementation. *J. Appl. Physiol.* 103: 1986-1998, 2007.

Dulloo AG, Decrouy A and Chinet A. Suppression of Ca^{2+}-dependent heat production in mouse skeletal muscle by high fish oil consumption. *Metabolism.* 43: 931-934, 1994.

Dulloo AG, Gubler M, Montani JP, Seydoux J and Solinas G. Substrate cycling between *de novo* lipogenesis and lipid oxidation: a thermogenic mechanism against skeletal muscle lipotoxicity and glucolipotoxicity. *Int. J. Obesity.* 28: S29-S37, 2004.

Dyck DJ, Heigenhauser GJF and Bruce CR. The role of adipokines as regulators of skeletal muscle fatty acid metabolism and insulin sensitivity. *Acta. Physiol.* 186: 5-16, 2006.

Echtay KS, Esteves TC, Pakay JL, Jekabsons MB, Lambert AJ, Portero-Otin M, Pamplona R, Vidal-Puig AJ, Wang S, Roebck SJ and Brand MD. A signalling role for 4-hydroxy-2-nonenal in regulation of mitochondrial uncoupling. *Embo. J.* 22: 4103-4110, 2003.

European Molecular Biology Laboratory-European Bioinformatics Institute (EMBL-EBI). http://www.ebi.ac.uk/gxa/, 2010.

Frank K, Tilgmann C, Shannon TR, Bers DM and Kranias EG. Regulatory Role of Phospholamban in the Efficiency of Cardiac Sarcoplasmic Reticulum Ca^{2+} Transport. *Biochem. 39:* 14176–14182, 2000.

Friedman JM and Halaas JL. Leptin and the regulation of body weight in mammals. *Nature.* 395: 763-770, 1998.

Goeger DE and Riley RT. Interaction of cyclopiazonic acid with rat skeletal muscle sarcoplasmic reticulum vesicles. *Biochem. Pharmacol.* 38: 3995-4003, 1989.

Goldsmith R, Joanisse DR, Gallagher D, Pavlovich K, Shamoon E, Leibel L and Rosenbaum M. Effects of experimental weight perturbation on skeletal muscle work efficiency, fuel utilization, and biochemistry in human subjects. *Am. J. Physiol.* 298: R79-R88, 2010.

Gong DW, He Y and Reitman ML. Genomic organization and regulation by dietary fat of the uncoupling protein 3 and 2 genes. *Biochem. Biophys. Res. Commun*. 256: 27-32, 1999.

Gramolini AO, Trivieri MG, Oudit GY, Kislinger T, Li W, Patel MM, Emili A, Kranias EG, Backx PH and MacLennan DH. Cardiac-specific overexpression of sarcolipin in phospholamban null mice impairs myocyte function that is resotred by phosphorylation. *Proc. Natl. Acad. Sci.* 103: 2446 - 2451, 2006.

Green HJ, Jones S, Ball-Burnett M. and Fraser I. Early adaptations in blood substrates, metabolites and hormones to prolonged exercise training in man. *Can. J. Physiol. Pharmacol.* 69: 1222-1229, 1991.

Griffin ME, Marcucci MJ, Cline GW, Bell K, Barucci N, Lee D, Goodyear LJ, Kraegen EW, White MF and Shulman GI. Free fatty acid-induced insulin resistance is associated with activation of protein kinase C theta and alterations in the insulin signallin cascade. *Diabetes.* 48: 1270-1274, 1999.

Grynkiewicz G, Poenie M. and Tsien RY. A new generation of Ca^{2+} indicators with greatly improved fluorescence properties. *J. Biol. Chem.* 260: 3440-2450,1985.

Guilherme A, Virbasius JV, Puri V and Czech MP. Adipocytes dysfunctions linking obesity to insulin resistance and type 2 diabetes. *Nat. Rev. Mol. Cell. Biol.* 9: 367-377, 2008.

Hasselbach W and Oetliker H. Energetics and electrogenicity of the sarcoplasmic reticulum calcium pump. *Annu. Rev. Physiol.* 45: 325-339, 1983.

Hawkins C, Xu A and Narayanan N. Comparison of the effects of fluoride on the calcium pumps of cardiac and fast skeletal muscle sarcoplasmic reticulum: evidence for tissue- specific qualitative difference in calcium-induced pump conformation. *Biochemica. Biophysica. Acta.* 1191: 231-243, 1994.

Haynes WG, Morgan DA, Walsh SA, Mark AL and Sivitz WI. Receptor-mediated regional sympathetic nerve activation by leptin. *J. Clin. Invest.* 100: 270-278, 1997

Hegarty BD, Furler SM, Ye J, Cooney GJ and Kraegen EW. The role of intramuscular lipid in insulin resistance. A*cta Physiol Scand.* 178: 373-383, 2003.

Henquin JC. Regulation of insulin secretion: a matter of phase control and amplitude modulation. *Diabetologia.* 52: 739-751, 2009.

Hojman P, Brolin C, Gissel H, Brandt C, Zerahn B, Pedersen BK and Gehl J. Erythropoietin over-expression protects against diet-induced obesity in mice through increased fat oxidation in muscles. *Plos One.* 4: e5894, 2009.

Homsher E. Muscle enthalpy production and its relationship to actinomyosin ATPase. *Annu. Rev. Physiol.* 49: 672-690, 1987.

Inesi G, Kurzmack M and Verjoversuski-Almeida S. ATPase phosphorylation and calcium ion translocation in the transient state of sarcoplasmic reticulum activity. *Ann. N.Y. Acad. Sci.* 307: 224-227, 1978.

Inesi G. Mechanism of Ca^{2+} transport. *Annu. Rev. Physiol.* 47: 573-601, 1985.

Inesi G and de Meis L. Regulation of steady state filling in sarcoplasmic reticulum: Roles of back-inhibition, leakage, and slippage of the calcium pump. *J. Biol. Chem.* 264: 5929-5936, 1989.

James PT. Obesity: the worldwide epidemic. *J. Clin. Dermato.* 22: 276-280, 2004.

Janovska A, Hatzinikolas G, Mano M and Wittert GA. The effect of dietary fat content on phospholipid fatty acid profile is muscle fibre-type dependent. *Am. J. Physiol.* 2010 (Epub ahead of print).

Kadambi VJ, Ponniah S, Harrer JM, Hoit BD, Dorn GW, Walsh RA and Kranias EG. Cardiac-specific overexpression of phospholamban alters calcium kinetics and resultant cardiomyocyte mechanics in transgenic mice. *J. Clin. Invest.* 97: 533-539,1996

Kahn R. Metabolic syndrome-what is the clinical usefullness? *Lancet.* 371: 1892-1893, 2008.

Katzmarzyk PT and Mason C. Prevalence of class I, II and III obesity in Canada. *CMAJ.* 174: 156-157, 2006.

Kennedy AJ, Ellacott KL, King VL, Hasty AH. Mouse models of the metabolic syndrome. *Dis. Model Mech.* 3: 156-66, 2010.

Kim JK. Hyperinsulinemic-euglycemic clamp to assess insulin sensitivity in vivo. *Methods Mol. Biol.* 560: 221-238, 2009.

Kontani Y, Wang Y, Kimura K, Inokuma KI, Saito M, Suzuki-Miura T, Wang Z, Sato Y Mori N and Yamashita H. UCP1 deficiency increases susceptibility to diet-induced obesity with age. *Aging Cell.* 4: 147-155, 2005.

Kopecky J, Clarke G, Enerback S, Spiegelman B and Kozak LP. Expression of the mitochondrial uncoupling protein gene from the aP2 promoter prevents genetic obesity. *J. Clin. Invest.* 96: 2914-2923, 1995.

Kopelman PG. Obesity as a medical problem. *Nature.* 404: 635-643, 2000.

Krauss S, Zhang CY and Lowell BB. The mitochondrial uncoupling-protein homologues. *Nat. Rev. Mol. Cell. Biol.* 6: 248-261, 2005.

Kus V, Prazak T, Braunner P, Hensler M, Kuda O, Flachs P, Janovska P, Medrikova D, Rossmeisl M, Jilkova Z, Stefl B, Pastalkova E, Drahota Z, Houstek J and Kopecky J. Induction of muscle thermogenesis by high-fat diet in mice: association with obesity-resistance. *Am. J. Physiol.* 295: E356-E367, 2008.

Laemmli UK. Cleavage of structural proteins during the assembly of the head of bacteriophage T4. *Nature.* 227: 680-685, 1970

Laaksonen DE, Niskanen L, Lakka HM, Lakka TA and Uusitupa M. Epidemiology and treatment of the metabolic syndrome. *Ann. Med.* 36: 332-346, 2004.

Lee, A.G. A calcium pump made visible. *Curr. Opin. Struct. Biol.* 12: 547-554, 2002.

Leibel R, Rosenbaum M and Hirsh J. Changes in energy expenditure resulting from altered body weight. *N. Eng. J. Med.* 332: 621-628, 1995.

Levine JA, Eberhardt NL and jensen MD. Role of non-exercise activity thermogenesis in resistance to fat gain in humans. *Science*. 283: 212-214, 1999.

Li B, Nolte LA, Ju J-S, Han DH, Coleman T, Holloszy JO and Semenkovich CF. Skeletal muscle respiratory uncoupling prevents diet-induced obesity and insulin resistance in mice. *Nat. Med.*
6: 1115-1120, 2000.

Lin B, Coughlin S and Pilch PF. Bidirectional regulation of uncoupling protein-3 and GLUT-4 mRNA in skeletal muscle by cold. *Am. J. Physiol.* 275: E386-E-391, 1998.

Lowell BB and Spiegelman BM. Towards a molecular understanding of adaptive thermogenesis. *Nature*. 404: 652-660, 2000.

Luo W, Grupp IL, Harrer J, Ponniah S, Grupp G, Duffy JJ, Doetschman T and Kranias EG. Targeted ablation of the phospholamban gene is associated with markedly enhanced myocardial contractility and loss of beta-agonist stimulation. *Circ. Res.* 75: 401-409, 1994.

Lytton J, Westlin M, Burk SE, Shull GE and MacLennan DH. Functional comparisons between isoforms of the sarcoplasmic or endoplasmic reticulum family of calcium pumps. *J. Biol. Chem.* 267: 14483-14489, 1992.

MacLennan DH, Yip CC, Iles GH and Seeman P. Isolation of sarcoplasmic reticulum proteins. *Cold Sping Harbor Symp. Quant. Biol.* 37: 469-478, 1972.

MacLennan DH. Isolation of proteins of the sarcoplasmic reticulum. *Methods Enzymol.* 32: 291-302, 1974.

MacLennan DH, Rice WJ and Green NM. The mechanism of Ca2+ transport by sarco(endo)plasmic reticulum Ca2+-ATPases. *J. Biol. Chem.* 272: 28815-28818, 1997.

MacLennan DH, Abu-Abed M and Kang C. Structure-function relationships in Ca^{2+} cycling proteins. *J. Mol. Cell. Cardiol.* 34: 897-918, 2002.

MacLennan DH, Asahi M and Tupling AR. The regulation of SERCA-type pumps by phospholamban and sarcolipin. *Ann. N.Y. Acad. Sci.* 986: 472 - 487, 2003.

MacLennan DH and Kranias EG. Phospholamban: a crucial regulator of cardiac contractility. *Nat. Rev. Mol. Cell. Biol.* 4: 566-577, 2003.

Mahmmoud YA. Capsaicin stimulates uncoupled ATP hydrolysis by sarcoplasmic reticulum calcium pump. *J. Biol. Chem.* 283: 21418-21426, 2008.

Maickel RP, Matussek N, Stern DN and Brodie BB. The sympathetic nervous system as a homeostatic mechanism. I. Absolute need for sympathetic nervous function in body temperature maintenance of cold exposed rats. *J. Pharmacol. Exp. Ther.* 157: 103-110, 1967.

Mall S, Broadbridge R, Harrison SL, Gore MG, Lee AG and East JM. The presence of sarcolipin results in increased heat production by Ca^{2+}-ATPase. *J. Biol. Chem.* 281: 36597-36602, 2006.

Mallinson J, Meissner J and Chang KC. Chapter 2. Calcineurin signalling and the slow oxidative skeletal muscle fiber type. *Int. Rev. Cell. Mol. Biol*. 277: 67-101, 2009.

Marmonier F, Duchamp C, Cohen-Adad F, Eldershaw TP and Barré H. Hormonal control of thermogenesis in perfused muscle of Muscovy ducklings. *Am. J. Physiol.* 273: R1638-R1648, 1997.

Matthias A, Ohlson KBE, Fredriksson JM, Jacobsson A, Nedergaard J and Cannon B. Thermogenis responses in brown fat cells are fully UCP-1 dependent. *J. Biol. Chem.* 275: 25073-25081, 2000.

McWhirter JM, Gould GW, East JM and Lee AG. Characterization of Ca^{2+}uptake and release by vesicles of skeletal-muscle sarcoplasmic reticulum. *Biochem. J.* 245: 731-738, 1987.

Millet L, Vidal H, AndreelliF, Larrony D, Riou JP, Ricquier D, Laville M and Langin D. Increased uncoupling protein-2 and -3 mRNA expression during fasting in obese and lean humans. *J. Clin. Invest.* 100: 2665-2670, 1997.

Morita T, Hussain D, Asahi M, Tsuda T, Kurzydlowski K, Toyoshima C and MacLennan DH. Interaction sites among phospholamban, sarcolipin, and the sarco(endo)plasmic reticulum Ca^{2+}-ATPase. *Biochem. Biophys. Res. Commun.* 369: 188-194, 2008.

Moro C, Galgani JE, Luu L, Pararica M, Mairal A, Bajpeyi S, Schmitz G, Langin D, Liebisch G and Smith SR. Influence of gender, obesity, and muscle lipase activity on intramyocellular lipids in sedentary individuals. *J. Clin. Endocrinol. Metab.* 94: 3440-3447, 2009.

Morrissette JM, Franck JPG and Block BA. Charaterization of ryanodine receptors and Ca^{2+}-ATPase isoforms in the thermogenic heater organ of blue marlin (*Makaira nigricans*). *J. Exp. Biol.* 206: 805-812, 2003.

Muniyappa R, Lee S, Chen H and Quon MJ. Current approaches for assessing insulin sensitivity and resistance in vivo: advantages, limitations, and appropriate usage. *Am. J. Physiol.* 294: E15-E26, 2008.

Muoio DM and Newgard CB. Molecular and metabolic mechanisms of insulin resistance and β-cell failure in type 2 diabetes. *Nature Rev.* 9: 193-205, 2009.

Murphy RM, Larkins NT, Mollica JP, Beard NA and Lamb GD. Calsequestrin content and SERCA determine normal and maximal Ca^{2+} storage levels in sarcoplasmic reticulum of fast- and slow-twitch fibres of rat. *J. Physiol.* 587: 443-460, 2009.

Must A, Spadano J, Coakley EH, Field AE, Colditz G and Dietz WH. The disease burden associated with overweight and obesity. *JAMA.* 282: 1523-1529, 1999.

Norris SM, Bombardier E, Smith IC, Vigna C and Tupling AR. ATP consumption by SR Ca^{2+}pumps accounts for 50% of resting metabolic rate in mouse fast and slow twitch skeletal muscle. *Am. J. Physiol.* 298: C521-529, 2010.

O'Brien PJ, Shen H, Weiler J, Mirsalimi M and Julian R. Myocardial Ca-sequestration failure and compensatory increase in Ca-ATPase with congestive cardiomyopathy: Kinetic characterization by a homogenate microassay using real-time ratiometric indo-1 spectrofluorometry. *Mol. Cell. Biochem.* 102: 1-12, 1991.

Odermatt A, Taschner PE, Scherer SW, Beatty B, Khanna VK, Cornblath DR, Chaudhry V, Yee WC, Schrank B, Karpati G, Breuning MH, Knoers N, and MacLennan DH. Characterization of the gene encoding human sarcolipin (SLN), a proteolipid associated with SERCA1: absence of structural mutations in five patients with Brody disease. *Genomics.* 45: 541-553, 1997.

Odermatt A, Becker S, Khanna VK, Kurzydlowski K, Leisner E, Pette D and MacLennan DH. Sarcolipin regulates the activity of SERCA1, the fast-twitch skeletal muscle sarcoplasmic reticulum Ca2+-ATPase. *J. Biol. Chem.* 273: 12360-12369, 1998.

Okada T, Kawano Y, Sakakibara T, Hazeki O, Ui M. essential role of phosphatidylinositol 3-kinase in insulin induced glucose transport and antilipolysis in rat adipocytes. Studies with selective inhibitor wortmannin. *J. Biol. Chem.* 269: 3568-3573, 1994.

Ottenheijm C, Fong C, Vangheluwe P, Wuytack F, Babu GJ, Periasamy M, Witt CC, Labeit S and Granzier H. Sarcoplasmic reticulum calcium uptake and speed of relaxation are depressed in nebulin-free skeletal muscle. *FASEB. J.* 22: 2912-2919, 2008.

Petersen KF and Shulman GI. Pathogenesis of skeletal muscle insulin resistance in type 2 diabetes mellitus. *Am. J. Cardiol*. **90**: 11G-18G, 2002.

Rasmussen H. The calcium messenger system. *N. Engl. J. Med.* 314: 1094-1101, 1986.

Reaven GM, Lithell H and Landsberg L. Hypertension and associated metabolic abnormalities-the role of insulin resistence and the sympathoadrenal system. *N. Eng. J. Med.* 334: 374-381, 1996.

Reis M, Farage M, de Souza ACL and de Meis L. Correlation between uncoupled ATP hydrolysis and heat production by the sarcoplasmic reticulum Ca2+-ATPase: coupling effect of fluoride. *J. Biol. Chem.* 276: 42793-42800, 2001.

Reis M, Farage M and de Meis L. Thermogenesis and energy expenditure: control of heat production by the Ca^{2+}-ATPase of fast and slow muscle. *Mol. Mem. Biol.* 19: 301-310, 2002.

Rezende EL, Garland Jr. T, Chappell MA, Malisch JL and Gomes FR. Maximum aerobic performance in lines of Mus selected for high wheel-running activity: effects of selection, oxygen availability and the mini-muscle phenotype. *J. Exp. Biol*. 209: 115-127, 2006.

Roden M, Price TB, Perseghin G, Petersen KF, Rothman DL, Cline GW and Shulman GI. Mechanism of free fatty acid-induced insulin resistance in humans. *J. Clin. Invest.* 97: 2859-2865, 1996.

Rolfe, D.F.S. and G.C. Brown, Cellular energy utilization and molecular origin of standard metabolic rate in mammals. *Physiol. Rev.* 77: 731-758, 1997.

Rosen ED and Spiegelman BM. Adipocytes as regulators of energy balance and glucose homoeostasis. *Nature.* 444: 847-853, 2006.

Rosenbaum M, Vandenborne K, Goldsmith R, Simoneau JA, Heymsfield S, Joanisse DR, Hirsch J, Murphy E, Mathews D, Segal KR and Leibel RL. Effects of experimental weight perturbation on skeletal muscle work efficiency in human subjects. *Am. J. Physiol.* 285: R183-R192, 2003.

Rousset S, Alves-Guerra MC, Mozo J, Miroux B, Cassard-Doulcier AM, Bouillaud F and Ricquier d. The biology of mitochondrial uncoupling proteins. *Diabetes*. 53(Suppl. 1): S130-S135, 2004.

Schacterle GR and Pollack RL. A simplified method for the quantitative assay of small amounts of protein in biological material. *Anal. Biochem.* 31: 654-655, 1973.

Scharrer E. Control of food intake by fatty acid oxidation and ketogenesis. *Nutrition.* 15: 704-714, 1999.

Schrauwen, P., Westerterp-Plantenga, M.S., Kornips, E., Schaart, G. and van Marken Lichtenbelt, W.D. The effects of mild cold exposure on UCP3 mRNAexpression and UCP3 protein content in humnas. *Int. J. Obes. Relat. Metab. Disord*. 26: 450-457, 2002.

Schrauwen P and Hasselink MK. The role of uncoupling protien 3 in fatty acid metabolism: protection against lipotoxicity. *Proc. Nutri. Soc*. 63: 287-292, 2004.

Schrauwen, P., Hoeks, J. and Hesselink, M.K. Putative function and physiological relevance of the mitochondrial uncoupling protein-3: involvement in fatty acid metabolism. *Prog. Lipid Res.* 45: 17-41,2006.

Schrauwen P, Hoppeler H, Billeter R, Bakker A and Pendergast D. Fibre type dependent upregulation of human skeletal muscle UCP2 and UCP3 mRNA expression by high fat diet. *Int. J. Obes. Relat. Metab. Disord.* 25: 449-456, 2001.

Seidler, N.W. , Jona, I., Vegh, M. and Martonosi, A. Cyclopiazonic acid is a specific inhibitor of the Ca^{2+}-ATPase of sarcoplasmic reticulum. *J. Biol. Chem.* 264: 17816-17823, 1989.

Shanik MH, Xu Y, Skrha J, Dankner R, Zick Y and Roth J. Insulin resistance and hyperglycemia: Is hyperinsulinemia the cart or the horse. *Diabetes Care*. 31: S262-S268, 2008.

Shiota M and Masumi S. Effect of norepinephrine on consumption of oxygen in perfused skeletal muscle from cold exposed rats. *Am. J. Physiol.* 254: E482-E489, 1988.

Simmerman HK and Jones LR. Phospholamban: protein structure, mechanism of action, and role in cardiac function. *Physiol. Rev.* 78: 921-947, 1998.

Simonides & Van Hardeveld (1990)
Sitnick M, Bodine SC and Rutledge JC. Chronic high fat feeding attenuates load-induced hypertrophy in mice. *J. Physiol.* 587: 5753-5765, 2009.

Smith WS, Broadbridge R, East JM and Lee AG. Sarcolipin uncouples hydrolysis of ATP from accumulation of Ca^{2+} by the Ca^{2+}-ATPase of skeletal muscle sarcoplasmic reticulum. *Biochem. J.* 361: 277-286, 2002.

Solinas G, Summermatter S, Mainieri D, Gubler M, Pirola L, Wymann MP, Rusconi S, Montani JP, Seydoux J and Dulloo AG. The direct effect of leptin on skeletal muscle thermogenesis is mediated by substrate cycling between de novo lipogenesis and lipid oxidation. *FEBS. Lett.* 577:5 39-544, 2004.

Son C, Hosoda K, Ishihara K, Bevilacqua L, Masuzaki H, Fushiki T, Harper ME and Nakao K. Reduction of diet-induced obesity in transgenic mice overexpressing uncoupling protein 3 in skeletal muscle. *Diabetologia*. 47: 47-54, 2004.

Statistics Canada, *Canadian Community Health Survey*, 2004.

Ste Marie L, Luquet S, Curtis W and Palmiter RD. Norepinephrine- and epinephrine-deficient mice gain weight normally on a high-fat diet. *Obes. Res.* 13: 1518-1522, 2005.

Sumbilla C, Cavagna M, Zhong L, Ma H, Lewis D, Farrance I and Inesi G. The slippage of the Ca2+ pump and its control by anions and curcumin in skeletal and cardiac sarcoplasmic reticulum. *J. Biol. Chem.* **277**: 13900-13906, 2002.

Summermatter S, Mainieri D, Russell AP, Seydoux J, Montani JP, Buchala A, Solinas G and Dulloo AG. Thrifty metabolism that favors fat storage after caloric restriction: a role for skeletal muscle phosphatidylinositol-3-kinase activity and AMP-activated protein kinase. *FASEB. J.* 22: 774-785, 2008.

Szentesi P, Zaremba R, van Mechelen W and Stienen GJ. ATP utilization for calcium uptake and force production in different types of human skeletal muscle fibres. *J. Physiol.* 531: 393-403, 2001.

Taylor BA and Phillips SJ. Detection of obesity QTLs on mouse chromosomes 1 and 7 by selective DNA pooling. *Genomics.* 34: 389-398, 1996.

Toyoshima, C., Nomura, H. and Sugita, Y. Crystal structure of Ca^{2+}ATPase in various physiological states. *Ann. N.Y. Acad. Sci.* 986: 1-8, 2003.

Toyoshima C, Nakasako M, Nomura H and Ogawa H. Crystal structure of the calcium pump of sarcoplasmic reticulum at 2.6 Å resolution. *Nature.* 405: 647-655, 2000.

Toyoshima C and Nomura H. Structural changes in the calcium pump accompanying the dissociation of calcium. *Nature*. 418: 605-611, 2004.

Toyoshima C and Inesi G. Structural basis of ion pumping by Ca2+-ATPase of the sarcoplasmic reticulum. *Annu. Rev. Biochem.* 73: 269-292, 2004.

Toyoshima C. Structural aspects of ion pumping by Ca^{2+}-ATPase of sarcoplasmice reticulum. *Arch Biochem Biophys* **476**, 3-11, 2008.

Tupling AR, Asahi M and MacLennan DH. Sarcolipin overexpression in rat slow twitch muscle inhibits sarcoplasmic reticulum Ca^{2+} uptake and impairs contractile function. *J. Biol. Chem.* 277: 44740 - 44746, 2002.

Tupling AR, Gramolini AO, Duhamel TA, Kondo H, Asahi M, Tsuchiya SC, Borrelli MJ, Lepock JR, Otsu K, Hori M, MacLennan DH and Green HJ. HSP70 binds to the fast-twitch skeletal muscle Sarco (endo)plasmic reticulum Ca2+-ATPase (SERCA1a) and prevents thermal inactivation. *J. Biol. Chem*. 279: 52382 - 52389, 2004.

Tupling R, Green H, Senisterra G, Lepock J and McKee N. Ischemia-induced structural change in SR Ca2+-ATPase is associated with reduced enzyme activity in rat muscle. *Am. J. Physiol.* 281: R1681-1688, 2001.

Tupling AR and Green H. Silver ions induce Ca2+ release from the SR in vitro by acting on the Ca2+ release channel and the Ca2+ pump. *J. Appl. Physiol.* 92: 1603-1610, 2002.

Tupling AR, Hussain D, Trivieri MG, Bapu G, Backx PH, Periasamy M, MacLennan DH and Gramolini AO. Improvement of Ca^{2+} transport and muscle relaxation in skeletal muscle from sarcolipin null mice. *FASEB J* 22(Meeting Abstracts): 962.34, 2008.

TUkropec J, Anunciado RP, Ravussin Y, Hulver MW and Kosak LP. UCP1-independent thermogenesis in white adipose tissue of cold-acclimated $Ucp1^{-/-}$ mice. *J. Biol. Chem.* 281: 31894-31908, 2006.

Vander EJ, Sherman JH and Luciano DS. *Human physiology: The mechanisms of body function*. 5th ed., 1990, pp 158-163,200, 498 and 635, McGraw Hill publishing, Toronto.

Vangheluwe P, Schuermans M, Zador E, Waelkens E and Raeymaekers L. Sarcolipin and phospholamban mRNA and protein expression in cardiac and skeletal muscle of different species. *Biochem. J.* 389: 151-159, 2005a.

Vaugheluwe, P., Raeymaekers, L., Dode, L. and Wuytack, F. Modulating sarco(endo)plasmic reticulum Ca2+ ATPase 2 (SERCA2) activity: cell biological implications. *Cell. Calcium.* 38: 291-302, 2005b.

Vidal-Puig AJ, Grujic D, Zhang CY, Hagen T, Boss O, Ido Y, Szczepanik A, Wade J, Mootha V, Cortright R, Muoio DM and Lowell BB. Energy metabolism in uncoupling protein 3 gene knockout mice. *J. Biol. Chem.* 275: 16258-16266, 2000.

Wawrzynow A, Theibert JL, Murphy C, Jona I, Martonosi A, Collins JH. Sarcolipin, the "proteolipid" of skeletal muscle sarcoplasmic reticulum, is a unique, amphipathic, 31-residue peptide. *Arch. Biochem. Biophys.* 298: 620-623, 1992.

Webber J and Macdonald IA. Signalling in body weight homeostatis: neuroendocrine efferent signals. *Proc. Nutr. Soc*. 59: 397-404, 2000.

Weicher, H., Feraudi, M., Hagele, H. and Plato, R. Electrochemical detection of catecholamines in urine and plasma after separation with HPLC. *Clin. Chim. Acta.* 141: 17-25, 1984.

West DB and York B. Dietary fat, genetic predisposition, and obesity: lessons from animal models. *Am. J. Clic. Nutr*. 67 (suppl): 505S-512S, 1998.

Wu KD and Lytton J. Molecular cloning and quantification of sarcoplasmic reticulum Ca(2+)-ATPase isoforms in rat muscles. *Am. J. Physiol.*264: C333-C341, 1993.

Yang G, Badeanlou L, Bielawski J, Roberts AJ, Hannun YA and Samad F. Central role of ceramide biosynthesis in body weight regulation, energy metabolism, and the metabolic syndrome. *Am. J. Physiol.* 297: E211-E224, 2009.

Yu X and Inesi G. Variable stoichiometric efficiency of Ca^{2+} and Sr^{2+} transport by the sarcoplasmic reticulum ATPase. *J. Biol. Chem.* 270: 4361-4367, 1995.

Zhai J, Schmidt AG, Hoit BD, Kimura Y, MacLennan DH and Kranias EG. Cardiac-specific overexpression of a superinhibitory pentameric phospholamban mutant enhances inhibition of cardiac function in vivo. *J. Biol. Chem.* 275: 10538-10544, 2000.

Zhang S-J, Anderson DC, E. SM, Westerblad H and Katz A. Cross brdges account for only 20% of total ATP consumption during submaximal isometric contraction in mouse fast-twitch skeletal muscle. *Am. J. Physiol.* 291: C147-C154, 2006.

Zurlo F., Larson K., Boqardus C and Ravussin E. Skeletal muscle metabolism is a major determinant of resting energy expenditure. *J. Clin. Invest.* 86: 1423-1427, 1990.

Zvaritch E, Backx PH, Jirik F, Kimura Y, de Leon S, Schmidt AG, Hoit BD, Lester JW, Kranias EG and MacLennan DH. The transgenic expression of highly inhibitory monomeric forms of phospholamban in mouse heart impairs cardiac contractility. *J. Biol. Chem.* 275: 14985-14991, 2000.

Appendix A: Product Sheet of High Fat Diet

Harlan Teklad — *Custom Research Diets*

TD.88137 Adjusted Calories Diet (42% from fat)

Formula	g/Kg
Casein	195.0
DL-Methionine	3.0
Sucrose	341.46
Corn Starch	150.0
Anhydrous Milkfat	210.0
Cholesterol	1.5
Cellulose	50.0
Mineral Mix, AIN-76 (170915)	35.0
Calcium Carbonate	4.0
Vitamin Mix, Teklad (40060)	10.0
Ethoxyquin, antioxidant	0.04

Key Planning Information

- *Products are made fresh to order*
- Store product at 4°C or lower
- Recommended use within 3 months
- Box labeled with product name, manufacturing date, and lot number
- Lead time:
  - Up to 2 weeks non-irradiated
  - Up to 4 weeks irradiated

Footnote

TD 88137 is often referred to as the Western Diet in the cardiovascular literature. The overall level of fat and the saturated nature of the fat are representative of diets that are linked to risk of cardiovascular disease in humans. The formula originated with researchers at Rockefeller University and is used primarily with genetically manipulated mouse models that are susceptible to atherosclerosis. The diet may also be useful in diet induced obesity, diabetes, and metabolic syndrome models.

Product Specific Information

- 1/2" Pellet or Powder (crumbly)
- Minimum order 3 Kg
- Irradiation available upon request
- Feed fresh diet at minimum one time per week (discard unused diet)

Related Diets

There are numerous modifications of TD 88137. Contact a nutritionist for more information about specific modifications, or to develop one that suits your needs.

Options (Fees Will Apply)

- Rush order (pending availability)
- Irradiation (see Product Specific Information)
- Vacuum packaging (0.5, 1, 2 Kg)

Selected Nutrient Information [1]

	% by weight	% kcal from
Protein	17.3	15.2
Carbohydrate	48.5	42.7
Fat	21.2	42.0

Kcal/g	**4.5**
Cholesterol [2]	**0.2%**

[1] Values are calculated from ingredient analysis or manufacturer data

[2] 0.15% added, 0.05% from fat source

International Inquiry

·*Outside U.S.A. or Canada*·

- **askanutritionist@teklad.com**

Speak With A Nutritionist

- **800·483·5523**
- **askanutritionist@teklad.com**

Place Your Order (U.S.A. & Canada)

· *Place Order* · *Obtain Pricing* · *Check Order Status* ·

- **800·483·5523**
- **608·277·2066** *facsimile*
- **customerservice@teklad.com**

Harlan TEKLAD — P.O. Box 44220 · Madison, WI 53744-4220 · 800 · 483 · 5523 — *Access to excellence*

Appendix A: Product Sheet of High Fat Diet

Harlan TEKLAD

TD.88137 - Adjusted Calories Diet (42% from fat)

Typical Fatty Acid Analysis

		Mean	SD
Saturated fat	% of diet	13.3	0.8
Monounsaturated fat	% of diet	5.9	0.6
Polyunsaturated fat	% of diet	0.9	0.4
Unknown	% of diet	0.9	0.2
Total	% of diet	20.8	0.1

Typical Profile

4:0	% of total fatty acids	1.2	0.1
6:0	% of total fatty acids	1.2	0.1
8:0	% of total fatty acids	0.9	0.1
10:0	% of total fatty acids	2.3	0.1
12:0	% of total fatty acids	3.0	0.3
14:0	% of total fatty acids	10.3	0.8
14:1	% of total fatty acids	0.8	0.1
15:0	% of total fatty acids	1.2	0.2
16:0	% of total fatty acids	29.4	1.3
16:1	% of total fatty acids	1.7	0.1
17:0	% of total fatty acids	0.8	0.1
18:0	% of total fatty acids	12.6	0.8
18:1 (Oleic)	% of total fatty acids	20.7	2.5
18:1 Isomers	% of total fatty acids	4.7	0.2
18:2 (Linoleic)	% of total fatty acids	2.3	1.0
18:2 Isomers	% of total fatty acids	1.0	0.2
18:3 (Linolenic)	% of total fatty acids	0.6	0.2
Others*	% of total fatty acids	5.1	1.1

Compilation of analytical data

n = 11

*Others are a combination of unidentified fatty acids and those contributing on average less than 0.5% of total fatty acids, such as EPA and DHA.

11/1/2007

PO BOX 44220 Madison, WI 53744-4220 Phone: (608) 277-2070 Fax: (608) 277-2066
www.tekladcustomdiets.com

Appendix B: Product Sheet of Mice chow

8640
Harlan Teklad 22/5 Rodent Diet

Product Description—Harlan Teklad 22/5 Rodent Diet is an economical, complete, and balanced fixed formula diet designed to provide consistent nutrition to research rodents. Also recommended for use with hamsters.

Ingredients—Dehulled soybean meal, ground corn, wheat middlings, flaked corn, fish meal, cane molasses, soybean oil, ground wheat, dried whey, dicalcium phosphate, brewers dried yeast, calcium carbonate, iodized salt, choline chloride, magnesium oxide, vitamin A acetate, vitamin D_3 supplement, vitamin E supplement, niacin, calcium pantothenate, riboflavin, thiamine mononitrate, pyridoxine hydrochloride, menadione sodium bisulfite complex (source of vitamin K activity), folic acid, biotin, vitamin B_{12} supplement, manganous oxide, ferrous sulfate, copper sulfate, zinc oxide, calcium iodate, cobalt carbonate, chromium potassium sulfate, kaolin.

Guaranteed Analysis		
Crude Protein	(Min.)	22.0%
Crude Fat	(Min.)	5.0%
Crude Fiber	(Max.)	4.5%
Average Nutrient Composition		
Protein	%	22.58
Fat	%	5.23
Fiber	%	3.94
Ash	%	7.06
Nitrogen-Free Extract	%	51.19
Gross Energy	Kcal/g	3.82
Digestible Energy	Kcal/g	3.38
Metabolizable Energy	Kcal/g	3.11
Linoleic Acid	%	3.32
Amino Acids		
Arginine	%	1.65
Methionine	%	0.37
Cystine	%	0.37
Histidine	%	0.52
Isoleucine	%	1.17
Leucine	%	1.88
Lysine	%	1.29
Phenylalanine + Tyrosine	%	2.04
Threonine	%	0.93
Tryptophan	%	0.29
Valine	%	1.17

Minerals		
Calcium	%	1.13
Phosphorus	%	0.94
Sodium	%	0.40
Chlorine	%	0.67
Potassium	%	1.00
Magnesium	%	0.24
Iron	mg/Kg	348.75
Manganese	mg/Kg	104.19
Zinc	mg/Kg	78.84
Copper	mg/Kg	24.07
Iodine	mg/Kg	2.69
Cobalt	mg/Kg	0.72
Selenium	mg/Kg	0.26
Vitamins		
Vitamin A	IU/g	15.93
Vitamin D_3	IU/g	2.99
Vitamin E	IU/Kg	109.54
Choline	mg/g	2.39
Niacin (Nicotinic Acid)	mg/Kg	65.61
Pantothenic Acid	mg/Kg	22.51
Pyridoxine (Vitamin B_6)	mg/Kg	14.45
Riboflavin (Vitamin B_2)	mg/Kg	6.56
Thiamine (Vitamin B_1)	mg/Kg	32.62
Menadione (Vitamin K_3)	mg/Kg	5.22
Folic Acid	mg/Kg	3.19
Biotin	mg/Kg	0.42
Vitamin B_{12}(Cyanocobalamin)	mcg/Kg	54.60
Vitamin C	mg/Kg	---

Reported nutrient values may vary due to the inherent variability in laboratory analysis.

www.teklad.com • customerservice@teklad.com • 1-800-483-5523

2/16/2006

Appendix C: Time-line for Study 2

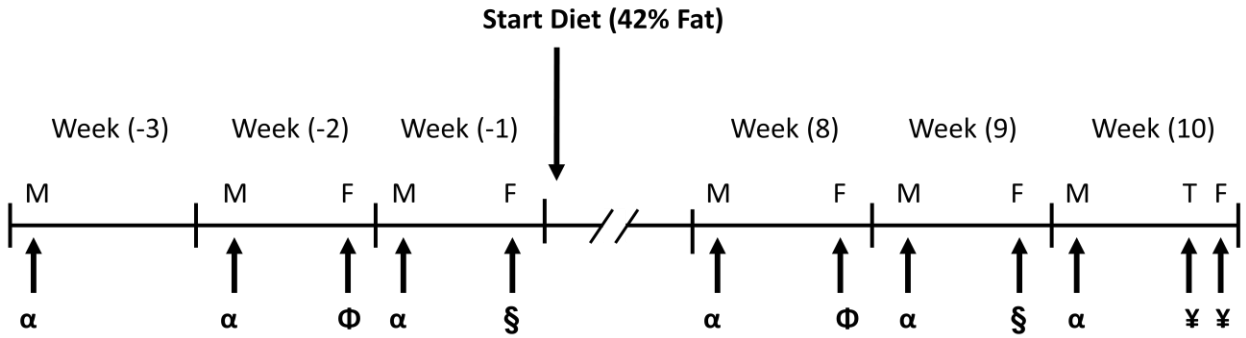

α Basal metabolic rate in CLAMS

Φ Glucose tolerance test

§ Insulin tolerance test

¥ Sacrifice